Muscle-associated *Drosophila* Adducin Regulates Larval Neuromuscular Junction Development and the Localization of Draper to the Synapse

by

Mannan Wang

B.Sc., Sun Yat-sen University, 2009

Thesis Submitted in Partial Fulfillment
of the Requirements for the Degree of
Master of Science

in the
Department of Biomedical Physiology and Kinesiology
Faculty of Science

SIMON FRASER UNIVERSITY

Spring 2013

Approval

Name: **Mannan Wang**

Degree: **Master of Science**

Title of Thesis: ***Muscle-associated Drosophila Adducin Regulates Larval Neuromuscular Junction Development and the Localization of Draper to the Synapse***

Examining Committee:

Chair: James Wakeling, Associate Professor

Wade Parkhouse
Senior Supervisor
Professor
Department of Biomedical Physiology and Kinesiology

Charles Krieger
Supervisor
Professor
Department of Biomedical Physiology and Kinesiology

Nicholas Harden
Supervisor
Professor
Department of Molecular Biology and Biochemistry

Esther Verheyen
External Examiner
Professor
Department of Molecular Biology and Biochemistry

Date Defended/Approved: 28 January 2013

Partial Copyright Licence

Abstract

Adducin, the cross linker of actin and spectrin, has important regulatory roles in the remodeling of submembranous cytoskeleton during synaptic development. In *Drosophila*, *Drosophila* adducins, encoded by *hu-li tai shao (hts)*, are localized to both pre-synaptic and post-synaptic larval neuromuscular junction (NMJ). In animals with muscle-specific knock-down of Hts, NMJs are underdeveloped, whereas overexpression of Hts in the muscle results in NMJ overgrowth. Draper, a transmembrane engulfment receptor, has also been shown to regulate larval NMJ development and may interact with Hts. *In vivo,* Draper colocalizes with Hts at the postsynaptic region. Moreover, in animals with muscle-specific knock-down of Hts, Draper is more tightly localized to the synapse, whereas overexpression of Hts causes delocalization of Draper immunoreactivity from the synapse. This delocalization of Draper induced by Hts highlights a new avenue by which Hts may be exerting its influence on NMJ development.

Keywords: adducin, Hu-li tai shao (Hts), Draper, Drosophila NMJ, synaptic development

To my lovely wife Clare Zheng,
my parents and friends.

Acknowledgements

I would like to express my sincere appreciation to my senior supervisor Dr. Wade Parkhouse for the opportunity to do a Master study at this great university and his continuing support, guidance and encouragements in the past three years; to my committee members: Dr. Charles Krieger and Dr. Nicholas Harden for their support, helpful suggestions and intellectual inputs in my project.

My thanks also go to members of the Harden Lab: Simon Wang, Xi Chen, Michael Chou, David Chung, Sharayu Jangam, Byoungjoo Yoo, Nicole Yoo and Mandeep Rau for their friendship and support. I especially thank Simon Wang, for teaching me the lab techniques and guiding me through this project. I also thank the members of the Krieger lab and the Verheyan lab for their support and friendship. Thanks to Timothy Heslip for his technical support on confocal microscopy.

I would also like to thank Susie Nugent, the graduate assistant of BPK, for always being there and giving me kind encouragements, thoughtful suggestions and always willing to help. Thanks to my friends Jesse Greiner, Michele Bruner, Tasneem Pirani, Mohammed Hassan-Ali, Clarissa Gilbson, John Manning for peer support during my Master study.

Thanks to my wife Clare Zheng and our parents for their constant love and support. None of this would be possible without them.

Table of Contents

List of Tables and Figures

List of Abbreviations

Add	Adducin
ALS	Amyotrophic lateral sclerosis
Brp	Bruchpilot
BSA	Bovine serum albumin
CamK	Ca/calmodulin-dependent protein kinase
CNS	Central nervous system
DFz2	*Drosophila* Frizzled2 receptor
Dlg	Discs-large
Drpr	Draper
ECL	Enhanced chemiluminescence
GluR-IIb	Glutamate receptor IIb
Hrp	Horseradish peroxidase
Hts	Hu-li tai shao
MARCKS	Myristoylated alanine-rich C kinase substrate
MHD	MARCKS-homology domain
mSOD	mutant superoxide dismutase
NMJ	Neuromuscular junction
Pak	p21-activated kinase
PBS	Phosphate buffered saline
PKA	cAMP-dependent kinase
PKC	protein kinase C
RNAi	RNA interference
SDS	Sodium dodecylsulphate
SDS-PAGE	SDS-Polyacrylamide gel electrophoresis
Ser	Serine
SSR	Subsynaptic reticulum

1. Introduction

1.1. Amyotrophic Lateral Sclerosis (ALS)

ALS, also called motor neuron disease or Lou Gehrig's disease in North America, is the third most common adult-onset neurodegenerative disease. It is characterized by degeneration of a selective group of motor neurons and pathways in the brain and spinal cord, which lead to progressive paralysis of the voluntary muscles (Eisen and Krieger, 1998). The clinical features includes initial muscle spasticity, cramps and fasciculations, and then muscle weakness, atrophy, and eventually paralysis and death within 5 years of diagnosis (Rowland and Shneider, 2001). Approximately 2500~3000 Canadians over 18 live with ALS. The vast majority (at least 90%) of ALS cases are sporadic with no family history. Familial forms of ALS, inherited in autosomal dominant or recessive patterns, account for approximately 5%~10% of all ALS cases (Schymick *et al*., 2007). Unfortunately the causes of ALS are still poorly understood.

Several causal and pathogenetic hypotheses for ALS have been proposed over the years, including toxic protein aggregation in motor neurons (Strong *et al*., 2005), glutamate excitotoxicity and hyperexcitability at synapses (Martin and Chang, 2012), oxidative stress caused by free radicals (Barber and Shaw, 2010) and axonal transport defect (Chevalier-Larsen and Holzbaur, 2006). In addition, several new pathogenic mutations such as TDP-43 and FUS/TLS have been identified as causatives of ALS (Bolah, 2011). ALS is increasingly recognized as a disorder of multiple etiologies that give rise to a common end-stage disease phenotype.

Aberrant expressions and activities of protein kinases and phosphoproteins have also been considered to contribute to neuronal death in ALS (Krieger *et al*., 2003). Previous work studying protein kinase and phosphoprotein expression in spinal cord tissues obtained from human ALS patients has shown elevated levels of adducin phosphorylation compared to samples from the control population (Hu *et al*., 2003b).

Consistently, increased phospho-adducin immunoreactivity was also observed in ventral and dorsal horn spinal cord regions of a murine ALS model (Shan *et al*., 2005). These results may indicate a close relationship between adducin and ALS.

1.2. Adducin, an membrane cytoskeletal protein, plays a role in synapse development

Adducin is a family of membrane cytoskeletal proteins which bind and regulate actin filaments and the actin-spectrin cytoskeletal complex (Matsuoka *et al*., 2000). In rat brain, adducin is highly enriched in regions with high synapses densities of the hippocampus, cerebral cortex and cerebellum (Seidel *et al*., 1995). Adducin was also shown to concentrate at the dendritic spines and growing cones of cultured neurons (Matsuoka *et al*., 1998). Collectively these findings indicate that adducins are constituents of synaptic structures and highly involved in promoting the assembly and dissembly processes underling synaptic plasticity.

1.2.1. The actin-spectrin cytoskeleton as a key component of synaptic maintenance and plasticity

In almost all cell types of metazoan organisms, it has been found that actin and spectrin form a cortical cytoskeletal network which lies beneath the plasma membrane (Bennett, 1990). At synapses, the actin-spectrin cytoskeleton supports the overall synaptic framework and functions as the mediator of synapse dynamics and plasticity. The basic unit of the actin-spectrin skeleton is a heterotetramer composed by α- and β-spectrin subunits (Bennett, 1990; Goeliner and Aberle, 2011), which cross-links to short actin filaments (forming the filamentous network) and tethers the network to the plasma membrane through binding to the membrane protein ankyrin and protein 4.1 (Matsuoka *et al.*, 2000). A schematic model of the actin-spectrin cytoskeleton is shown in **Figure 1.1**.

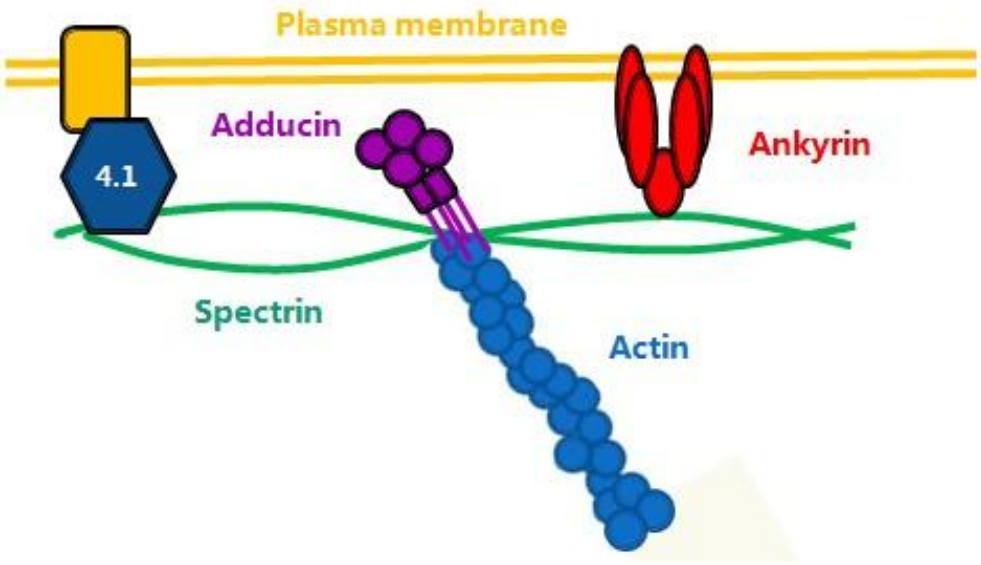

Figure 1.1 A schematic model of the physical model of actin-spectrin cytoskeletal complex.

The spectrin heterotetramer is composed by two α- and two β-spectrin subunits. The heterotetramers bind actin filaments through the N-terminal actin-binding domain of β-spectrin. β-spectrin also has sites for interacting with the membrane protein ankyrin and protein 4.1, which tethers the actin-spectrin cytoskeleton to the plasma membrane. Adducin is the cross-linker that recruits spectrin to actin filaments. (adapted from Matsuoka *et al*., 2000)

The actin-spectrin cytoskeleton has also been termed a “protein accumulation machine” because it serves as a scaffold for protein recruitment and interactions. Presynaptically, the spectrin-actin cytoskeleton acts as a scaffold to organize the neurotransmitter release machinery, recruit regulators to the sites of transmitter release, and facilitate vesicle trafficking and endocytosis. Postsynaptcially, the spectrin-actin cytoskeleton organizes the postsynaptic density where neurotransmitter receptors and other signaling machineries are located (Dillon and Goda, 2005). Proper organization and regulation of actin-spectrin cytoskeleton is critical for synaptic stabilization.

In addition, actin-spectrin cytoskeleton is also the location where dynamic actin network remodeling facilitates morphological changes of synapses in order to grow or retract in response to activity or injury (Honkura *et al*., 2008). Regulation of actin polymerization, as well as of the interactions between actin and other cytoskeletal and synaptic proteins underlies a variety of processes that potentially contribute to synaptic plasticity (Dillon and Goda, 2005; Gu *et al*., 2010 and Zhou *et al*., 2011).

Given the importance of actin-spectrin cytoskeleton in scaffolding synaptic proteins and maintaining synaptic connection, and the fact that proper actin cytoskeletal dynamics is critical for synaptic plasticity, it is intriguing to study the structural proteins localized to the actin-spectrin cytoskeleton and their potential regulatory effects on synaptic integrity and plasticity. Adducin, the cross-linker of spectrin and actin filaments in the actin-spectrin cytoskeletal complex, is the main interest in the present study.

1.2.2. Adducin and its function at actin-spectrin cytoskeleton

Mammalian adducins are a family of submembranous cytoskeletal proteins encoded by three closely related genes: *α*, *β*, and *γ-adducin*. These forms of genes are differently expressed: while *α* and *γ-adducin* are expressed ubiquitously, β-adducin is mainly present in the CNS and erythrocytes (Citterio *et al*., 2003). Proper oligomerization appears to be necessary for adducin activity. Functional adducin is a heterotetramer composed by α/β or α/γ subunit combinations (Matsuoka *et al*., 2000). Structurally, all three adducin proteins contain an N-terminal globular head domain, a short connecting neck domain, a C-terminal tail domain. The head and neck domains mediate oligomerization, while the C-terminal tail domain contains a 22-residue MARCKS-homology domain (MHD), which is named after a similar sequence in the effector domain of myristoylated alanine-rich C kinase subtract (MARCKS) protein (Li *et al*., 1998). The MARCKS-homology domain embeds key residues and binding sequences, which involve a serine residue that is the target for phosphorylation by protein kinase C (PKC), a sequence for Ca^{2+}-dependent calmodulin binding and many other lysine residues of unknown function (Matsuoka *et al.*, 2000).

Adducin is essential for the actin-spectrin cytoskeleton because it is the cross-linker of spectrin and actin. By recruiting spectrin to actin filaments, adducin stabilizes a network of short actin filaments connected together by spectrin heterotetramers, which forms the basis of the actin-spectrin cytoskeleton (Matsuoka *et al*., 2000). Adducin also has regulatory activities in bundling actin filaments and capping the fast-growing (barbed) ends of actin filaments (Kuhlman *et al*., 1996). All of these functions of adducin are important for structural modification during synapse development. Regulation of adducins provides a switch between dynamically growing actin filaments and the stable spectrin cytoskeleton. The specific binding sites of adducin to actin-spectrin complex are

not known, however it is shown that the MHD in C-terminal domain is necessary but not sufficient for binding, and the neck domain also contributes to binding (Li *et al*., 1998) (**Figure 1.2**).

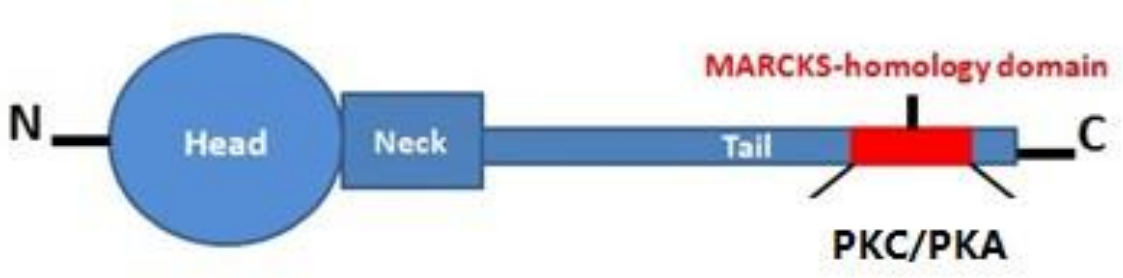

Figure 1.2 A schematic model of adducin monomer.

Adducin is composed of an N-terminal globular head domain, a neck domain and a C-terminal tail containing a MARCKS-homology domain. The major phosphorylation sites of PKA and PKC are localized to the MARCKS-homology domain. (adapted from Matsuoka *et al*., 2000)

The activity of adducin is regulated by different protein kinases and signaling molecules. The C-terminal MARCKS domain of adducin contains target sites for phosphorylation by protein kinase C (PKC) and cyclic AMP-dependent protein kinase (PKA) (Matsuoka *et al*., 1996). Both the actin-capping and actin-spectrin cross-linking activities of adducin are inhibited by PKC/PKA phosphorylation (Matsuoka *et al*., 1998). The C-terminal MARCKS domain also provides the binding site for Ca^{2+}-dependent calmodulin, which has similar inhibitory effects on the activities of adducin (Kuhlman *et al*., 1996).

1.2.3. Adducin and its role in synaptic plasticity and nervous system

In *Aplysia*, Increased phosphorylation of γ-adducin was observed during long-term synaptic facilitation (Gruenbaum *et al*., 2003). In addition, high levels of phosphorylated adducin have been observed in hippocampal dendritic spines (Matsuoka *et al.*, 1998). These observations suggest that the actin-capping activity of adducin could be regulated during morphological synaptic plasticity by phosphorylation.

Phosphorylation by PKC/PKA abolishes the actin capping activity of adducin, which as a result releases the barbed end of actin filaments for further actin polymerization (Matsuoka *et al*., 1996 and 1998). This dynamic growth of actin filaments is hypothesized to give rise to actin-based filopodia extensions at the nerve terminal and promote new synapse formation (Pielage *et al*., 2011).

Adducin loss of function or misregulation has been shown to cause learning and memory defects. β-adducin knock-out mice showed impaired synaptic plasticity and defects in memory and learning (Porro *et al*., 2010). In a recent study using the nematode *Caenorhabditis elegans*, it is found that animals lacking the homologue of mammalian adducin failed to consolidate the changes after synaptic remodeling during memory formation, resulting in impaired short- and long-term memory (Vukojevic *et al*., 2012). These results suggest that during memory formation and learning, adducin not only facilitate enhanced synaptic plasticity, but also is required for the maintenance of the newly formed synapses.

Despite the well studied regulatory roles of adducin in memory formation and learning processes, how adducin and its regulation on synaptic plasticity affect other neurological functions remains poorly studied. Aberrant hyperphosphorylation of adducin is observed in spinal cord tissues from both human ALS patients and a murine ALS model (Hu *et al*., 2003b; Shan *et al*., 2005). How these observed changes of phospho-adducin levels relate to the etiology of ALS is unknown. Reduced synaptic connectivity and dysregulated synaptic activity are hallmarks of several psychiatric disorders and neurodegenerative diseases (Lin and Koleske, 2010). In ALS, the disassembly of neuromuscular junction is an early pathological feature (Fischer *et al*., 2004). The loss of muscle-neuronal contact and impaired retrograde uptake/transport in motor neuron axons has also been speculated to contribute to the debility in a murine model of ALS (Parkhouse *et al*., 2008). In addition, the dysregulation of synaptic activity in the central nervous system has long been proposed to cause motor neuron death in ALS (Martin and Chang, 2012). All the above studies support the study of adducin and its regulatory roles in synapse maintenance and development in order to better understand ALS. In the present study, I used Drosophila 3rd instar larval neuromuscular junction (NMJ) system as the model to study adducin and its regulatory roles in synaptic development.

1.3. Drosophila 3rd instar larval NMJ as a preeminent model for studying synaptic development

The *Drosophila* larval neuromuscular junction (NMJ) system has emerged as an increasingly popular model for studying axonal guidance, synaptic development, synaptic electrophysiology, vesicle trafficking and synaptic plasticity (Jan and Jan, 1976a). Compared to about 25,000 genes on 23 chromosomes for humans, the *Drosophila* genome encodes only about 13,600 genes on 4 chromosomes (Adams *et al*., 2000). This much reduced complexity avoids the gene redundancy observed in mammalian subjects (Zhang, 2012). In addition, the *Drosophila* larval neuromuscular junction (NMJ) is easily accessible for analysis, with a wide range of molecular and genetic tools available to permit sophisticated genetic manipulations.

1.3.1. The formation of Drosophila neuromuscular system

The entire *Drosophila* metamorphosis takes about 12 days at 25°C. Once an egg is laid, it goes through embryogenesis and takes about 24 hours to hatch, and then 6 days to go through three larval stages (1st, 2nd, 3rd instar larval stage) to turn into an immobile pupa. During the next four days of metamorphosis, most larval tissues in the pupa get destroyed and replaced by adult tissue derived from the imaginal discs, and the pupa finally turn into an adult fly. Adult flies then break the pupa shell and emerge themselves, which is called eclosion. After an adult fly ecloses, it takes another 12 hours for it to become fertile (Miller, 2008).

The formation of neuromuscular system happens during embryonic development, when motoneurons in the brain stem start to extend axons along major nerve trunks and then branch into their corresponding muscle area (Johansen *et al*., 1989b). Meanwhile, each individual muscle is formed from the fusion of a single founder cell with one or more fusion-capable myoblasts (Bate, 1990). The establishment of neuromuscular junctions begins at about embryonic stage 15, around 13 hours after an egg is laid, when axonal growth cones of motoneurons reach their target muscles (Ritzenthaler *et al*., 2000). Membrane processes (called myopodia) from the muscle firstly make contacts with axonal growth cones and initiate a target-recognizing process (Kohsaka and Nose, 2009). Recognition between myopodia from each muscle and its specific neuronal

counterpart is mediated by a balance between attractive and repellent cues, and interaction between cell-specific membrane proteins (Rose and Chiba, 2000; Inaki *et al.*, 2010). Myopodia contacts with their specific partner motoneurons are stabilized to form synapses, while those with non-partner motoneurons are retracted and disassembled (Kohsaka and Nose, 2009). By embryonic stage 17, about 18 hours after egg lying, all synapses with mature morphological and functional features will have been established (Broadie and Bate, 1993).

1.3.2. Drosophila 3rd instar larval NMJ as an important model system to study synaptic development

One of the most exploited features of *Drosophila* larval NMJ system is the fact that larval NMJ is a continuously developing synapse. During the growth of a *Drosophila* larva from hatching to late 3rd instar stage, its muscle cells undergo a dramatic increase (~150 times) in volume (Ruiz-Canada and Budnik, 2006). Although the general wiring of neuromuscular connections has virtually established by the end of embryogenesis, in response to the dramatic growth of muscle fibers during larval stage, the NMJ needs to continuously expand in size and develop to maintain synaptic efficacy (Ruiz-Canada and Budnik, 2006).

It is well established that the development of larval NMJ requires combined activities of synapse formation and retraction (Zito *et al.*, 1999; Eaton *et al*., 2002). The molecular mechanisms underlying synapse formation have been studied extensively and include target recognition, cell adhesion, modulation of the neuronal cytoskeleton, synapse assembly and stabilization (Luo, 2002; Schuster *et al.*, 1996a; Goda and Davis, 2003). The opposing mechanisms that cause synaptic retraction include modulation of submembranous spectrin/ankyrin skeleton, axonal transport, and growth factor signaling (Pielage *et al*., 2005; Koch *et al*., 2008; Eaton *et al*., 2002; Luo and O'Leary, 2005).

Drosophila 3rd instar larval NMJ is an excellent model to study the molecular mechanisms underlying synaptic development. Taking advantage of the well established genetic tools in *Drosophila*, a wide range of genetic manipulation is available, including stage- and tissue-specific induction or knockdown of gene expression. In addition, Drosophila larval body walls have genetically predetermined layout with well defined

synapses, which allows consistent and reliable comparisons between animals of different genotypes. Mutations that perturb NMJ development can be easily examined.

1.3.3. Structure and organization of the Drosophila 3rd instar larval NMJ system

A 3rd instar larva can be easily dissected to obtain its body wall preparation containing all the abdominal muscles and neuromuscular junctions. 3rd instar larval body wall is composed of 7 abdominal segments (A1 to A7) of repetitive musculature display. Each abdominal segment has two identical hemisegments located at each side of the ventral midline (**Figure 1.3A**). Each hemisegment is composed of 30 skeletal, supercontractile muscle fibers appearing in a stereotyped pattern. Individual muscles are uniquely identifiable, based on their sizes, shapes, positions and sites of insertion in the larval cuticle (Cossley, 1978).

Muscles in each hemisegment of the larval body wall are innervated by 30 motoneurons located in ventral ganglion. Each motoneuron axon specifically innervates its target muscles with a high degree of accuracy (Keshishian and Chiba, 1993). Most muscles are poly-innervated by no less than two moroneurons, with only one exception, muscle 4 is mono-innervated (Ruiz-Canada and Budnik, 2006). When a motoneuron axon reaches its target muscle, it branches over the muscle and forms a structure called axonal terminal. The axonal terminal consists of branched chains of roughly spherical swollen tips (also called synaptic boutons) to make synaptic connections with the muscle. The synaptic boutons are imbedded into the surface of the muscle tissue but remain interconnected by the axonal tract (Keshishian and Chiba, 1993). Each synaptic bouton contains many presynaptic active zones, where synaptic vesicles fuse and the neurotransmitter is released to the synaptic cleft. The neurotransmitter is then bound by neurotransmitter receptors on the muscle surface clustering at sites that directly appose to the active zones (**Figure 1.3D**).

The size and arrangement of synaptic boutons at each muscle is determined by the innervating motoneurons. There are three classes of motoneurons in Drosophila: type-I, type-II and type-III (Jan and Jan, 1976a). Type-I is the most abundant class of motorneurons which gives rise to the largest boutons. Type-I motoneurons can be further subdivided into Type-I big (Type-Ib) motoneurons and Type-I small (Type-Is)

motoneurons. Type-Ib boutons have bigger size than type-Is boutons. The axonal terminal of type-Ib tends to be short and minimally branching, whereas that of type-Is is usually much longer with more elaborate branching (Jan and Jan, 1976a; Johansen et al., 1989b). Type-II motoneurons form relatively small boutons. Axonal terminals of type-II motoneurons are very long and elaborate (Johansen et al., 1989a; Monastirioti et al., 1995). Type-III motoneurons are rare and only found to innervate muscle 12 with smaller boutons than type I (Hoang and Chiba, 2001) (**Figure 1.3B**).

Type-I motoneurons (both type-Ib and type-Is) are the primary stimulatory motorneurons that innervate all the larval muscles. Type-I boutons are purely glutamatergic releasing glutamate (the main excitatory neurotransmitter) at active zones (Jan and Jan, 1976b). Type-Is boutons contain vesicles with larger diameter than those in type-Ib boutons. Type-Is boutons are likely to release larger quantities of transmitter and have a higher probability of releasing transmitter than type-Ib boutons (Atwood *et al*., 1997; Karunanithi *et al*., 2002). The other two classes of motoneurons, type-II and type-III, mainly form neuromodulatory boutons that release the biogenic amine octopamine (Monastirioti *et al*., 1995), or a variety of peptides (Gorczyce *et al*., 1993), though they also contain glutamate-filled vesicles (Johansen *et al.*, 1989b).

Different classes of motoneurons also have different corresponding postsynaptic structures. The subsynaptic reticulum (SSR) is an elaborate network of membrane invaginations formed in the plasma membrane of the muscle surrounding the presynaptic boutons (Guan *et al*., 1996). The specific function of the SSR in unknown, though proper formation of the SSR has been shown to be important for localization of synaptic scaffolding protein discs-large (Dlg) and cytoskeletal protein spectrin (Lahey *et al.*, 1994; Pielage *et al.*, 2006). Type-Ib boutons are surrounded by a larger SSR than type-Is boutons. There is no SSR surrounding type-II and type-III boutons (Jia et al., 1993).

The neuromuscular junction located between the two major ventral longitudinal abdominal muscles (muscle 6/7) has been quite commonly used as the model to study synaptic development (**Figure 1.3C**), owning to its well-defined structure and the large size of muscle 6/7. Muscle 6 and 7 are only innervated by two types of boutons, type-Ib

and type-Is (**Figure 1.3B**). Type-II and type-III are absent from muscle 6/7 (Guan *et al*., 1996; Jan and Jan, 1976a, b).

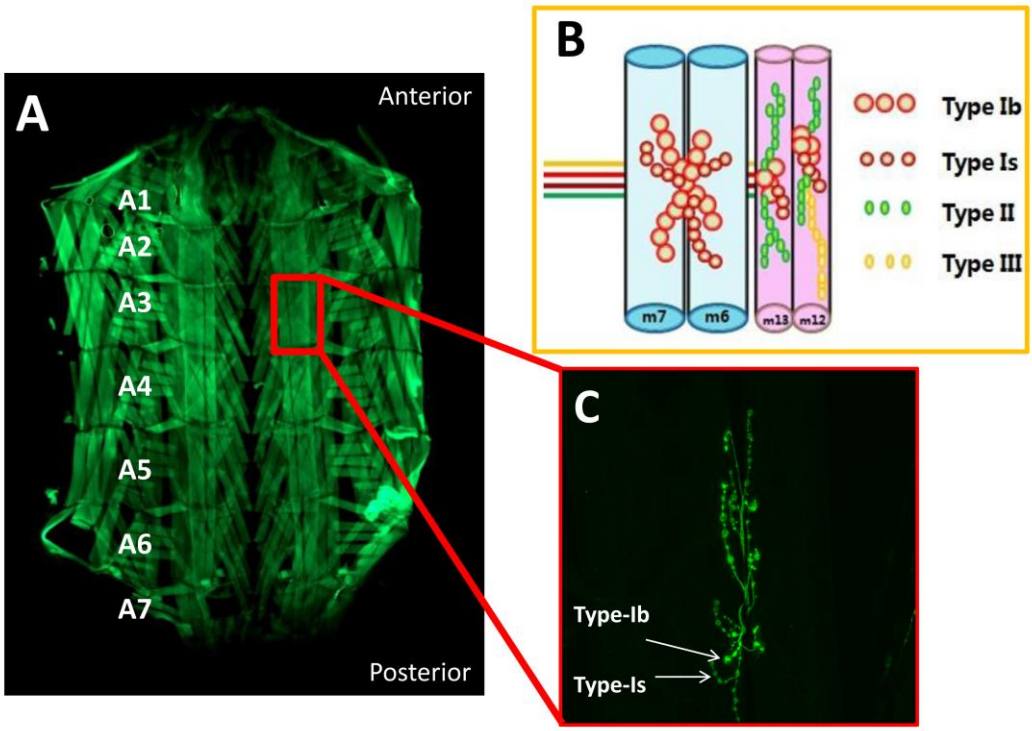

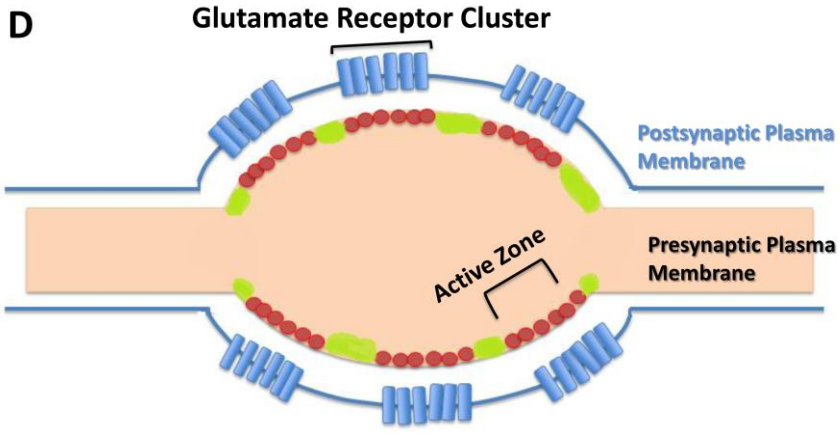

Figure 1.3 Structure and organization of Drosophila 3rd instar NMJ system.

(A)---Dissected late third instar larval body wall preparation. The body wall preparation is stained with FITC-phalloidin to show musculature. 3rd larva has seven abdominal segments (A1-A7). A2 to A7 have identical muscle arrangement and display pattern, A1 is slightly different from the others (Gorczyca and Budnik, 2006). (B)---Schematic model of innervations patterns at muscle pairs 6/7 and 12/13. Muscle 6/7 is only innervated by two types of motoneurons, type-Ib and type-Is. (adapted from Guan et al., 1996). (C)---Wild type muscle 6/7 NMJ in A3 segment, immunostained against the neuronal marker Hrp. (D)---The cartoon of a single synaptic bouton (in pink) imbedded in the postsynaptic muscle membrane (in blue). Each bouton contains many active zones (in red), which locate in precise apposition to postsynaptic Glutemate receptor clusters. Synaptic vesicles fuse at active zones and release neurotransmitter (Glutamate) when excitatory signals come. (adapted from Roos and Kelly, 1999)

1.4. Hu-li tai shao (Hts), the Drosophila adducin, regulates larval NMJ development

Drosophila orthologs of adducin are encoded by the *Hu-li tai shao* (*hts*) locus. Meaning “too little nursing” in Chinese, *hts* was firstly characterized during oogenesis where mutant females are sterile and produce egg chambers with fewer than the normal 15 nurse cells (Yue and Spradling, 1992). Data from oogenesis studies suggests that Hts proteins associate with actin and spectrin and may have a conserved role as a regulator of actin-spectrin networks in a manner similar to the mammalian adducins (Zaccai and Lipshitz, 1996a, b).

1.4.1. Structure of Hts

Alternative splicing of *hts* transcripts results in four distinct Hts proteins: Add1, Add2, ShAdd and Ovhts. These four protein isoforms share common N-terminal head and neck domains, but differ in C-terminal tail regions (**Figure 1.4**). Add1 and Add2 exhibit homology to the mammalian adducins as they both contain the MARCKS homology domain (the main regulatory domain) in their C-terminal regions (Petrella *et al.*, 2007). Add1 shares 38% overall identity with vertebrate α-adducin and 64% identity within the MARCKS domain (www.flybase.org; Blast NCBI). Add2 only differs from Add1 by having an extra 23 amino acids in the C-terminal region. ShAdd has a truncated C-terminal domain, whereas Ovhts has a novel C-terminal domain termed the Ring Canal (RC) domain (Petrella *et al.*, 2007).

Four antibodies (htsF, hts1B1, htsM and htsRC) are available to detect different Hts protein domains. htsF antibody (Lin *et al.*, 1994) recognizes the common head and neck domains of all four Hts proteins. hts1B1 antibody (Zaccai and Lipshitz, 1996b) recognizes a portion of the C-terminal tail domain shared by Add1, Add2 and Ovhts. Because the C-terminal domain is truncated in ShAdd, it cannot be detected by hts1B1. As htsM recognizes the MARCKS homology domain it only detects Add1 and Add2. htsRC detects specifically against Ovhts by recognizing its unique RC domain in the C-termial tail (Petrella *et al*., 2007).

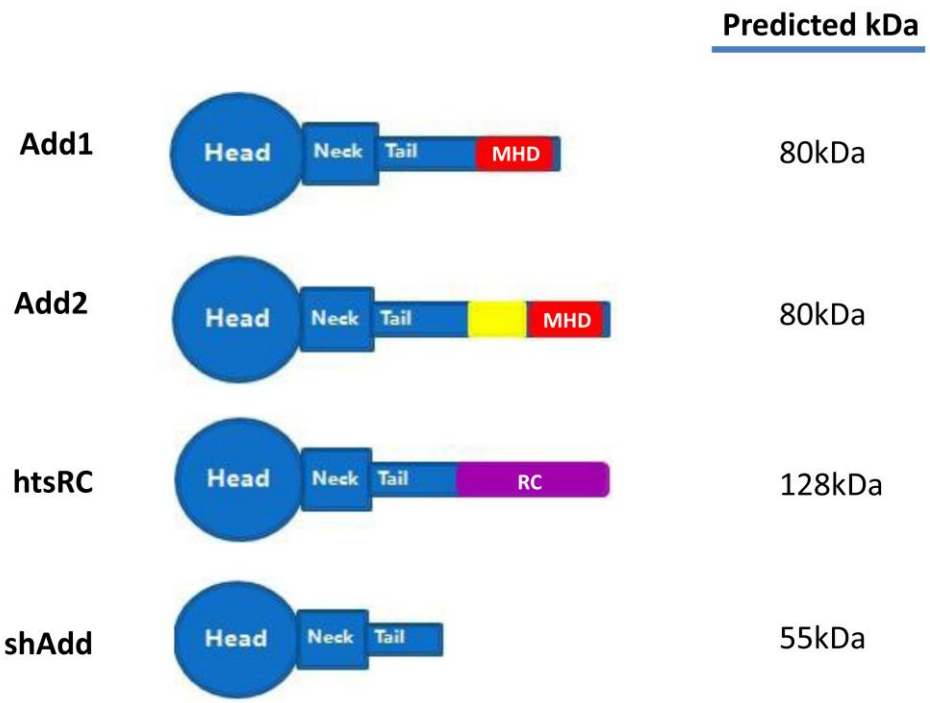

Figure 1.4 Domain structure and predicted sizes of four Hts proteins

All the four Hts proteins contain the common head (H) and neck (N) domains. Four Hts proteins have distinct C-terminal tail domains: ShAdd contains a truncated tail domain, Ovhts contains a novel Ring Canal domain (in purple), Add1 and Add2 are the only isoforms of Hts with a MARCKS-homology domain (MHD, in red) in their tail domain. Add2 only differs from Add1 by containing an extra exon of 23 amino acids (in yellow). (adapted from Petrella et al., 2007)

1.4.2. Hts regulates larval NMJ development

Two previous studies have identified the localization of Hts in the Drosophila 3rd instar larval neuromuscular junction (NMJ). Hts has been shown to localize to the postsynaptic membrane of NMJ with staining more specifically localized to type-I glutamatergic boutons (Wang *et al*., 2011). Three different Hts antibodies were used in the study to detect different Hts isoforms at the NMJ. No immunoreactivity was detected using htsRC antibody, indicating Ovhts is not present to the postsynaptic NMJ. Both hts1B1 (detecting Add1, Add2 and ShAdd) and htsM (only detecting Add1 and Add2) showed similar immunostaining at the postsynaptic NMJ, indicating that Add1 and Add2 (the only Drosophila homologs of adducin) are the predominant isoforms at postsynaptic NMJ (Wang *et al*., 2011). Pielage *et al*. (2011) showed that in addition to its postsynaptic localization, Hts is also present in the presynaptic axons. Only one isoform of Hts proteins, Add1, was observed in larval brain, indicating Add1 is the predominant isoform in presynaptic axons (Pielage *et al*., 2011).

Both the above two groups studied Hts regulation on Drosophila larval NMJ development and showed conflicting results. Wang *et al*. (2011) showed that 3rd instar larvae which are homozygous mutant for hts^{01103}, a null allele that contains a P-element insertion upstream of the *hts* gene, have severely underdeveloped synaptic terminals at muscle 6/7 compared to wild-type control. This underdeveloped phenotype is characterized by decreased branch length and less branch number. However, Pielage *et al*. (2011) showed that loss of Hts caused overdeveloped NMJs in muscle 4, characterized by an increase in bouton numbers and NMJ span, and the formation of long actin-rich presynaptic protrusions. A possible explanation of this discrepancy is that these two groups were looking at synapses in different muscles. Muscle 6/7 is innervated by both type-Ib and type-Is motoneurons, whereas muscle 4 is mono-innerved by only type-Ib motoneuron. Different muscle properties and innervating profiles may affect the outcomes of *hts* mutations. Indeed, subgroups of motor neurons and muscles demonstrate a diversity in their susceptibility to an ALS-related gene mutation has been documented in the *Drosophila* NMJ system (Xia *et al*., 2012).

The regulatory roles of Hts in Drosophila larval NMJ development were further studied using transgenic flies with Hts overexpressions. Wang *et al*. (2011)

overexpressed endogenous *hts* in the muscle by crossing the muscle specific *mef2-GAL4* driver to *UAS-hts*^{GS13858} (a Gene Search line where UAS sequences were inserted upstream of the endogenous *hts* gene). Overexpression of endogenous *hts* in the muscle gave rise to significant NMJ overgrowth at muscle 6/7, characterized by increased bouton number, branch extension and overall NMJ span. On the other side, Pielage *et al*. (2011) specifically overexpressed the cDNA encoding Add1 in the presynaptic neurons and observed its impact on NMJ development at muscle 12/13. Wild type muscle 12 and 13 are innervated by motoneurons that form type-Ib boutons as well as small-caliber type-II and type-III synaptic terminals. Presynaptic overexpression of hts severely restrained the growth and extensiton of the small-caliber type-II and type-III synaptic terminals (Pielage *et al*., 2011). These two findings together suggest that Hts may play distinct roles presynaptically or postsynaptically. In this respect, presynaptic Hts restrains the NMJ growth whereas postsynaptic Hts promotes NMJ growth. More study is needed to better understand Hts and its regulatory roles in the *Drosophila* larval NMJ system.

1.4.3. Hts regulates larval NMJ development through interactions with synaptic proteins

Adducin/Hts localizes to the actin-spectrin cytoskeleton complex where other synaptic proteins are gathered and assembled. Some synaptic proteins have also been shown to affect synapse development. Exploring the potential interactions between Hts and these synaptic proteins may aid in the understanding of Hts regulation at the NMJ.

1.4.3.1. Hts regulates the phosphorylation and localization of Dlg at *Drosophila* larval NMJ

Discs-large (Dlg) is a Drosophila homolog of the mammalian postsynaptic density 95 (PSD-95), which is a member of the membrane-associated guanylate kinase (MAGUK) family of scaffolding proteins. Like other members of MAGUK family, Dlg contains three PSD-95-Discs Large-Zonula Adhesion (PDZ) domains followed by a Src homology 3 (SH3) and a C-terminal guanylate kinase like (GUK) domain (Wood and Bryant, 1991; Budnik *et al*, 1996).

Dlg was originally identified as a tumor suppressor which when mutated causes tumor growth in imaginal discs due to loss of epithelial apicobasal polarity (Wood and

Bryant, 1991). At the *Drosophila* larval NMJ, Dlg is concentrated at type I bouton postsynaptic specializations, and to a lesser extent, to the presynaptic bouton border (Lahey *et al*., 1994). Dlg recruits a variety of synaptic proteins to the postsynaptic membrane and mediates many protein-protein interactions via its three Class-I PDZ repeats and SH3 domain (Chen and Featherstone, 2005; Zito *et al*., 1997). Dlg also facilitates the accumulation and assembly of Fasciclin2 (Fas2), a homophilic transmembrane cell adhesion molecule, at both postsynaptic and presynaptic membranes to stabilize the synapse (Zito *et al*., 1997). The breaking and restoration of Fas2/Dlg-mediated adhesion between presynaptic and post-synaptic membranes is likely a critical process underlying synaptic plasticity. Proper localization and regulation of Dlg to the postsynaptic area is required for normal synapse structure, function and development (Lahey *et al.*, 1994; Budnik *et al*, 1996; Koh *et al*. 2000). Dlg is regulated by phosphorylation at Ser48 and Ser797 by Ca2+/calmodulin-dependent kinase II (CaMKII) and PAR-1 kinase respectively. Phosphorylation induced by either kinase causes delocalization of Dlg away from the NMJ and impairs its scaffolding function (Koh *et al*., 1999; Zhang *et al.*, 2007).

It has been shown that Hts and Dlg colocalize with each other at postsynaptic NMJ. In addition, Hts and Dlg were shown to co-immunoprecipitate with each other in 3rd instar larval extracts (Wang *et al*., 2011). These indicate that Hts and Dlg physically exist in the same protein complex and suggest potential interactions between the two. Consistently, Hts has been found to regulate the phosphorylation and localization of Dlg at postsynaptic NMJ and muscle-specific overexpression of Hts caused Dlg to delocalize form the postsynaptic NMJ in a diffusing pattern. Increased level of phosphorylated Dlg (p-Dlg) was detected in cytoplasmic muscle area, along with increased immunoreactivity of both CamKII and PAR-1 detected at the NMJ of larvae with muscle-specific Hts overexpression. These findings indicate that Hts may be regulating Dlg phosphorylation and localization via CamKII and PAR-1, and that interactions between Hts and Dlg may be involved in Hts regulation on NMJ development (Wang *et al*., 2011).

1.4.3.2. Draper, an engulfment receptor, could be a potential candidate involved in Hts regulation of NMJ development

Draper, the *Drosophila* ortholog of CED-1 in the nematode *Caenorhabditis elegans*, is an engulfment receptor expressed in phagocytic cells, where it acts to

recognize cell corpses and initiate engulfment and phagocytosis of the corpses (Zhou *et al.*, 2001). Draper was initially found to be required in embryonic glia for glial clearance of the neuronal cell corpses generated during embryonic neurogenesis (Freeman *et al*., 2003). Draper also recognizes and engulfs neural debris during axon pruning (Awasake et al., 2006) and removes severed axons in the CNS (MacDonald *et al*., 2006).

Structurally, Draper is a transmembrane receptor containing 15 extracellular atypical epidermal growth factor (EGF) repeats and a single intracellular domain. The extracellular EGFs are important for recognizing the "eat me" signals sent out from the cell corpses or neuronal debris. A single transmembrane domain (once activated) initiates engulfment events by activating its downstream Drosophila CED-6 (dCED-6) and Src family signaling cascade composed of the non-receptor tyrosine Kinases Src42a and Shark (Ziegenfuss *et al*., 2008). It has been shown that loss of Draper signaling blocks the initial activation of glial responses to axon injury in vivo, which entails upregulation of engulfment genes and extension of glial membranes to injury sites (MacDonald *et al*., 2006; Ziegenfuss *et al*., 2008).

At the Drosophilal larval NMJ system, Draper localizes to the postsynaptic regions in the muscle and the surrounding glia cells. Interestingly, Draper has also been shown to be involved in *Drosophila* larval NMJ development (Fuentes-Medel *et al*., 2009). During normal NMJ development, an excessive number of axonal projections and synaptic connections are initially established. As the appropriate synaptic contacts are strengthened, excessive contacts are destabilized and shed, generating presynaptic debris (neuronally derived membrane and cell fragments) and "ghost boutons" (immature boutons without postsynaptic membranes surrounding them) (Luo and O'Leary, 2005). The clearance of presynaptic debris and "ghost boutons" are dependent on Draper mediated engulfment and phagocytosis. In *draper* null mutant larvae ($drpr^{\Delta 5}$), accumulated presynaptic debris and "ghost boutons" were observed. Interestingly, impaired synaptic growth (characterized by oversimplified synaptic terminals and decreased type-Ib bouton number) was observed at the same time (Fuentes-Medel *et al*., 2009). This suggests that proper clearance of neuronal debris is critical for synaptic plasticity during larval NMJ development. It has been shown that both glia and muscular Draper are important in the clearance process, with glial Draper mainly mediating the

clearance of presynaptic debris and muscular Draper mainly clearing “ghost boutons” away (Fuentes-Medel *et al*., 2009).

Several factors suggest that Draper is a potential candidate to interact with Hts during regulation of NMJ development. Both Draper and Hts have been shown to co-localize with Dlg at the postsynaptic region (Fuentes-Medel *et al*., 2009; Wang *et al*., 2011). In addition, a previous yeast two-hybrid based screen of the Drosophila proteome has identified Hts and Draper as putative binding partners (Giot *et al*., 2003). Thus it is highly possible that Draper and Hts co-localize to the post-synaptic membrane and physically interact with each other. Furthermore, both *hts* and *draper* null mutant larvae show similar NMJ defects characterized by severely decreased synaptic terminal span (Fuentes-Medel *et al*., 2009; Wang *et al*., 2011). Potential genetic interactions between *hts* and *draper* likely exist.

1.5. Rationale and research goals

Previous studies have revealed that Hts products are expressed both pre- and postsynaptically at the *Drosophila* larval NMJ (Wang *et al*., 2011; Pielage *et al*., 2011). The function of presynaptic Hts has been well studied. Regulation of presynaptic Hts provides a switch between actin dependent synaptic growth and spectrin dependent synaptic stabilization (Pielage *et al*., 2011). However, the function of postsynaptic Hts during *Drosophila* larval NMJ development remains unclear. Homozygous *hts* null mutant larvae (hts^{01103}) were shown to have underdeveloped NMJs. It is unclear if this underdeveloped phenotype is caused by the loss of pre- or postsynaptic Hts. In the present study, the roles of postsynaptic Hts in larval NMJ development will be studied, by examining the effects of muscle-specific Hts knock-down or overexpression on Drosophila larval NMJ development.

Hts contains protein interaction domains that initiate binding to other synaptic proteins (Matsuoka *et al*., 1996) and the interaction between Hts and other synaptic proteins is likely involved in regulating synaptic development (Wang *et al*., 2011). Draper, a transmembrane engulfment receptor, localizes to the *Drosophila* larval NMJ and is involved in regulating synaptic development (Fuentes-Medel *et al*., 2009). Given

that both Hts and Draper have postsynaptic localization at the *Drosophila* larval NMJ (Wang *et al*., 2011; Fuentes-Medel *et al*., 2009), and that Hts and Draper have been shown to be putative binding partners in a yeast two-hybrid based screen (Giot *et al*., 2003), it is possible that protein-protein interactions between Hts and Draper exists. To evaluate this possibility, colocalization of Draper and Hts will be first examined using immunohistochemical technique. Then the immunoreactivity of Draper will be further examined at NMJs with different genetic manipulations of Hts.

2. Materials and Methods

2.1. Fly strains and crosses

w^{1118} flies were used as wild type controls and flies that are homozygous for hts^{01103}*, a null allele* that contains a p-element insertion upstream of the *hts* gene, were used as *hts* loss of function flies (Wilson, 2005). *UAS-*$hts^{GS13858}$, is a gene search line whereby UAS sequences are inserted upstream of the endogenous *hts* gene (Toba *et al*., 1999). Using the UAS-GAL4 system (Duffy, 2002), a muscle specific Hts gain of function line can be made by crossing *UAS-htsGS13858* with *mef2-GAL4* (a muscle-specific driver line). Another hts transgene line used in these experiments was *UAS-*hts^{S705S}, which is a wild type transgene of *htsR1/Add1* transcriptional isoform (Whittaker *et al*., 1999). This transgene was used to study the function of Add1/HtsR1, an isoform of Hts proteins that is found to be highly expressed in the central nervous system of the late stage embryo and suggested to play a role during synapse development (Zaccai and Lipshitz, 1996a, b). *CG9325*, a *UAS-htsRNAi* line, was used to cross with mef2-GAL4 to generate a muscle-specific Hts knock-down model. Flies that are homozygous for $drpr^{\Delta 5}$, a truncated drpr null allele, are used to study Draper loss of function (Freeman *et al*., 2003). The fly strains used in this study are summarized in **Table 1**.

w^{1118}, hts^{01103}, *mef2-GAL4* flies were from Bloomington Drosophila Stock Center. $hts^{GS13858}$ was from Drosophila Genetic Resource Center, Japan. $hts^{1889\text{-}1\text{-}7F}$ (referred to as hts^{S705S} in the text) was generated by Vincent Chui in the Krieger Lab (Chui, 2011). *CG9325* (the *hts-RNAi* stock) and *UAS-dlg1RNAi* were from Vienna Drosophila RNAi Centre. $drpr^{\Delta 5}$, *UAS-drprRNAi, UAS-drpr-I* were gifts from Dr. Freeman (Fuentes-Medel *et al*., 2009). *UAS-*Dlg^{A} *and UAS-*Dlg^{S97} were gifts from Dr. Thomas (Ataman et al., 2006).

Table 1 Drosophila lines used for experiments

Fly lines	***Description***	***Function***
w^{1118}	wild type fly line (Bloomington)	wild type control
hts^{01103}	*hts* null allele (P element interruption)	*hts* loss of function
mef2>GAL4	muscle specific driver	specifically overexpresses transgenes in the muslce
UAS-$hts^{GS13858}$	Gene search line, with UAS sequence inserted upstream of endogenous *hts* gene	creating *hts* gain of function when crossed to *mef2>GAL4* flies
UAS-hts^{S705S}	wild type transgene of ADD1 transcroptional isoform	overexpressing ADD1 in the muscle when crossed to *mef2>GAL4* flies
CG9325	a *UAS-htsRNAi* line	initiating muscle-specific *hts* knock-down when crossed to *mef2>GAL4* flies
$drpr^{\Delta 5}$	*drpr* null allele (P-element induced truncation)	*drpr* loss of function
UAS-drpr-I	Transgene of Drpr-I transcroptional isoform	overexpressing Drpr-1 in the muscle when crossed to *mef2>GAL4* flies
UAS-drprRNAi	Transgene of drprRNAi	initiating muscle-specific *drpr* knock-down when crossed to *mef2>GAL4* flies
UAS-Dlg1RNAi	Transgene of RNAi that targeting on Dlg	initiating muscle-specific *dlg* knock-down when crossed to *mef2>GAL4* flies
UAS-Dlg^{A}	Transgene of Dlg^{A} transcroptional isoform	overexpressing Dlg^{A} in the muscle when crossed to *mef2>GAL4* flies
UAS-Dlg^{S97}	Transgene of Dlg^{S97} transcroptional isoform	overexpressing Dlg^{S97} in the muscle when crossed to *mef2>GAL4* flies

2.2. Experimental sample preparation

2.2.1. Drosophila 3rd instar larval body wall preparation and fixation

A modified protocol based on Brent et al., (2009) was performed to make the 3rd instar larval body wall preparations for immunostaining and visualization of the NMJ. Procedures are briefly described below.

The larval body wall dissection was operated under a dissecting microscope with 4X lens. The 3rd instar larva extracted from the cultures was cleaned in phosphate-buffered saline (PBS, pH 7.4). The larva was placed on the dissection platform (made from Sylgard 184 silicone elastomer) with dorsal surface facing up. The larva was stunned with cold PBS buffer and a minutien pin (0.15 mm) was placed between the posterior spiracles of the larva to pin it to the platform. Another pin was placed in the head of the larva near the mouth hook to stretch the animal out lengthwise. A small horizontal incision was made near the posterior pin on the dorsal side of the larva using a pair of fine micro-dissection scissors. The larva was cut open along the dorsal midline and its internal organs were removed. The larval body wall was then stretched with a pin placed to each corner of the body wall. The body wall was rinsed in PBS three times before fixation.

Body walls were fixed in Bouin's solution for 15 minites and then rinsed thoroughly with PBT (0.1% w/v Triton in PBS). Fixed body walls were stored in PBT at 4°C until ready for immunostaining.

2.2.2. Protein extraction and protein concentration assay

In order to prepare body wall lysates for western blotting, twelve 3rd instar larvae of each experimental genotype were dissected and then transferred into a pre-cooled Eppendorf tube containing 150µL NP-40 lysis buffer (150mM NaCl, 1.0% NP-40, 50mM pH8.0 Tris-Cl and protease inhibitor (1 tablet/ 50mL) in H_2O). Larval body walls were homogenized on ice for 2-3 minutes. Homogenized body wall samples were centrifuged for 10 minutes at 13,000 rpm at 4°C. The supernatant was collected and stored at -80°C for protein concentration assay.

A Bradford assay was used to determine the protein concentration of body wall lysates as described (http://labs.fhcrc.org/fero/Protocols/BioRad_Bradford.pdf). After the concentration of each protein lysate was determined, lysates were diluted in NP-40 lysis buffer, 5x protein loading buffer and 20x reducing agent to get samples with a target concentration (usually 100 µg proteins / 100 µL total solution). Samples can be further diluted accordingly. The diluted samples were stored at -20°C for western blotting.

2.3. Immunohistochemistry

2.3.1. Antibody preparation

Primary antibodies were diluted in blocking solution (1% w/v bovine serum albumin in PBT). Goat anti-HRP (1:100, Santa Cruz Biotechnology Inc.) was used to label the entire surface of presynaptic neurons by reacting with a neural-specific carbohydrate epitope (Jan and Jan, 1982). The mouse monoclonal 4F3 antibody (1:10, Developmental Studies Hybridoma Bank) was used to label the postsynaptic area by identifying Discs-large (Dlg). The mouse monoclonal nc82 antibody (1:200, Developmental Studies Hybridoma Bank) was used to label the presynaptic active zones by identifying Bruchpilot (Fouquet *et al*., 2009).The mouse monoclonal 1B1 antibody (1:5, DSHB) was used to label Hts (Wang *et al*., 2011). Rabbit anti-Draper (1:500) was a gift from Marc Freeman (Fuentes-Medel *et al*., 2009). Rabbit anti-GluRIIb (1:2500) was a gift from Dr. DiAntonio (DiAntonio *et al*., 1999). Rabbit anti-PAK (1:1000) was made by Dr. Nicholas Harden.

Secondary antibodies were all used at a dilution of 1:200. FITC anti-goat, CY3 anti-rabbit, CY5 anti-mouse and Dylight^{405} anti-mouse were from Jackson Immuno-Research Laboratories, Inc. FITC anti-mouse and Texas Red anti-rabbit were from Vector Laboratories.

2.3.2. Immunofluorescence staining

Body wall samples were washed with PBT 3 times for 10 minutes each, to wash off the yellow stain from the Bouin's solution. Body walls were then incubated in blocking solution (1% w/v bovine serum albumin in PBT) at room temperature for 1 hour. Body

walls were then incubated in primary antibody solution at 4°C overnight. After three 10-minute washes in PBT, body walls were incubated in secondary antibody solution in dark at room temperature for 2 hours. After another three 10-minute washes in PBT, body walls were left in Vectashield fluorescent mounting medium (Vector Laboratories, CA, USA) overnight at 4°C prior to mounting.

2.3.3. Mounting of the body wall samples onto the slides

Platform slides were made by gluing a pair of 22x22mm No.1 coverslips with nail polish onto each side of a sample slide, leaving a 13mm gap in between. One or two drops of the Vectashield were pipetted onto the central gap of a platform slide. Body walls were then transferred to and aligned in the gap area of each slide, ensuring that the inner side of the body wall was facing up. A 22x40mm No.1.5 coverslip was then slowly positioned to cover the central gap area. Nail polish was applied to each corner of the coverslip to secure its position. Slides were then stored in slide box at -20°C until ready to be imaged.

2.4. Immunostained sample imaging and data analysis

2.4.1. Confocal fluorescence microscopy

Immunostained body wall samples were imaged on a Nikon A1R laser scanning confocal microscope. Using Nikon NIS-Elements software, the NMJs at muscles 6/7 in abdominal segment 3 (A3 segment) were selected and imaged using the 40x oil-immersion objective. A 20x oil-immersion objective was used to image the whole area of muscle 6/7. A z-series stack of muscle 6/7 NMJ images of samples and controls were taken using identical exposure parameters. The spacing of successive z-images was set as 0.5 µm. Images were extracted from NIS-Elements software as maximum intensity projections of confocal stacks for analysis.

2.4.2. Quantitative analysis of NMJ phenotypes

To examine effects of Hts expression on morphology of the NMJs, NMJ samples were compared and analyzed in the following four aspects: 1) bouton number, 2) nerve

branch number, 3) area of individual NMJ standardized by the area of corresponding muscle 6/7.

Images taken by 40x objective were used to analyze bouton number and branch number of each NMJ with Nikon NIS-Elements software. Anti-HRP staining was used to define presynaptic domains (including both axons and nerve terminal boutons), anti-Bruchpilot (Brp) staining was used to label active zones on each bouton. The number of anti-Brp positive boutons (indicating functional boutons) of each NMJ was counted. The number of branching nerve terminals from the arbor was also counted in each individual NMJ.

Images taken with the 20x objective were used to measure the size of each NMJ area and its corresponding muscle 6/7. Analysis was conducted using Adobe Photoshop CS3. The area of each NMJ was selected using the "color range selection" function. The area of corresponding muscle 6/7 of each NMJ was selected manually using the "Lasso Tool". The sizes of selected areas can be determined using the "Analysis" function. Then a ratio was calculated between the size of each NMJ area and the size of its residing muscle 6/7 to standardize the data.

Sample mean of bouton number, branch number and standardized size of NMJ area were compared among different *hts* variants. Data were expressed as the mean ± the standard error of the mean (SEM). Student's t-test was applied to evaluate statistical significance.

2.4.3. Quantification of protein levels in immunohistochemistry

Images of each NMJs were processed and analyzed using Adobe Photoshop CS3 to determine the fluorescence intensity of the target protein staining. Images were firstly switched into "Grayscale' mode. Signal at the NMJ was selected using "Color Range" selection tool and the intensity was determined by measuring the mean gray value. Quantification of target protein levels at each NMJ was calculated as a ratio between the mean gray value of target protein signal and the mean gray value of HRP, which was used as a control to standardize the data. Data were expressed as the mean ± the standard error of the mean (SEM). Student's t-test was applied to evaluate statistical significance.

2.5. Western blotting analysis

To determine if Hts affects Draper expression level, larval body wall lysates made from three different *hts* genotypes including *mef2>wt* (Control), *mef2>hts*^{5881} (muscle specific *hts* gain of function) and mef2>htsRNAi (muscle specific *hts* knockdown) were immunoblotted with anti-Draper antibody.

Diluted protein lysates were boiled for 5 minutes and then loaded and separated on sodium dodecylsulphate-polyacrylamide gel electrophoresis (SDS-PAGE) gels (5% stacking gels and 8% separating gels). The electrophoresis was conducted at constant voltage of 100V for around 2 hours. After electrophoresis, separated proteins on the separating gel were transferred to a polyvinylidene difluoride (PVDF, Bedford, MA, USA) membrane for 1 hour at constant voltage of 15V. The membrane is then washed with TBS buffer (50mM Tris base, 150 mM NaCl, pH 7.4) three times, 10 minutes each, followed by incubation in blocking solution (5% BSA dissolved in TBST buffer) for 1 hour. After blocking, the membrane was incubated in primary antibody solution (3µL rabbit anti-Draper antibody diluted in 5mL 2.5% BSA solution) at 4°C overnight. The membrane was washed with TBST buffer (50mM Tris base, 150 mM NaCl, 0.1% Tween-20 (v/v), pH 7.4) twice, 10 minutes each, followed by two 10-minute incubations in 2.5% BSA solution for blocking. The membrane was incubated in secondary antibodies (2.5 µL HRP anti-rabbit antibody in 5mL 2.5% BSA solution) for 1 hour, followed by four 15-minute washes with TBST buffer.

The blots were developed by incubating in enhanced chemiluminescence reagent (ECL, Amersham, Piscataway, NJ, USA) for 1 minute. Films of different exposure time were developed with a Kodak developing machine. Signals were captured and analyzed using Image J software (http://rsb.info.nih.gov/ij/index.html). Band intensities on immunoblots were determined by performing densitometry as described (http: www.lukemiller.org/journal/2007/08/quantifying-western-blots-without.html). For quantification of Draper levels, mouse anti-β-actin (1:2000) (DHSB) was used as loading control. Results of normalized mean optical density (Draper/ β-actin) were expressed as mean ± SEM. Statistical comparison of Draper expression level among three genotypes was evaluated by independent t-test.

3. Results

3.1. Muscle specific knock-down of Hts in *Drosophila* causes neuromuscular defect

To examine the effects of muscle associated Hts on Drosophila neuromuscular function, male *UAS-htsRNAi* transgenic flies were crossed with virgin female *mef2-GAL4* driver flies to obtain progeny (referred to as *mef2>htsRNAi* in the text) with muscle-specific knock-down of Hts. The effectiveness of *hts* knock down in *mef2>htsRNAi* was previously examined in the Harden lab, the immunoreactivity of postsynaptic Hts is significant dimished at the 3rd instar larval muscle6/7 NMJ, whereas the presynaptic stainging of Hts retained (Simon Wang, unpublished data), indicating an effective postsynaptic *hts* knockdown. Wild type control flies were obtained by crossing male W^{1118} flies with virgin female *mef2-GAL4* driver flies. Parent flies were removed from the food vials 3 days after the crosses were made. Around 5 days after the crosses were made, both wild type control and *mef2>htsRNAi* 3rd instar larvae crawled out of the food base indicating that they are both larval viable. Around 2-3 days after, all viable larvae developed into pupal stage. Two weeks after the crosses were made, the majority of wild type control flies eclosed from the pupal shells and developed into mature adult flies. However, most *mef2>htsRNAi* flies failed to eclose and were trapped within the pupal shells (**Figure 3.1 A-B**). This observation suggests that muscle-specific knockdown of Hts in *Drosophila* causes neuromuscular defects so that the flies were too weak to break the pupa shells and eclose, and eventually starved to death.

To test the above hypothesis, late stage fly-filled pupas of each genotype (2 *wild type control* and 5 *mef2>htsRNAi*) were picked out from the food vials and ripped open at the anterior side. Flies within the shell were gently pulled out to examine whether the flies were alive and would move. Both *wild type control* flies were still alive and showed normal crawling and escape behavior. Of five pulled-out *mef2>htsRNAi* flies, three were found already dried out indicating that these flies had died previously. The other two flies

were still alive. However, these two flies showed severe neuromuscular defects characterized by their inability to crawl and lack of escape behavior. To further evaluate the neuromuscular defects in *mef2-htsRNAi* flies, all live flies were placed dorsal side down on a double-sided tape mounted to a slide. The movement and behavior of the flies were observed and video recorded using a dissecting microscope (**see appendix**). Compared to wild type control flies, mef2>htsRNAi flies showed dramatic decreased movement and escaping behavior. They were only able to partially move their legs with a substantial decrease in range of motion in a shivering pattern. A series of time-frame images captured every 5 seconds from videos of representative flies of each genotype are shown in **Figure 3.2 A-B**. These results support the hypothesis that muscle-specific knockdown of Hts can cause neuromuscular defects in *Drosophila*.

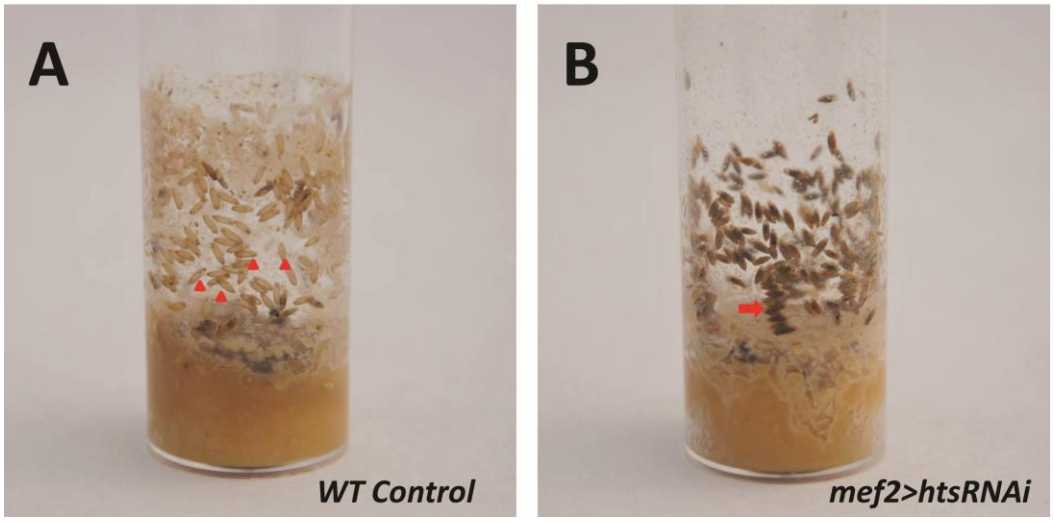

Figure 3.1 mef2>htsRNAi flies failed to eclose indicating potential neuromuscular defect caused by muscle-specific Hts knockdown.

Images of food vials of both wild type control and mef2>htsRNAi taken two weeks after the original cross date. **A)** shows food vial culture of wild type control. Arrow heads indicate empty pupal shells which were left in the vial after flies eclosed. **B)** shows food vial culture of mef2>htsRNAi. As indicated by the arrow, most flies were unable to eclose and were trapped in the pupal shells (dark shells). (Images taken by Simon Wang)

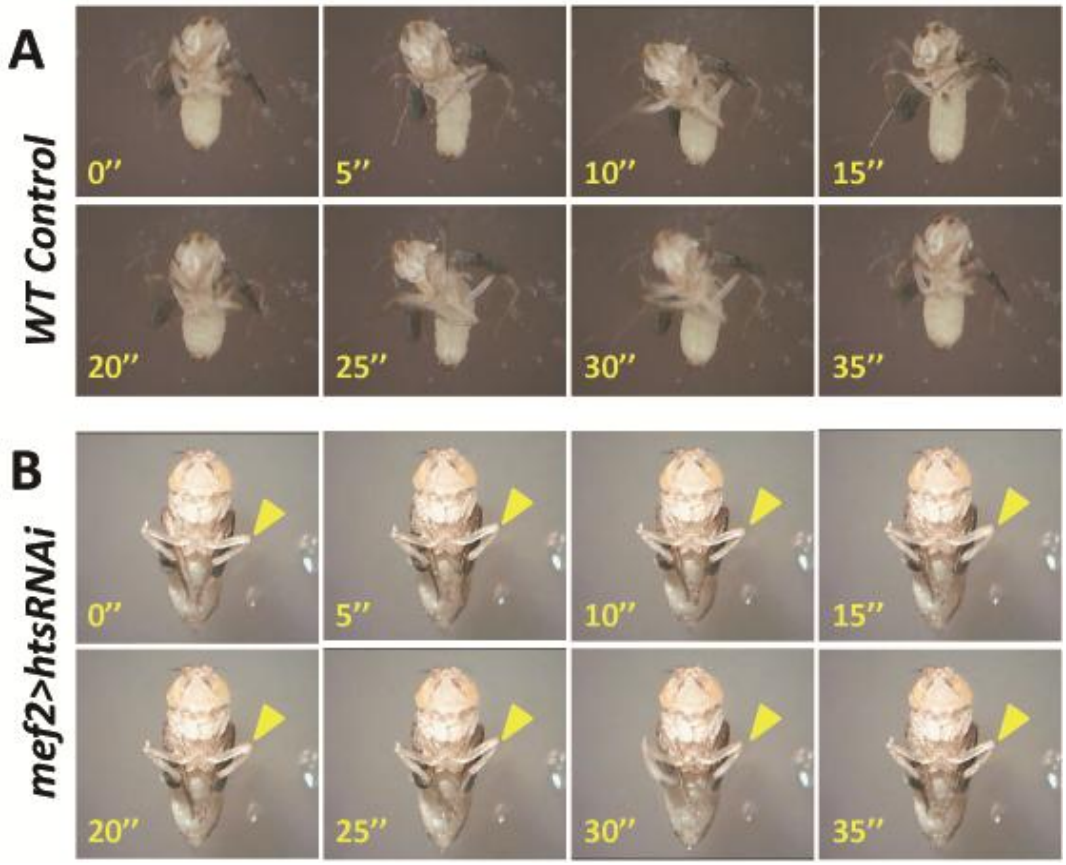

Figure 3.2 Flies with muscle-specific Hts knockdown have reduced movement and neuromuscular strength.

Series of images were captured in every 5 seconds from a video of wild type control fly **(A)** and a video of mef2-htsRNAi fly **(B)** that were released from the late stage pupae. **A)** The wild type control fly showed normal escape behavior and neuromuscular strength, characterized by a full range of motion of all of its legs, high frequency on moving its thorax and abdomen, and the strength to struggle and move its body for a short distance on the sticky tape surface. **B)** Compared to wild type control, the mef2>htsRNAi fly showed severe neuromuscular weakness, characterized by limited movement of its legs with dramatically decreased range of motion (indicated by the yellow arrow heads) and restrained ability to move its thorax and abdomen.

3.2. Muscle associated Hts regulates *Drosophila* larval NMJ development

The neuromuscular defect found in *mef2>htsRNAi* flies suggests that muscle associated Hts plays a role in Drosophila neuromuscular junction development. To evaluate the potential effects of muscle-associated Hts on NMJ development, wild type control larvae (*wt*), larvae with muscle specific *hts* knockdown (*mef2>htsRNAi*), and larvae with muscle specific *hts* gain of function (*mef2>hts*^{S705S}) were examined. Third instar larvae were dissected to access the NMJs for immunostaining. Anti-HRP antibodies were used to label overall presynaptic regions (Jan and Jan, 1982) and anti-Bruchpilot were used to label active zones which are the sites for neurotransmitter release within each synaptic terminal/bouton (Fouquet *et al*., 2009).

Immunostained images of NMJs at muscle 6/7 show obvious differences of morphology between wild type control, *mef2>htsRNAi* and *mef2>hts*^{S705S} larvae (**Figure 3.3 A-C**). Compared to wild type control larvae (**Figure 3.3 A-A'''**), *mef2>htsRNAi* larvae demonstrated an oversimplified NMJ morphology characterized by fewer boutons and less nerve branching into the muscle (**Figure 3.3 B-B'''**). However, *mef2>hts*^{S705S} larvae had overgrown NMJs characterized by more boutons and highly branched nerve terminals (**Figure 3.3 C-C'''**). Quantitative analysis of average bouton number per NMJ showed that compared to wild type control (57 ± 2.2 boutons; mean ± SEM, n=22), the mean bouton number of *mef2>htsRNAi* NMJs was significantly decreased (41 ± 2.0; mean ± SEM, n=23, $p<0.01$), and the mean bouton number of *mef2>hts*^{S705S} NMJs was significantly increased (65 ± 0.4; mean ± SEM, n=22, $p<0.05$) (**Figure 3.3D**). Quantitative analysis of average nerve branch number per NMJ showed that compared to wild type control (5.6 ± 0.23 branches; mean ± SEM, n=22), the mean nerve branch number per NMJ in *mef2>htsRNAi* larvae was significantly decreased (3.5 ± 0.28; mean ± SEM, n=23, $p<0.05$). Whereas the mean nerve branch number per NMJ in *mef2>hts*^{S705S} larvae was significantly increased (8.6 ± 0.06; mean ± SEM, n=22, $p<0.01$) (**Figure 3.3E**).

The effect of muscle-associated hts on NMJ development was further examined by conducting a quantitative analysis comparing the sizes of NMJ area. The NMJs were immunolabelled by anti-Hrp (neuronal marker) and anti-Draper (muscle marker)

antibodies. Images taken with lower magnification showed not only the NMJ staining, but also the whole area of muscle 6/7 that contains each individual NMJ (**Figure 3.4 A-C**). To standardize the data, a ratio was calculated between the area of each NMJ and its residing muscle 6/7 area (presented as a percentile). The calculated ratios can then be used to compare sizes of NMJs. This data (**Figure 3.4D**) shows that compared to sample mean of standardized NMJ area (each NMJ area / muscle 6/7 area, %) of wild type control (1.66% ± 0.07%; mean ± SEM, n=18), the mean of standardized NMJ area in *mef2>htsRNAi* larvae is decreased by ~10% (1.48% ± 0.05%; mean ± SEM, n=18, $p<0.05$), indicating an underdeveloped phenotype. However, the mean of standardized NMJ area in *mef2>hts*^{S705S} larvae is increased by ~20% (1.98% ± 0.09%; mean ± SEM, n=18, $p<0.01$), indicating an overgrown phenotype.

These results suggest that muscle-associated Hts regulates *Drosophila* larval NMJ development. Muscle-specific *hts* knockdown causes underdeveloped NMJs, whereas muscle-specific *hts* gain of function causes NMJ overdevelopment.

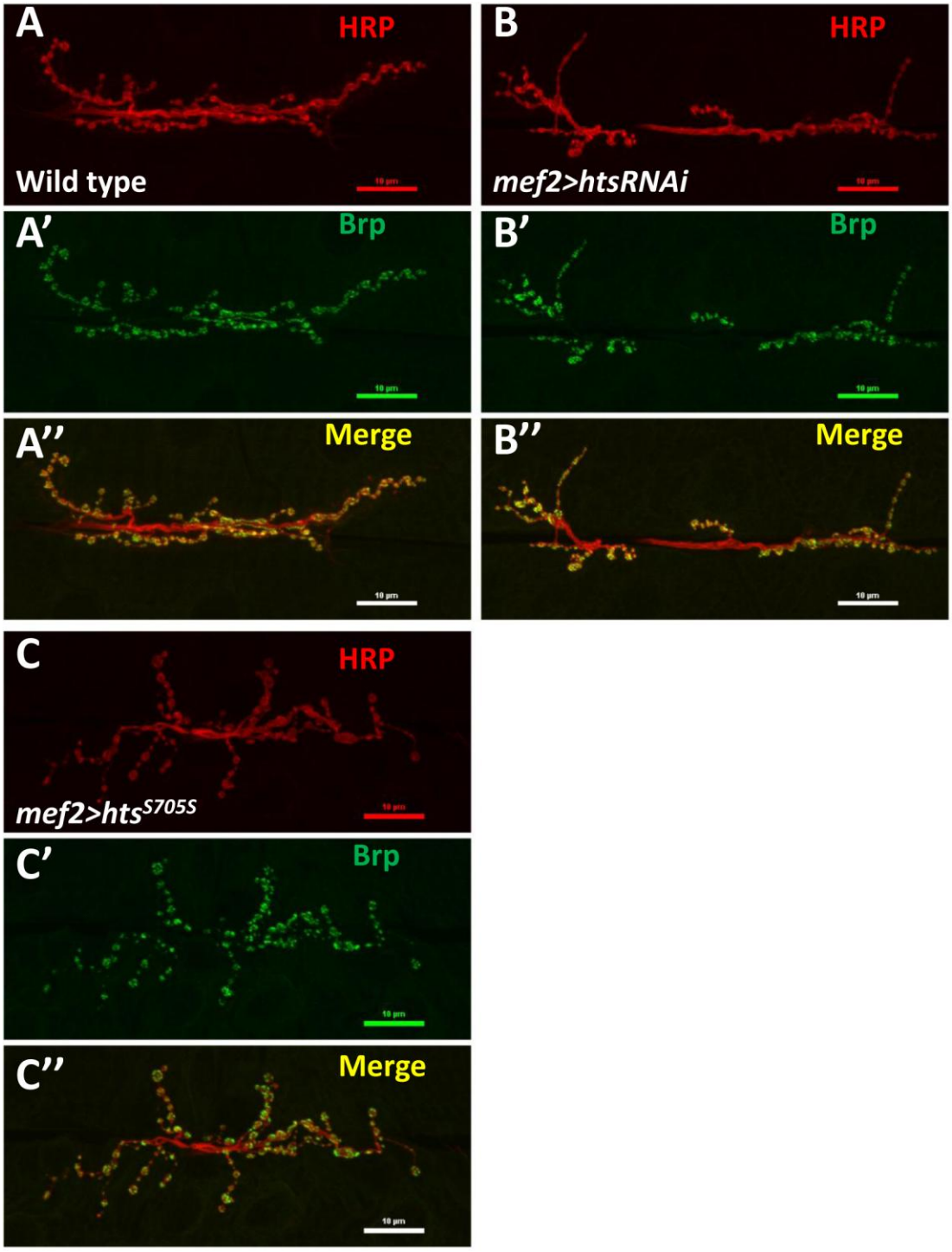
A
HRP
Wild type
B
HRP
mef2>htsRNAi
A'
Brp
B'
Brp
A''
Merge
B''
Merge
C
HRP
mef2>hts^S705S
C'
Brp
C''
Merge

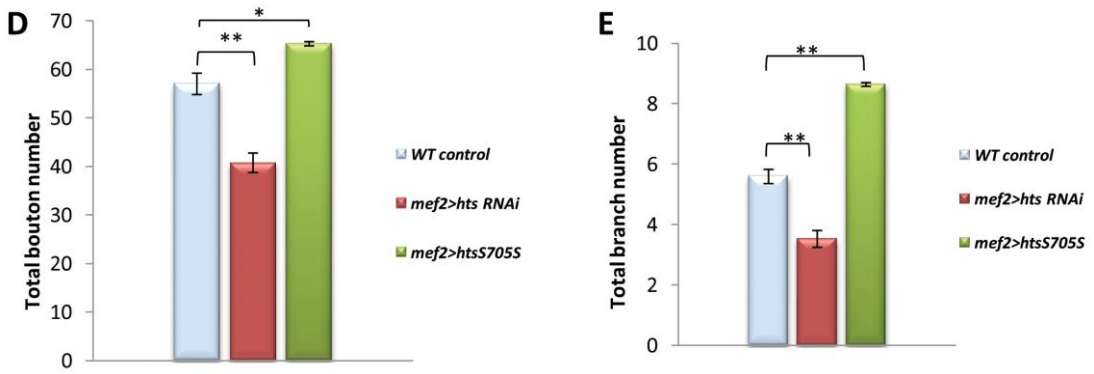

Figure 3.3 Effect of muscle-associated hts on Drosophila larval NMJ morphology

(A to C) Immunostaining of representative neuromuscular synapses on muscle 6/7 (segment A3) in third instar larvae stained with anti-Hrp and anti-Brp antibodies. All confocal images were taken using the 40x oil lens. Wild type NMJs are shown with immunolabelling against Hrp (A', red) and Brp (A'', green). (A) is the merged image of the above two color channels. (B to B'') Muscle-specific hts knockdown (*mef2>htsRNAi*) larvae show abnormal and oversimplified NMJ morphology, characterized by less synaptic boutons and less nerve branches. (C to C'') NMJs from muscle-specific *hts* overexpression (*mef2>hts*^{S705S}) show overgrown NMJ morphology showing more synaptic boutons and highly branched and over-extending nerve terminals. Scale bars, 10 µm (A-C''). (D and E) Quantification of nerve terminal growth of NMJs at muscle 6/7 showing total bouton number per NMJ (D) and total nerve branch number per NMJ (E). Each column (from left to right) represents wild type control (light blue, sample size n= 22), *mef2>htsRNAi* (red, sample size n=23) and *mef2>hts*^{S705S} (green, sample size n=22) respectively. Error bars represent SEM. Student t-test was used to examine statistical significance. One asterisk (*) indicates significant difference at $p<0.05$. Double asterisks indicate significant difference at $p<0.01$.

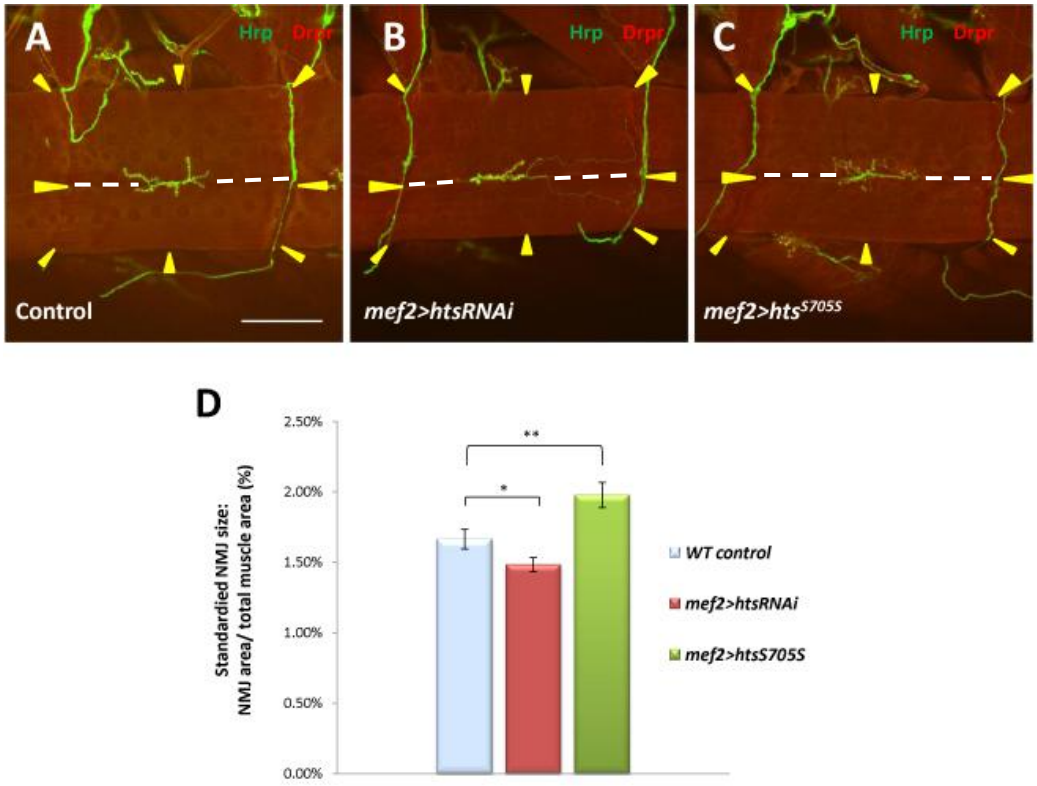

Figure 3.4 Muscle-associated hts affects the size of Drosophila larval NMJs.

(A to C) Immunostaining of muscle 6/7 NMJs and corresponding muscles. Anti-Hrp antibodies were used to label NMJ area (green). Anti-Draper (Drpr) was used to label muscle area (red). Scale bar: 100 µm. White discontinuous lines indicate the midline between muscle 6 and muscle 7. The muscle above the midline is muscle 6, the muscle below the midline is muscle 7. (D) Quantification of standardized NMJ size demonstrates that *mef2>htsRNAi* larvae (red bar) have smaller NMJs at muscle 6/7 than do wild type control (light blue bar), whereas *mef2>hts*^{S705S} larvae (green bar) have larger NMJs at muscle 6/7 compared to those in wild type (light blue bar). For each group, sample size is n=18 NMJs. Error bars represent SEM. Student t-test was used to examine statistical significance. One asterisk (*) indicates significant difference at $p<0.05$. Double asterisks (**) indicate significant difference at $p<0.01$.

3.3. Hts co-localizes with Draper at the post-synaptic region of *Drosophila* larval NMJ

To study the mechanism of how *hts* affects the Drosophila larval NMJ development, it is helpful to search for molecules that may interact with *hts* in the synaptic compartment. Here I examined the potential interaction between hts and Draper, a synaptic molecule that has been shown to regulate Drosophila larval NMJ development (Fuentes-Medel *et al*., 2009).

Immunostaining of Hts and Draper at muscle 6/7 NMJs showed that Hts immunoreactivity localized to each bouton evenly in donut-like pattern (**Figure 3.5A**, **Figure 3.5B'**). The immunoreactivity of Draper localized to each bouton in clusters making a discontinuous donut-like shape (**Figure 3.5B''**). The clusters of Draper immunostaining overlapped with Hts staining (**Figure 3.5B'''**) suggesting that Draper is co-localized with Hts at the synapse. The Draper immunoreactivity localized predominantly to the peripheral portion of each bouton, suggesting that Draper localization at NMJ was largely post-synaptic. This co-localization of Draper and Hts suggests that Hts may interact with Draper in the postsynaptic area.

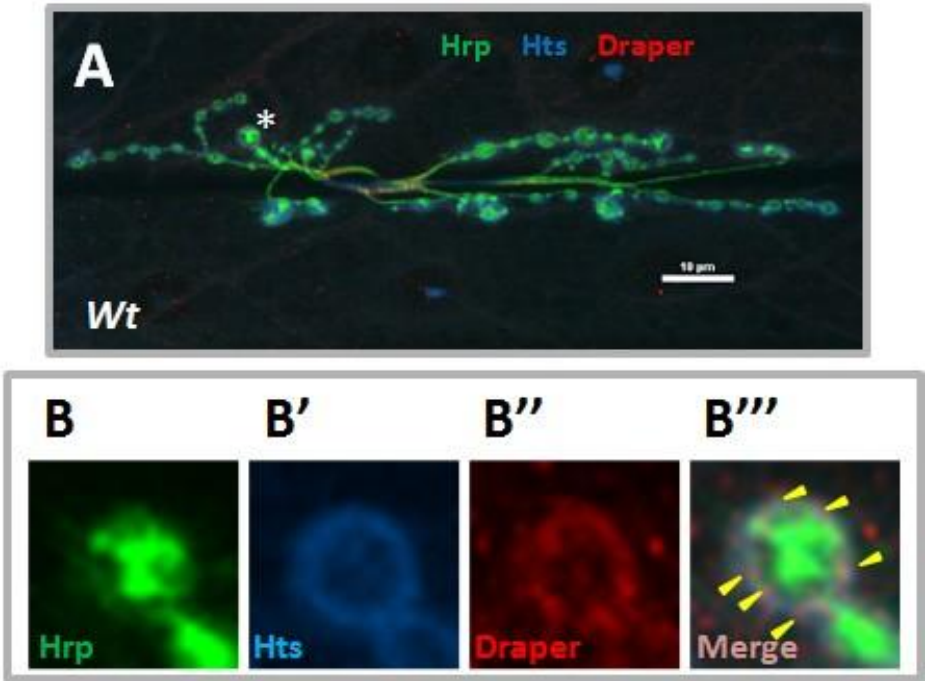

Figure 3.5 Draper co-localizes with Hts at postsynaptic NMJ.

Wild type larval body walls were co-stained with anti-Hrp, anti-Hts and anti-Draper antibodies. (A) is a representative immunostaining image of wild type larval NMJ at muscle 6/7. Scale bar: 10 µm. (B-B''') are higher power images of a bouton indicated by the asterisk in (A). (B) shows anti-Hrp staining (green channel). (B') shows the anti-Hts staining (blue channel). (B'') shows anti-Draper staining (Red channel). (B''') is the merged image of (B)-(B''), arrow heads indicates co-localization of Hts and Draper at postsynaptic NMJ area.

3.4. Muscle-associated Hts affects Draper localization at *Drosophila* larval NMJ

3.4.1. Effects of hts mutations on Draper immunoreactivity at Drosophila larval NMJ

To study the potential interactions between Hts and Draper (Drpr), Drpr immunoreactivity at NMJ was examined in wild type, hts^{01103} (null mutation of *hts*) and *mef2>*$hts^{GS13858}$ (muscle-specific overexpression of all endogenous Hts proteins) larvae. Body wall preparations were co-stained using anti-Hrp and anti-Draper antibodies. As shown in Figure 3.6, immunostaining images revealed that compared to wild type, hts^{01103} larvae have stronger immunoreactivity of Draper at the NMJ, whereas the immunoreactivity of Draper in *mef2>*$hts^{GS13858}$ larvae is de-localized from the NMJ (**Figure 3.6 A-C''**).

Quantification of the relative fluorescence intensity of Draper immunoreactivity was conducted using Adobe Photoshop CS3 software. Fluorescence intensities of both Draper and Hrp immunoreactivity (using Hrp as the control) were captured and measured. A ratio (relative fluorescence intensity of Draper) was then calculated at each NMJ between Draper fluorescence intensity and Hrp fluorescence intensity. The results show that there is about a 25% increase of relative fluorescence intensity of Draper at the NMJ in hts^{01103} (0.52 ± 0.02; mean ± SEM, n=23, $p<0.01$) compared to wild-type (0.40 ± 0.01; mean ± SEM, n=23) (**Figure 3.6D**). Because the distribution of Draper immunoreactivity at NMJ is severely delocalized and weak in *mef2>*$hts^{GS13858}$ larvae, the NMJ area cannot be accurately selected by Adobe Photoshop CS3 software (**Figure 3.6C'**) and the relative fluorescence intensity of Draper cannot be calculated.

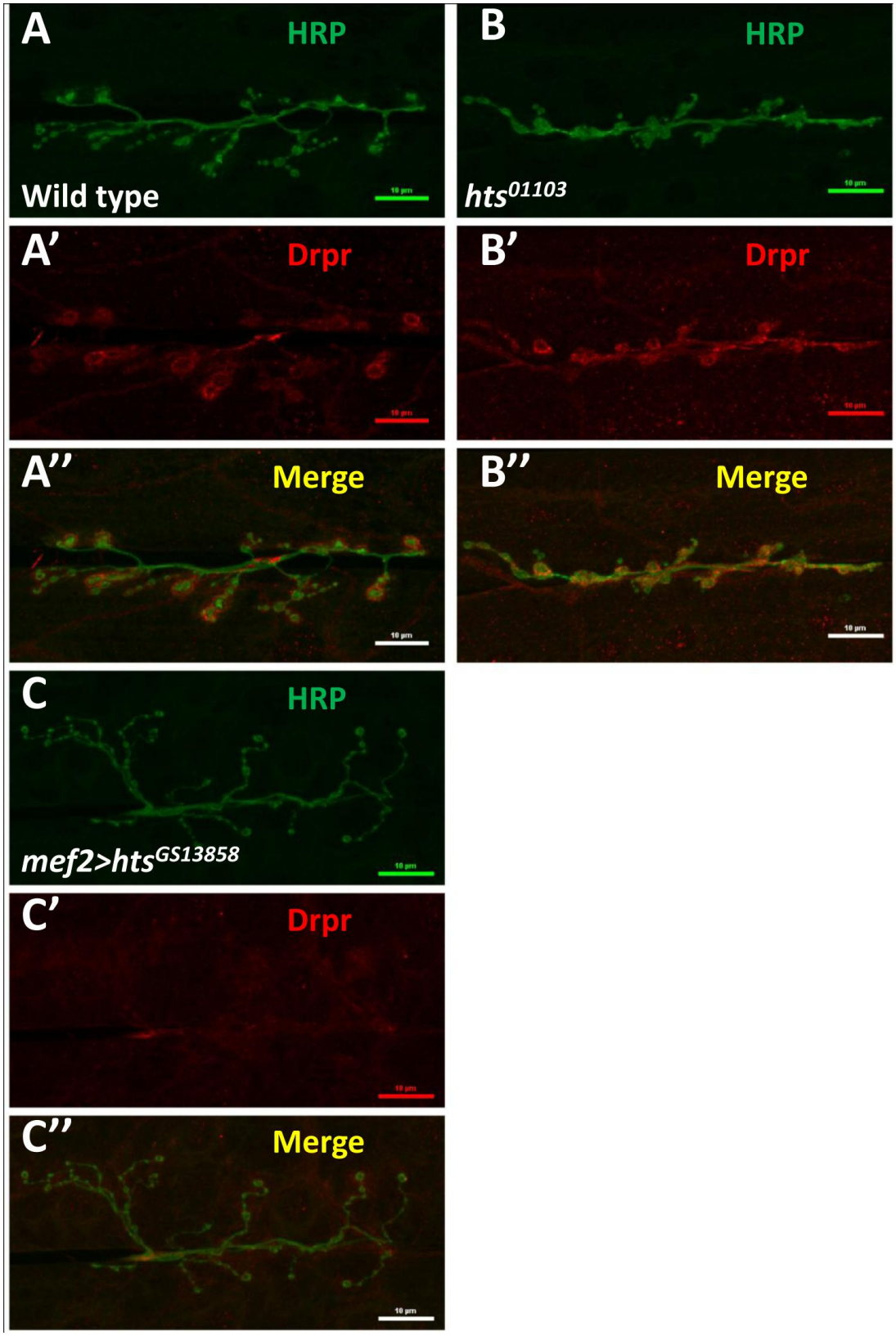
A
HRP
Wild type
B
HRP
hts01103
A'
Drpr
B'
Drpr
A''
Merge
B''
Merge
C
HRP
mef2>htsGS13858
C'
Drpr
C''
Merge

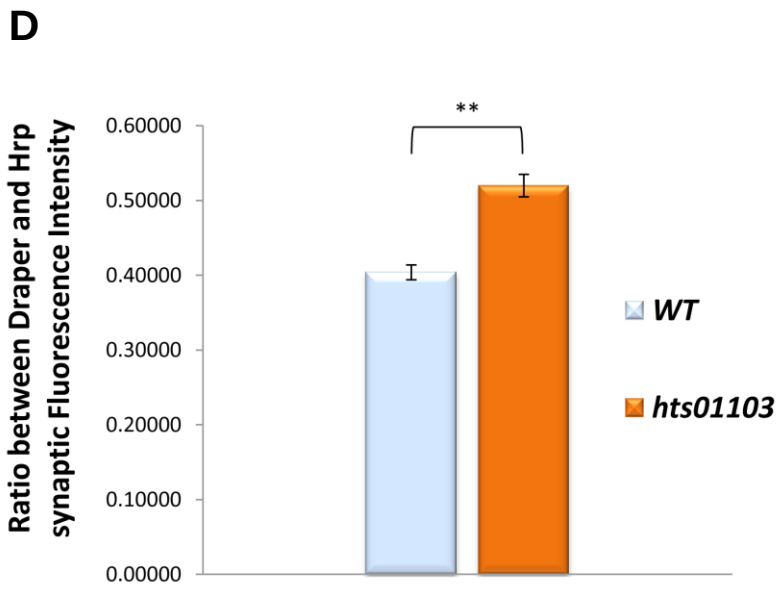

Figure 3.6 Hts regulates the localization of Draper at Drosophila larval NMJ.

Representative immunostainings of NMJs (muscle 6/7, A3 segment) in wild type (A to A''), *hts* null mutation hts^{01103} (B to B'') and muscle-specific endogenous *hts* overexpression ($mef2>hts^{GS13858}$) larvae (C to C''). Anti-Hrp staining is shown in green channel (A', B', C'), and anti-Draper staining is shown in red channel (A'', B'', C''). Scale bar: 10 µm. *hts* null mutant (hts^{01103}) larvae show tighter localization of Draper staining at NMJ (B'') compared to wild type (A''). $mef2>hts^{GS13858}$ larvae show severe loss of Draper immunoreactivity at the NMJ (C''). (D) Quantification of the ratio between Draper and Hrp synaptic fluorescence intensity (relative fluorescence intensity of Draper) shows that *hts* null mutation hts^{01103} (orange bar) have about 25% stronger relative fluorescence intensity of Draper compare to in wild type (light blue bar). For both wild type and hts^{01103}, sample size is n=23 NMJs. Double asterisks (**) indicate significant difference at $p<0.01$.

3.4.2. Muscle-associated Hts regulates Draper localization at Drosophila larval NMJ

In the previous data, a 'tighter' distribution of Draper immunoreactivity was observed at NMJs in *hts*^{01103} null mutant larvae where both presynaptic neuronal Hts and postsynaptic muscular Hts are knocked off. To determine whether this 'tighter' Draper localization at the NMJ is caused by a pre- or postsynaptic loss of Hts, I used *mef2>htsRNAi* to examine the effects of muscle-specific knockdown of Hts on the localization of Draper at the NMJ. Double labeling was performed using anti-Hrp and anti-Draper antibodies. Compared to wild type, mef2>htsRNAi is observed to have stronger Draper immunoreactivity at the NMJ (**Figure 3.7A to 3.7B'''**). Quantitative analysis of fluorescence intensity of the Draper signal supports the above observation by showing that compared to wild type (0.50 ± 0.01; mean ± SEM, n=20), there is a 20% increase of Draper relative fluorescence intensity in mef2>htsRNAi NMJs (0.60 ± 0.01; mean ± SEM, n=24, p<0.01) (**Figure 3.7C**). These results indicate that muscle-specific knockdown of Hts cause tighter localization of Draper at NMJ. The increased level of Draper relative fluorescence intensity in muscle-specific *hts* knock-down larvae (20%) is very close to the increased level in *hts* null mutation (~25%), suggesting that muscle-associated Hts is an important regulator of Draper localization at NMJ, not presynaptic Hts.

In the same experiment, I also observed that Draper delocalized from the NMJ in *mef2>hts*^{GS13858} larvae where endogenous Hts proteins were overexpressed in the muscle. However, the specific isoform(s) of Hts proteins that is/are actually causing the delocalization of Draper is unknown. Given that Add1 is the main isoform of Hts protein during Drosophila synapse development (Pielage *et al*., 2011), and as Add1 is speculated to be one of the predominant isoforms of Hts at the post-synaptic muscle region (Wang *et al*, 2011; Petrella *et al*., 2007), it was intriguing to examine the effect of muscle-specific overexpression of Add1 on the distribution of Draper immunoreactivity at the NMJ. I then crossed the muscle driver *mef2-GAL4* flies with *UAS-hts*^{S705S} (Add1 transgene) to obtain larvae with muscle-specific overexpression of Add1. Double immunostaining of anti-Hrp and anti-Draper shows that compared to the 'tight' localization of Draper at the NMJ of wild type (**Figure 3.8A', 3.8A'''**), the immunostaining of Draper in *mef2>hts*^{S705S} delocalized from the NMJ and gave a 'fuzzy' appearance

(**Figure 3.8B', 3.8B'''**). Quantification of relative fluorescence intensity of Draper supports the above observation by showing that compared to in wild type (0.52 ± 0.01; mean ± SEM, n=21), the relative fluorescence intensity of Draper at NMJ is decreased in *mef2>hts*^{S705S} larvae (0.46 ± 0.01; mean ± SEM, $p<0.01$, n=22). This indicates that overexpression of Add1, a predominant isoform of Hts proteins in the muscle, can delocalize Draper from the postsynaptic region.

All the above results suggest that muscle-associated Hts plays a role in regulating the localization of Draper protein at the postsynaptic NMJ. Loss of Hts in muscle causes tighter localization of Draper at the NMJ, whereas up-regulation of Hts in muscle causes delocalization of Draper from the NMJ.

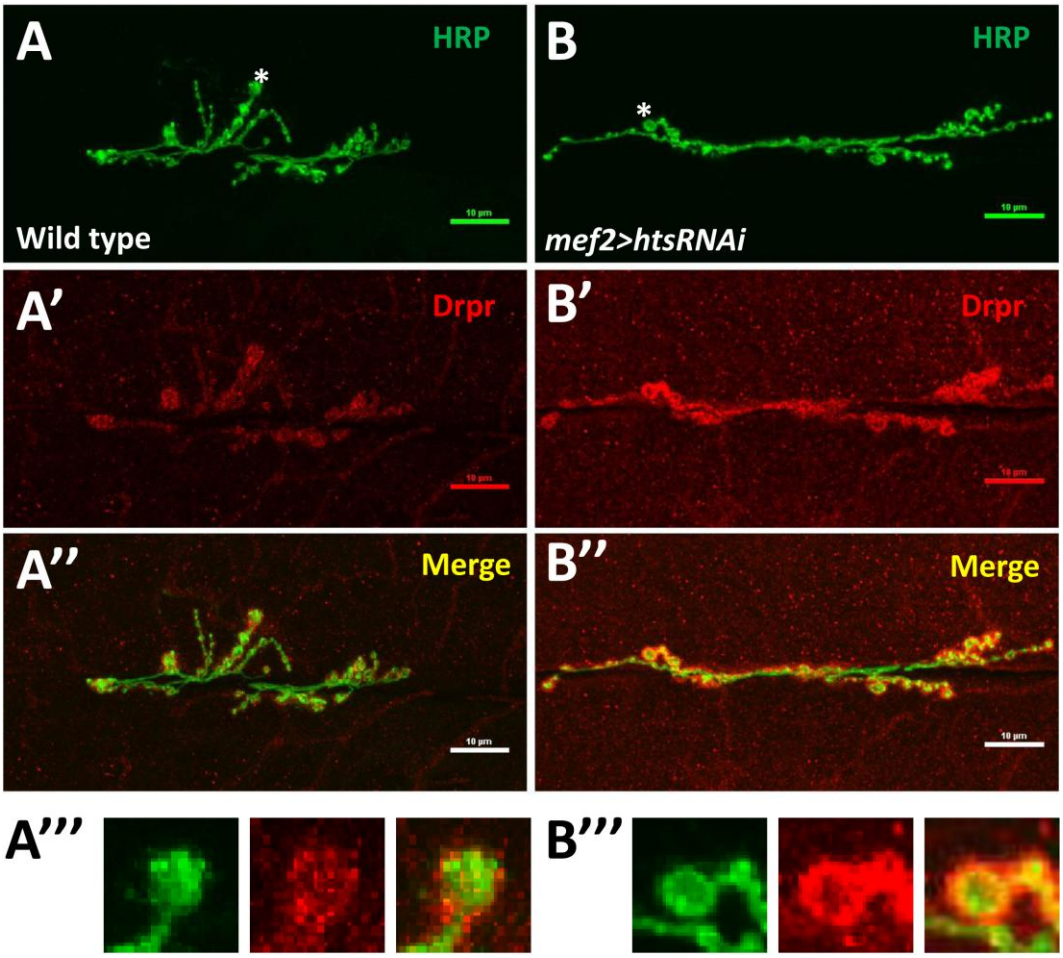
A
HRP
Wild type
B
HRP
mef2>htsRNAi
A'
Drpr
B'
Drpr
A''
Merge
B''
Merge
A'''
B'''

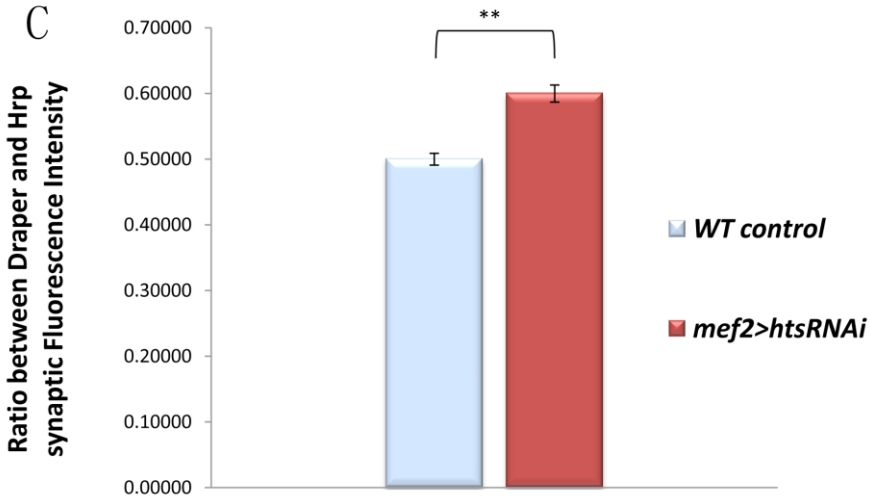
C
Ratio between Draper and Hrp synaptic Fluorescence Intensity
0.70000
0.60000
0.50000
0.40000
0.30000
0.20000
0.10000
0.00000
**
WT control
mef2>htsRNAi

Figure 3.7 Muscle-specific knockdown of Hts causes tighter localization of Draper at the NMJ

Representative immunostainings of NMJs (muscle 6/7, A3 segment) in wild type (A to A'') and muscle-specific *hts* knockdown (*mef2>htsRNAi*) larvae (B to B''). Anti-Hrp staining is shown in green channel (A, B), and anti-Draper (Drpr) staining is shown in red channel (A', B'). Merged images of the two channels are (A'', B''). Scale bar: 10 µm. (A''' and B''') are higher power images of the boutons indicated by the asterisks in (A) and (B). Muscle-specific *hts* knockdown (*mef2>htsRNAi*) show tighter localization of Draper staining at NMJ (B', B''') compared to wild type (A', A'''). (C) Quantification of the ratio between Draper and Hrp synaptic fluorescence intensity (relative fluorescence intensity of Draper) shows that muscle-specific *hts* knockdown (*mef2>htsRNAi)* larvae (red bar) have 20% stronger relative fluorescence intensity of Draper at the NMJ compared to in wild type (light blue bar). Sample size of wild type is n=20 NMJs. Sample size of *mef2>htsRNAi* is n=24 NMJs. Double asterisks (**) indicate significant difference at $p<0.01$.

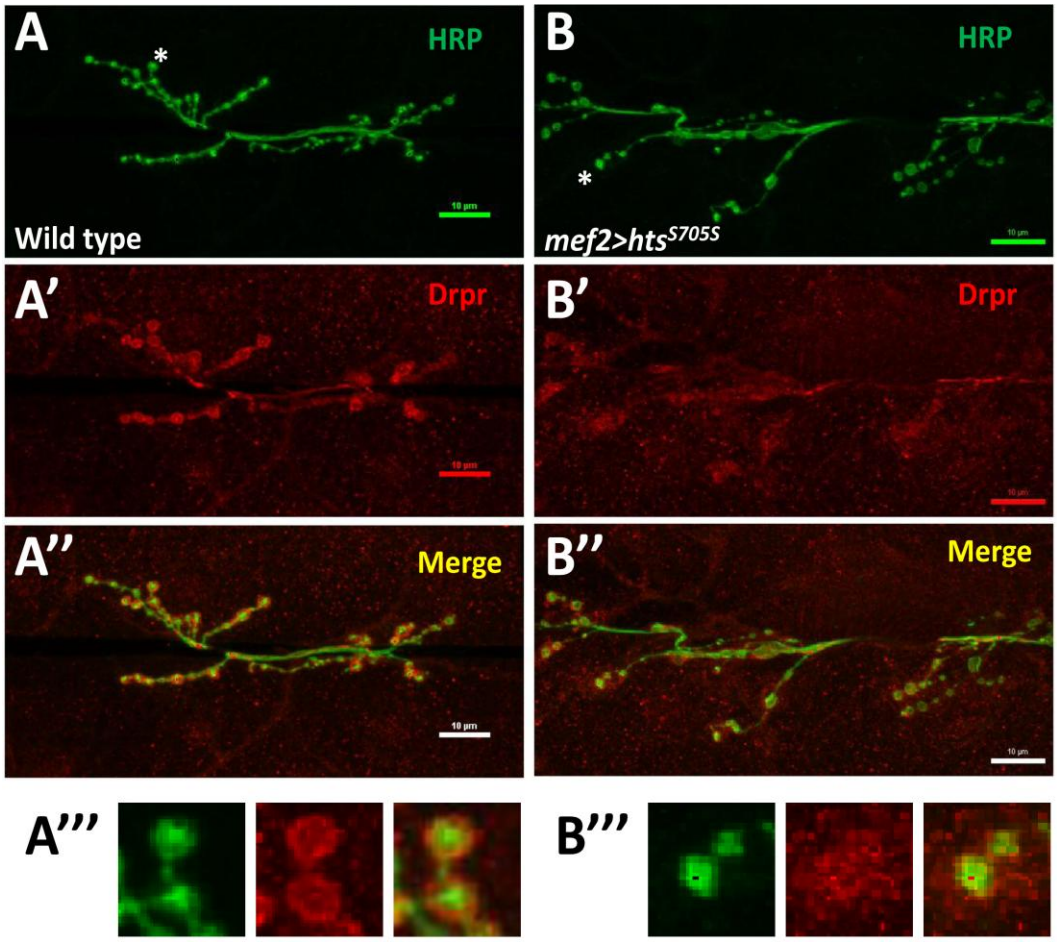
A
HRP
Wild type
B
HRP
mef2>hts^S705S
A'
Drpr
B'
Drpr
A''
Merge
B''
Merge
A'''
B'''

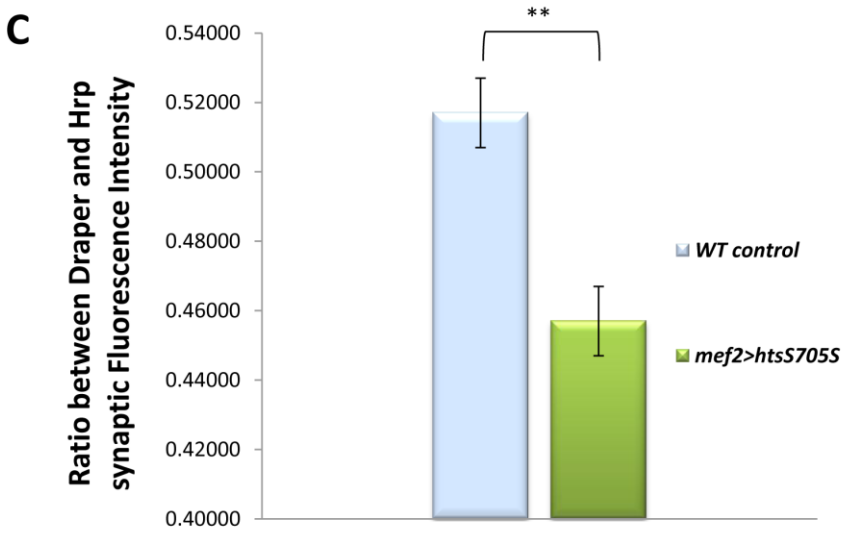
C
Ratio between Draper and Hrp synaptic Fluorescence Intensity
0.54000
0.52000
0.50000
0.48000
0.46000
0.44000
0.42000
0.40000
**
WT control
mef2>htsS705S

Figure 3.8 Muscle-specific overexpression of Add1 causes delocalization of Draper from postsynaptic NMJ

Representative immunostaining of NMJs (muscle 6/7, A3 segment) in wild type (A to A'') and with muscle-specific overexpression of Add1 (*mef2>hts*^{S705S}) larvae (B to B''). Anti-Hrp staining is shown in green channel (A, B), and anti-Draper staining is shown in red channel (A', B'). Merged images of the two channels are (A'', B''). Scale bar: 10 µm. (A''') and (B''') are higher power images of the boutons indicated by the asterisks in (A) and (B). Compared to the tight localization of Draper at NMJ in wild type (A', A'''), the immunostaining of Draper in *mef2>hts*^{S705S} delocalizes from the NMJ and gives a fuzzy appearance (B', B'''). (C) Quantification of the ratio between Draper and Hrp synaptic fluorescence intensity (relative fluorescence intensity of Draper) shows that compared to in wild type (light blue bar), the relative fluorescence intensity of Draper at NMJ in *mef2>hts*^{S705S} larvae (green bar) is significantly decreased, which indicates that Draper is delocalized from NMJ. Sample size of wild type is n=21 NMJs. Sample size of *mef2> hts*^{S705S} is n=22 NMJs. Double asterisks (**) indicate significant difference at $p<0.01$.

3.4.3. The delocalization of Draper seen in muscle-associated Hts gain of function larvae is not caused by a general muscle defect

It is possible that muscle-specific *hts* overexpression could interfere with muscle development. This possible developmental defect of muscle could affect the proper targeting of all the postsynaptic proteins to the NMJ. If this is true, the delocalization of Draper seen in muscle-associated *hts* gain of function animals might not be caused by specific Hts-Draper interactions.

To evaluate this possibility, the distributions of immuno-reactivity of two postsynaptic proteins, Pak and Glutamate receptor IIb (GluR-IIb), were investigated in *mef2>hts*^{S705S} larvae. The results show that both the immunoreactivity of Pak (**Figure 3.9 B'**, **3.9B'''**) and GluR-IIb (**Figure 3.10B', 3.10B'''**) are 'tightly' localized to the postsynaptic area in *mef2>hts*^{S705S} larvae. The relative fluorescence intensity of Pak at NMJ is even slightly stronger in *mef2>hts*^{S705S} larvae (0.54 ± 0.03; mean ± SEM, n=8, $p<0.05$) than in wild type larvae (0.48 ± 0.01; mean ± SEM, n=8) (**Figure 3.9C**). The relative fluorescence intensity of GluR-IIb at NMJ is decreased in *mef2>hts*^{S705S} larvae (0.44 ± 0.01; mean ± SEM, n=8, $p<0.01$) compared to wild type larvae (0.58 ± 0.03, mean ± SEM, n=8) (**Figure 3.10C**). However the immunostaining of GluR-IIb is still tight and sharp at the NMJ. The 'fuzzy' staining pattern of Draper was not observed in GluR-IIb staining.

The above data indicate that other postsynaptic proteins were properly targeted to the NMJ area. Therefore the delocalization of Draper seen in larvae with muscle associated *hts* overexpression is likely not be caused by a general developmental defect of muscle.

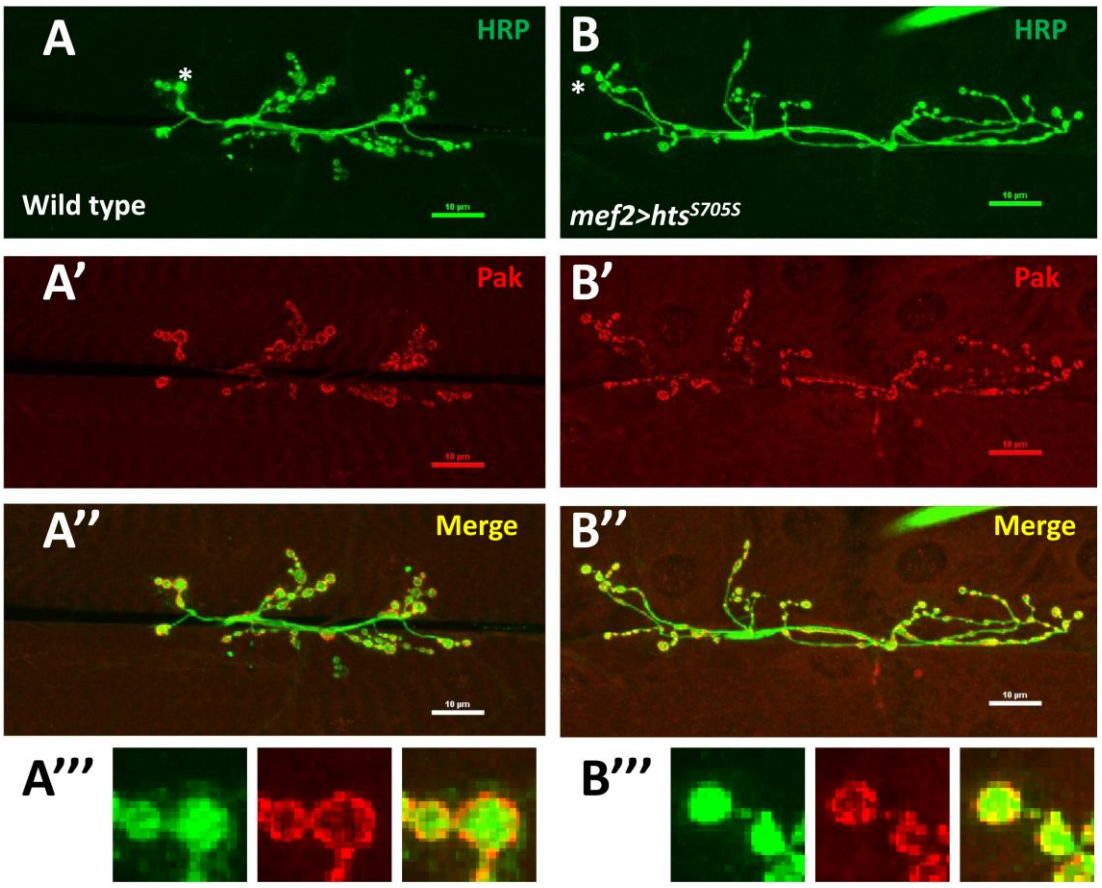
A
HRP
Wild type
B
HRP
mef2>hts^S705S
A'
Pak
B'
Pak
A''
Merge
B''
Merge
A'''
B'''

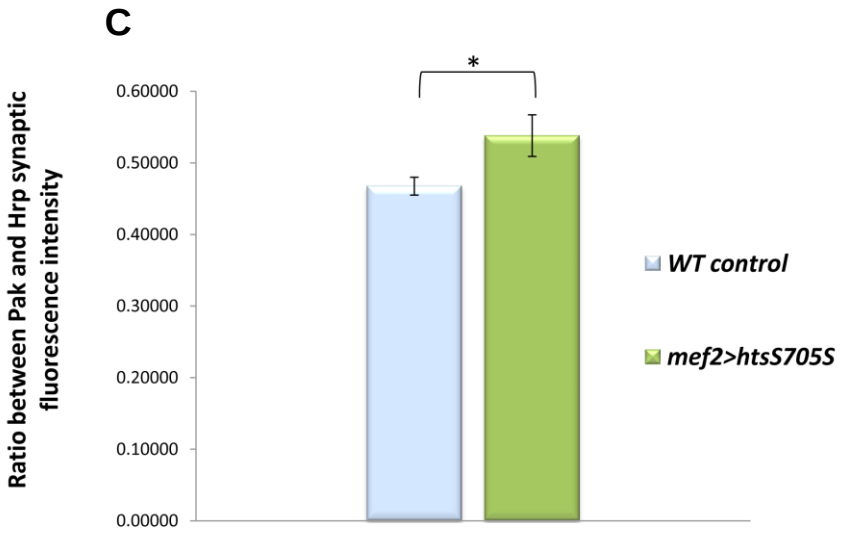
C
Ratio between Pak and Hrp synaptic fluorescence intensity
0.60000
0.50000
0.40000
0.30000
0.20000
0.10000
0.00000
*
WT control
mef2>htsS705S

Figure 3.9 Anti-Pak immunostaining is tightly localized to the postsynaptic NMJ area in muscle-specific hts gain of function larvae.

Representative immunostainings of NMJs (muscle 6/7, A3 segment) in wild type (A to A'') and with muscle-specific *hts* gain of function (*mef2>hts*^{S705S}) larvae (B to B''). Anti-Hrp staining is shown in the green channel (A, B), and anti-Pak staining is shown in the red channel (A', B'). Merged images of the two channels are (A'', B''). Scale bar: 10 µm. (A''') and (B''') are higher power images of the boutons indicated by the asterisks in (A) and (B). The immunoreactivity of Pak is tightly localized to postysynaptic NMJ in both wild type (A', A''') and *mef2>hts*^{S705S} larvae (B', B'''). (C) Quantification of the ratio between Pak and Hrp synaptic fluorescence intensity (relative fluorescence intensity of Pak) shows that compared to in wild type (light blue bar), the relative fluorescence intensity of Pak at NMJ is increased in *mef2>hts*^{S705S} larvae. For both wild type and *mef2>hts*^{S705S} larvae, sample size is n=8 NMJs. One asterisk (*) indicates significant difference at $p<0.05$.

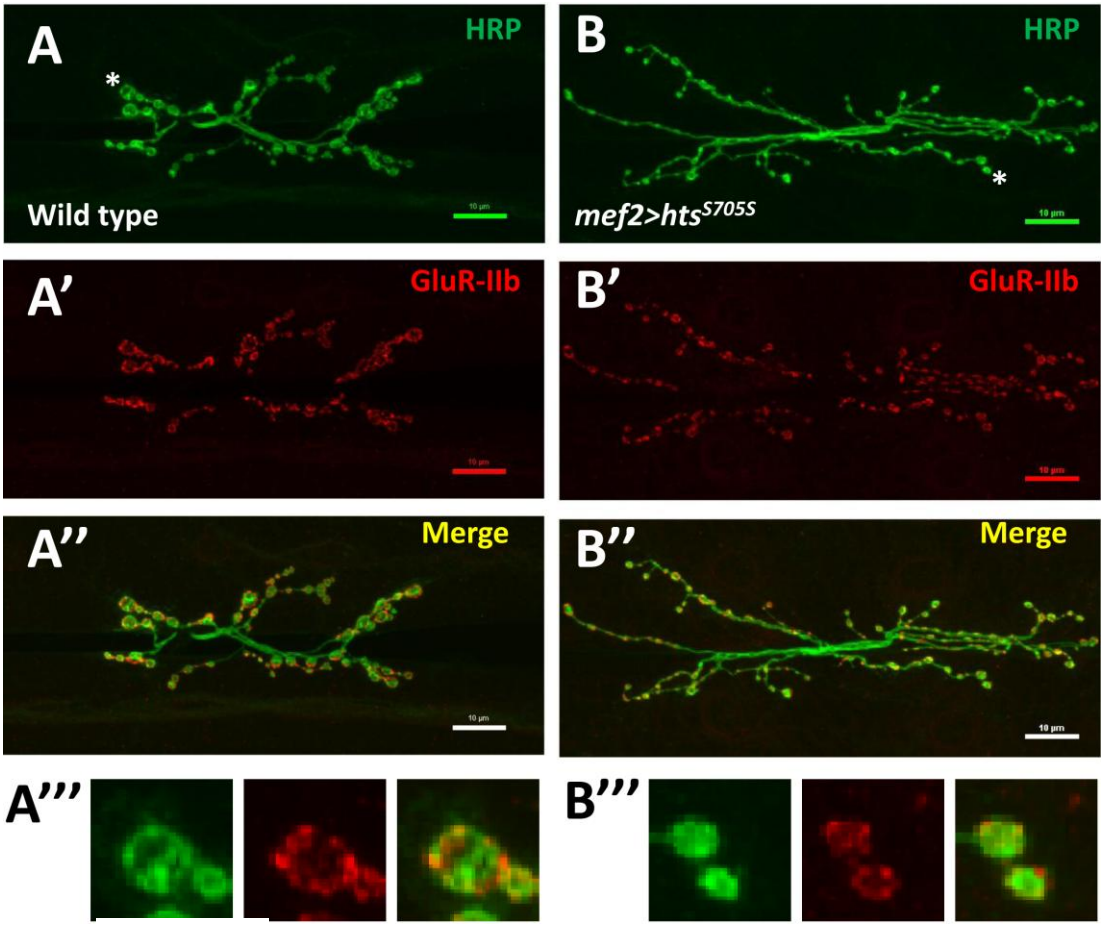
A
HRP
Wild type
B
HRP
mef2>hts^S705S
A'
GluR-IIb
B'
GluR-IIb
A''
Merge
B''
Merge
A'''
B'''
C
Ratio between GluR-IIb and H
synaptic fluorescence intensi
0.70000
0.60000
0.50000
0.40000
0.30000
0.20000
0.10000
0.00000
**
WT control
mef2>htsS705S

Figure 3.10 Anti-GluR-IIb immunostaining is tightly localized to the postsynaptic area in muscle-specific hts gain of function larvae.

Representative immunostainings of NMJs (muscle 6/7, A3 segment) in wild type (A to A'') and with muscle-specific *hts* gain of function (*mef2>hts*^{S705S}) larvae (B to B''). Anti-Hrp staining is shown in the green channel (A, B), and anti-GluR-IIb staining is shown in the red channel (A', B'). Merged images of the two channels are (A'', B'').Scale bar: 10 µm. (A''') and (B''') are higher power images of the boutons indicated by the asterisks in (A) and (B).The immunoreactivity of GluR-IIb is tightly localized to postysynaptic NMJ in both wild type (A', A''') and *mef2>hts*^{S705S} larvae (B', B'''). (C) Quantification of the ratio between GluR-IIb and Hrp synaptic fluorescence intensity (relative fluorescence intensity of GluR-IIb) shows that compared to in wild type (light blue bar), the relative fluorescence intensity of GluR-IIb at NMJ is decreased in *mef2>hts*^{S705S} larvae. For both wild type and *mef2>hts*^{S705S} larvae, sample size is n=8 NMJs. Double asterisks (**) indicate significant difference at $p<0.01$.

3.5. Muscle-associated Hts does not affect the protein level of Draper in larval body walls

3.5.1. Identifying the positions of Draper protein bands in Western blotting

In order to study whether manipulations of muscle-associated Hts affect the protein level of Draper in larval body walls using Western blotting, it is helpful to firstly identify the band positions of corresponding Drpr proteins. There are three isoforms of Draper proteins (Drpr-I, II, III) in Drosophila, having different structures and molecular weights (Fuentes-Medel *et al*., 2009). To identify their band positions, Western blotting of larval body wall lysates of wild type control larvae and three transgenic larvae (*mef2>drpr-I, mef2>drpr-II, mef2>drpr-III*) can be performed using the anti-Draper antibody (detecting all three Draper isoforms). Because the cDNA of each Draper isoform is specifically overexpressed in the muscle of corresponding transgenic larvae, we should be able to identify the band position of each isoform by picking out the band with a significant increase of signal intensity in each *drpr* transgenic sample.

In this experiment, the protein concentration of loading samples needed to be diluted to 10 µg/100 µL to obtain a clean blotting result. When the protein concentration of loading samples was so diluted, the signal of endogenous Draper proteins was below the level of detection in the blots. This explains why no blotting signal was detected in wild type body wall lysates (**Figure 3.11**). However, the signal of overexpressed Draper isoforms is detectable in the samples of *drpr* transgenes. As shown in **Figure 3.11**, the blots demonstrated a protein band of Draper-I (~130KD), a band of Draper-II and a band of Draper-III (both ~70KD) specifically in each corresponding sample of *drpr* transgenes. The positions of these bands are consistent with a previous observation of Western blotting for Draper in *Drosophila* salivary glands (McPhee *et al*., 2010).

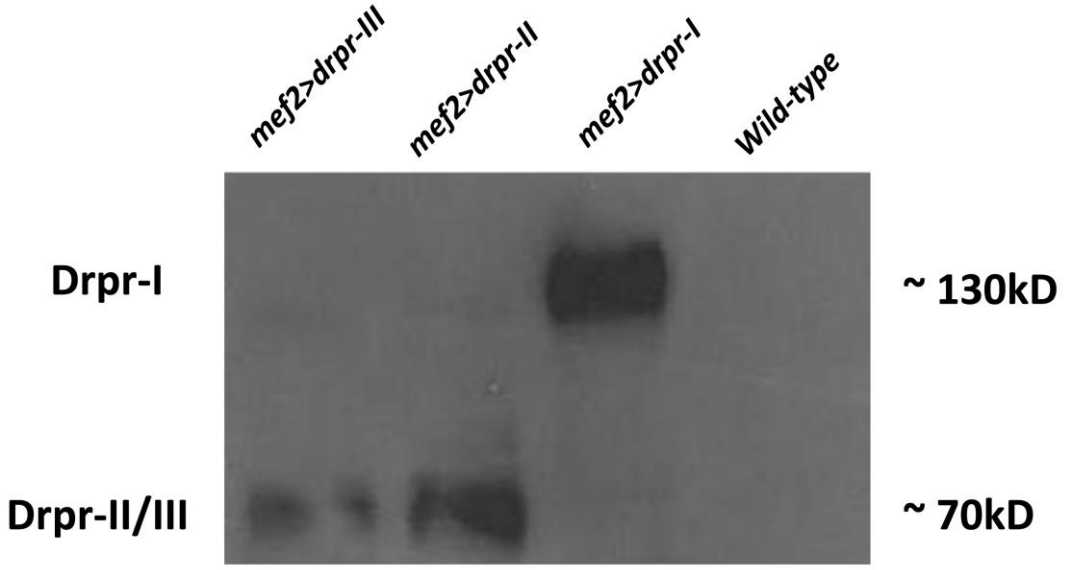

Figure 3.11 Western blotting of Draper identified the band position of every isoform of Draper proteins

Sample lysates loaded into the gels are (from right to left): wild-type, *mef2>drpr-I* (where *drpr-I* is specifically overexpressed in muscle), *mef2>drpr-II* (where *drpr-II* is specifically overexpressed in muscle) and *mef2>drpr-III* (where *drpr-III* is specifically overexpressed in muscle). The anti-Draper antibodies used in this blotting detects all three isoforms of Draper proteins. There is no band signal detected in wild-type, because the sample lysates was too diluted to give detectable signal of endogenous Draper bands. The band of Draper-I is detected (at the molecular weight of about 130kD) in *mef2>drpr-I* sample lysates. The band of Draper-II is detected (at the molecular weight of around 70kD) in *mef2>drpr-II*. The band of Draper-III appears at a similar position to the Draper-II band in *mef2>drpr-III*.

3.5.2. *Protein levels of Draper proteins in larval body wall lysates are not affected by muscle-associated Hts variation*

Western blotting of Draper was performed to compare Draper protein level in wild-type control (*mef2>w*^{1118}), muscle-associated *hts* knock-down (*mef2>htsRNAi*) and muscle-specific *hts* gain of function (*mef2>hts*^{S705S}) larval body wall lysates. The body wall lysates of *drpr*$^{\Delta 5}$, a *drpr* null mutation, was also used as a negative control. β-actin was also blotted using a mouse monoclonal antibody (JLA20, DHSB) to serve as a loading control.

A previous study has shown that only *drpr-I* and *drpr-III* are expressed in *Drosophila* larval body wall tissues, whereas *drpr-II* is not expressed (Fuentes-Medel *et al*., 2009). Thus the band signals appearing at ~70kD in this blotting should correspond to Draper-III only. As shown in **Figure 3.12**, Western blotting of Draper did not reveal significant difference in either Draper-I or Draper-III protein level among wild type control, *mef2>htsRNAi* and *mef2>hts*^{S705S} larval body wall lysates. Quantification of normalized relative band densities of Draper-I showed no significant difference among the samples evaluated (wild-type control: 1.000 ± 0.000; *mef2>htsRNAi*: 0.997 ± 0.110, p=0.9482; *mef2>hts*^{S705S}: 1.023 ± 0.149, p=0.7140; mean ± SEM, n=6). Quantification of normalized relative band intensities of Draper-III did not reveal significant difference among *hts* variants either (wild-type control: 1.000 ± 0.000; *mef2>htsRNAi*: 1.021± 0.090, p=0.8202; *mef2>hts*^{S705S}: 1.136 ± 0.158, p=0.4059; mean ± SEM, n=6). These results suggest that muscle-associated Hts does not affect the expression level of *drpr* in Drosophila larval body wall.

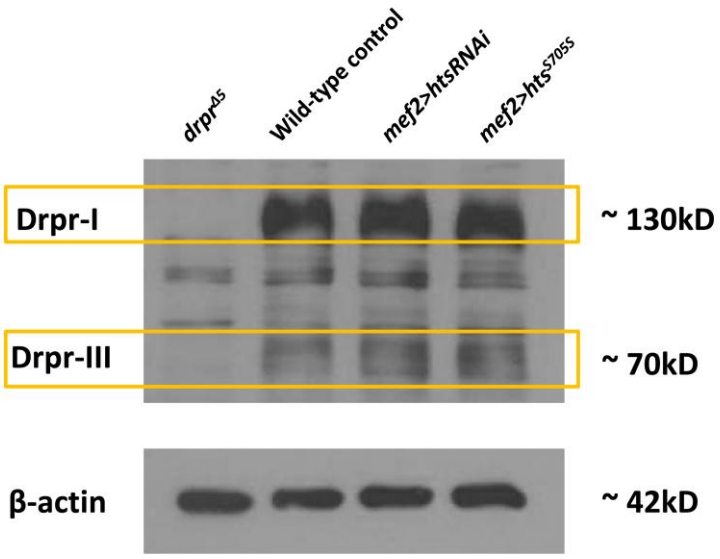

Figure 3.12 Muscle-associated Hts variation does not affect the protein levels of Draper-I/-III in Drosophila larval body wall lysates.

Protein levels of Draper-I and Draper-III were compared among the body wall lysates of three *hts* variants using Western blotting with a-Draper antibodies. $drpr^{\Delta 5}$, a null mutation of *draper,* was used as the negative control. All the three hts variants showed detectable protein bands at ~ 130kD indicating Draper-I, and protein bands at ~ 70kD indicating Draper-III. Protein bands of Draper-I and Draper-III were not detected in $drpr^{\Delta 5}$. No significant differences were found in the protein level of either Draper-I or Draper-III in body wall lysates from three *hts* variants. Blots were standardized by loading control β-actin.

3.6. Dlg is also delocalized from NMJ in a similar pattern to Drpr in larvae overexpressing *Drosophila* adducin in the muscle

Dlg has been previously shown to be delocalized from the NMJ in larvae overexpressing endogenous *hts* (using Gene search line) in the muscle by Hts overexpression in the muscle (Wang et al., 2011). However, since all the isoforms of Hts protein are overexpressed, it is not cleat if this delocalization of Dlg is caused by adducin-like Hts isoforms. Here I overexpressed Add1 (the adducin-like isoform) in the muscle by crossing *UAS-hts*^{S705S} transgenic line with *mef2-GAL4* driver flies, and examined how Add1 overexpression affects Dlg localization to the NMJ.

As shown in **Figure 3.13 A'', B''**, Dlg is delocalized from the NMJ in *mef2>hts*^{S705S} larvae. Interesting, the delocalization pattern of Dlg is similar to that of Drpr (**Figure 3.13 A', A'', B' B''**), suggesting that Dlg and Drpr may exist in the same protein complex and a potential interactions between Dlg and Drpr.

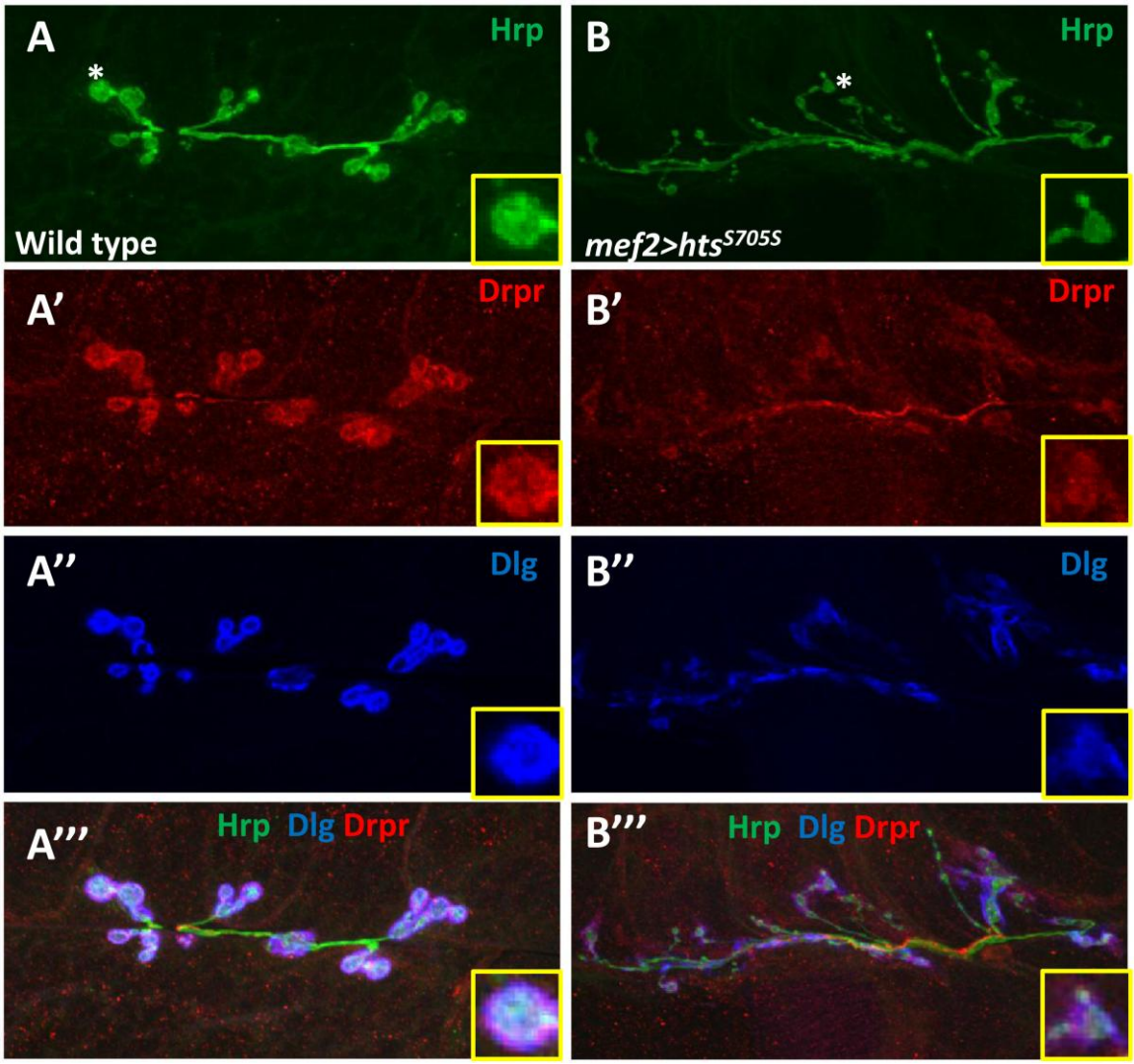

Figure 3.13 Dlg is delocalized from the NMJ in a similar pattern to Drpr in larvae overexpressing Drosophila adducin in the muscle.

Representative immunostainings of NMJs (muscle 6/7, A3 segment) in wild type (A to A''') and larvae with muscle-specific overexpression of Drosophila adducin (*mef2>hts*^{S705S}) (B to B'''). Higer power image of a individual bouton (indicated by the asterisk) is shown at the bottom right corner in each panel. Anti-Hrp staining is shown in the green channel (A, B), anti-drpr staining is shown in the red channel (A', B'), anti-Dlg staining is shown in the blue channel (A'', B''). Merged images of the three channels are (A''', B'''). Scale bar: 10 μm. Sample size: wild type=12 NMJs, *mef2>hts*^{S705S} =12 NMJs.

3.7. Dlg regulates Draper immunoreactivity at the NMJ

Given that overexpression of Hts in the muscle also delocalized Dlg from the NMJ (in the present study and Wang et al., 2011), and that the immunoreactivity of Draper colocalizes with that of Dlg at the postsynaptic NMJ (Fuentes-Medel et al., 2009), it is possible that Dlg interacts with Draper at the postsynaptic NMJ, so that the delocalization of Draper caused by Hts overexpression is mediated by Dlg.

To examine the above hypothesis, Draper immunoreactivity at the NMJ was examined in wild type control larvae, and larvae with muscle specific Dlg knockdown (*mef2>dlgRNAi*). In wild type control larvae, Draper immunoreactivity is sharp and 'tightly' localized to the postsynaptic NMJ (**Figure 3.14A'**). However, in *mef2>dlgRNAi* larvae where Dlg immunoreactivity is absent (**Figure 3.14B'**), the immunostaining of Draper is 'fuzzy' (**Figure 3.14B''**) indicating that the localization of Draper to the postsynaptic NMJ is affected. However, Draper immunoreactivity is not totally absent from the NMJ in *mef2>dlgRNAi* larvae, suggesting that Draper targeting to the NMJ is not solely dependent on Dlg.

If Dlg interacts with Draper and affects Draper distribution at the NMJ, we should expect an upregulation of Draper immunoreactivity at the NMJ in larvae overexpressing Dlg in the muscle compared to wild type larvae. Two Dlg isoforms (Dlg-A and Dlg-S97) are present at the *Drosophila* larval NMJ (Ataman et al., 2006). The effects of overexpression of each Dlg isoform on Draper immunoreactivity were examined here. Larvae with muscle-specific overexpression of Dlg-A showed a 20% increase of Draper immunoreactivity at the NMJ compared to wild type control (**Figure 3.15A', B' and D**). Whereas there is no significant change of Draper immunoreactivity detected in larvae overexpressing Dlg-S97 compared to wild type (**Figure 3.15A',C' and D**). These data suggest that only the isoform Dlg-A interacts with Draper at postsynaptic NMJ.

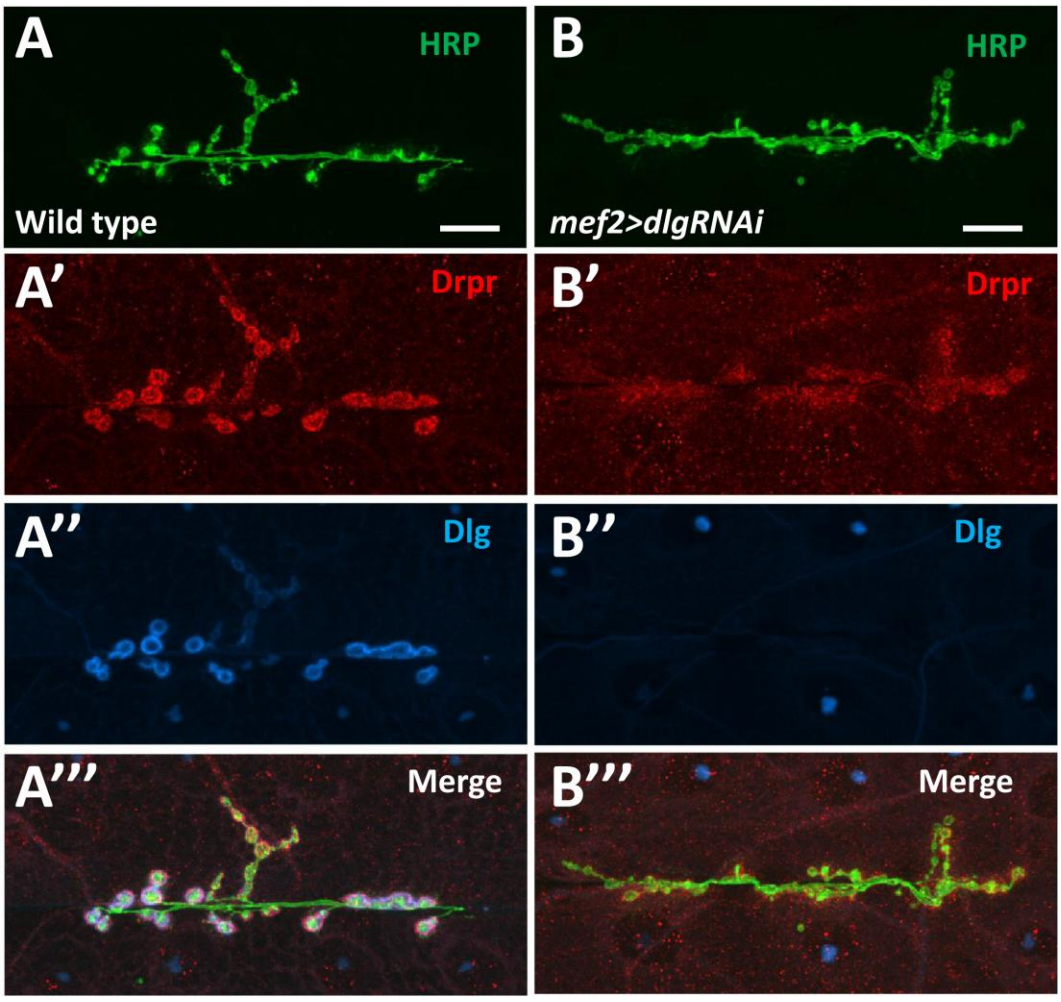

Figure 3.14 Draper localization at the postsynaptic NMJ is affected in larvae with muscle-specific knock-down.

Representative immunostainings of NMJs (muscle 6/7, A3 segment) in wild type (A to A''') and larvae with muscle-specific knockdown of Dlg (mef2>dlgRNAi) (B to B''). Anti-Hrp staining is shown in the green channel (A, B), anti-drpr staining is shown in the red channel (A', B'), anti-Dlg staining is shown in the blue channel (A'', B''). Merged images of the three channels are (A''', B'''). Scale bar: 10 µm. Sample size: wild type=12 NMJs, mef2>dlgRNAi =12 NMJs.

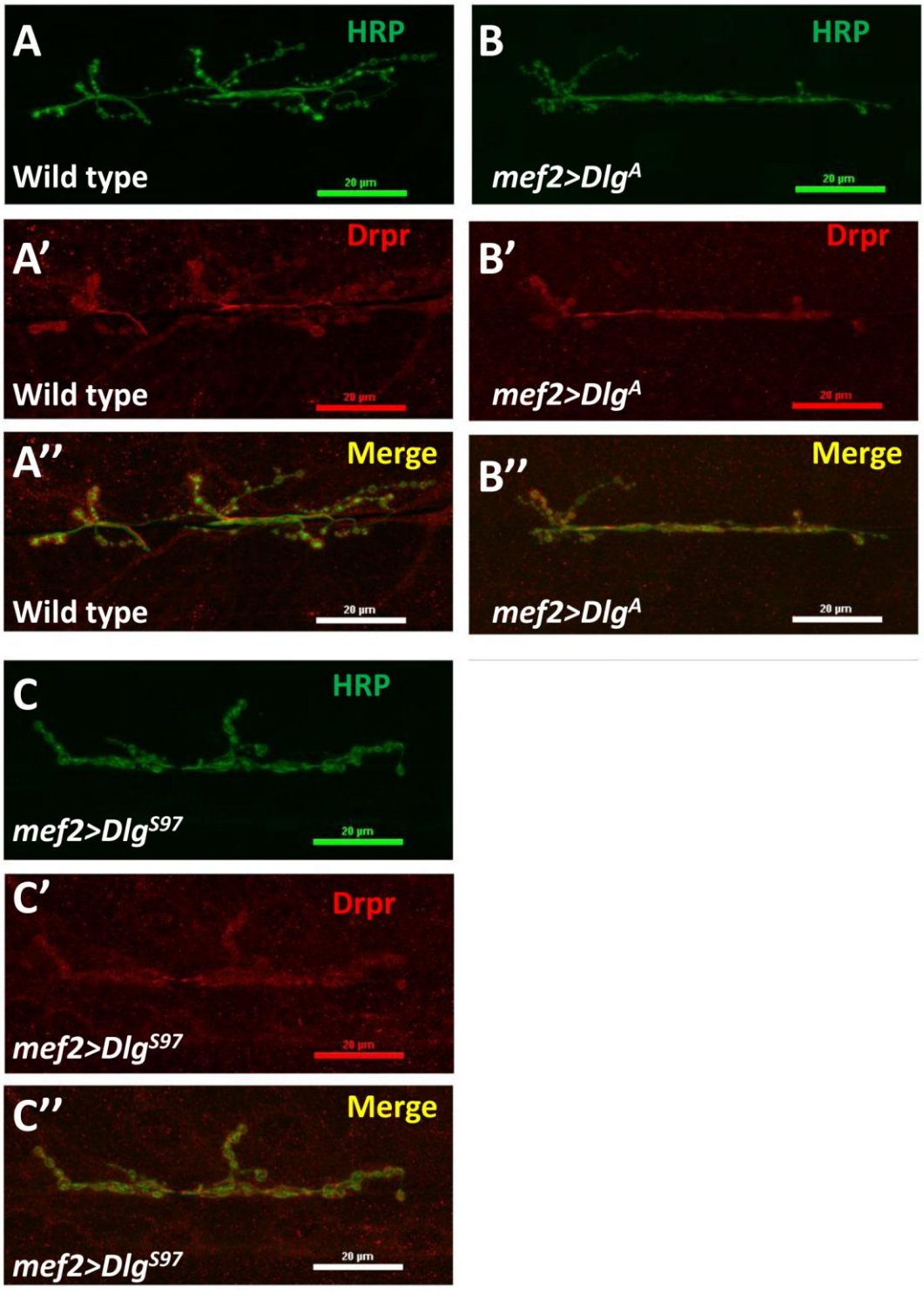
A
HRP
Wild type
20 µm
B
HRP
mef2>Dlg^A
20 µm
A'
Drpr
Wild type
20 µm
B'
Drpr
mef2>Dlg^A
20 µm
A''
Merge
Wild type
20 µm
B''
Merge
mef2>Dlg^A
20 µm
C
HRP
mef2>Dlg^S97
20 µm
C'
Drpr
mef2>Dlg^S97
20 µm
C''
Merge
mef2>Dlg^S97
20 µm

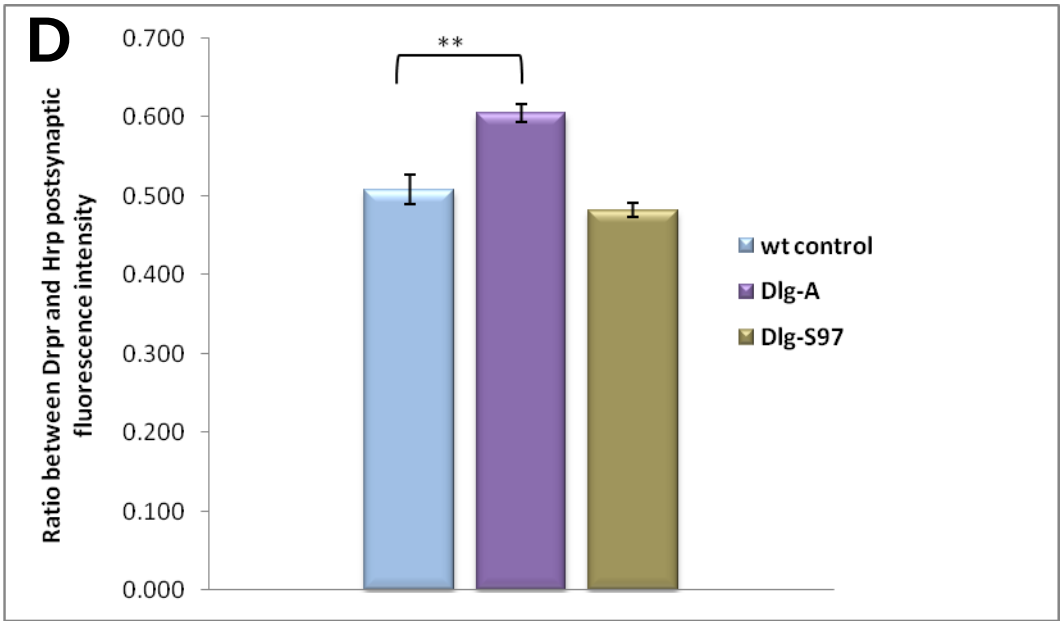

Figure 3.15 Muslce specific overexpression of Dlg-A, but not Dlg-S97, results in stronger Draper immunoreactivity at the NMJ.

Representative immunostainings of NMJs (muscle 6/7, A3 segment) in wild type (A to A''), larvae with muscle-specific overexpression of Dlg-A (*mef2>dlg^{A}*) (B to B''), and larvae with muscle-specific overexpression of Dlg-S97 (*mef2>dlg^{S97}*) (C to C''). Anti-Hrp staining is shown in the green channel (A, B, C), and anti-Draper staining is shown in the red channel (A', B', C'). Merged images of the two channels are (A'', B'', C''). (C) Quantification of the ratio between Draper and Hrp synaptic fluorescence intensity. Sample size: wild type=17 NMJs, *mef2>dlg^{A}* =18 NMJs, *mef2>dlg^{S97}*. Double asterisks (**) indicate significant difference at $p<0.01$

3.8. *Draper* null mutant larvae exhibit decreased Hts immunoreactivity at the NMJ and possibly affects Hts function.

Given the morphological similarities between *hts* and *drpr* mutant NMJ, their colocalization at the post-synaptic region, and that Hts negatively regulates Draper localization via a specific Hts-Draper interaction, it is intriguing to examine if genetic manipulations of *draper* affects Hts immunoreactivity.

The $drpr^{\Delta 5}$ putative null allele was examined for changes in Hts levels by immunostaining. As shown in **Figure 3.16**, NMJs from larvae homozygous for drpr null mutant alleles showed similar Hts localization patterns compared to wildtype (**Figure 3.16 A' and B'**), but had a 30% decrease in Hts immunoreactivity (**Figure 3.16 A', B' and C**). Consistently, mild decreases in Hts immunoreactivity (by ~17%) were also observed in two other hypomorphic drpr alleles (Chui, 2011). These results suggest that the expression level of Hts is affected by *Drpr* loss of function. When the immunoreactivity of Hts was examined in larvae with muscle-specific knock down of Draper (*mef2>drprRNAi*), there is only a slight decrease of Hts immunoreactivity detected compared to wildtype (**Figure 3.17 A', B' and C**).

Long, small-caliber neuronal protrusions were observed in *hts* mutant NMJs (Pielage et al., 2011). In my study, *Drpr* null mutant NMJs were observed to have a higher frequency on presenting long, small-caliber neuronal protrusions (**Figure 3.18**). About 44% examined drpr null mutant NMJs (n=18) had neuronal protrusions, whereas no protrusions were observed in wildtype NMJs (n=18). This similar phenotype suggests that Hts function is affected at the *drpr* null mutant NMJ.

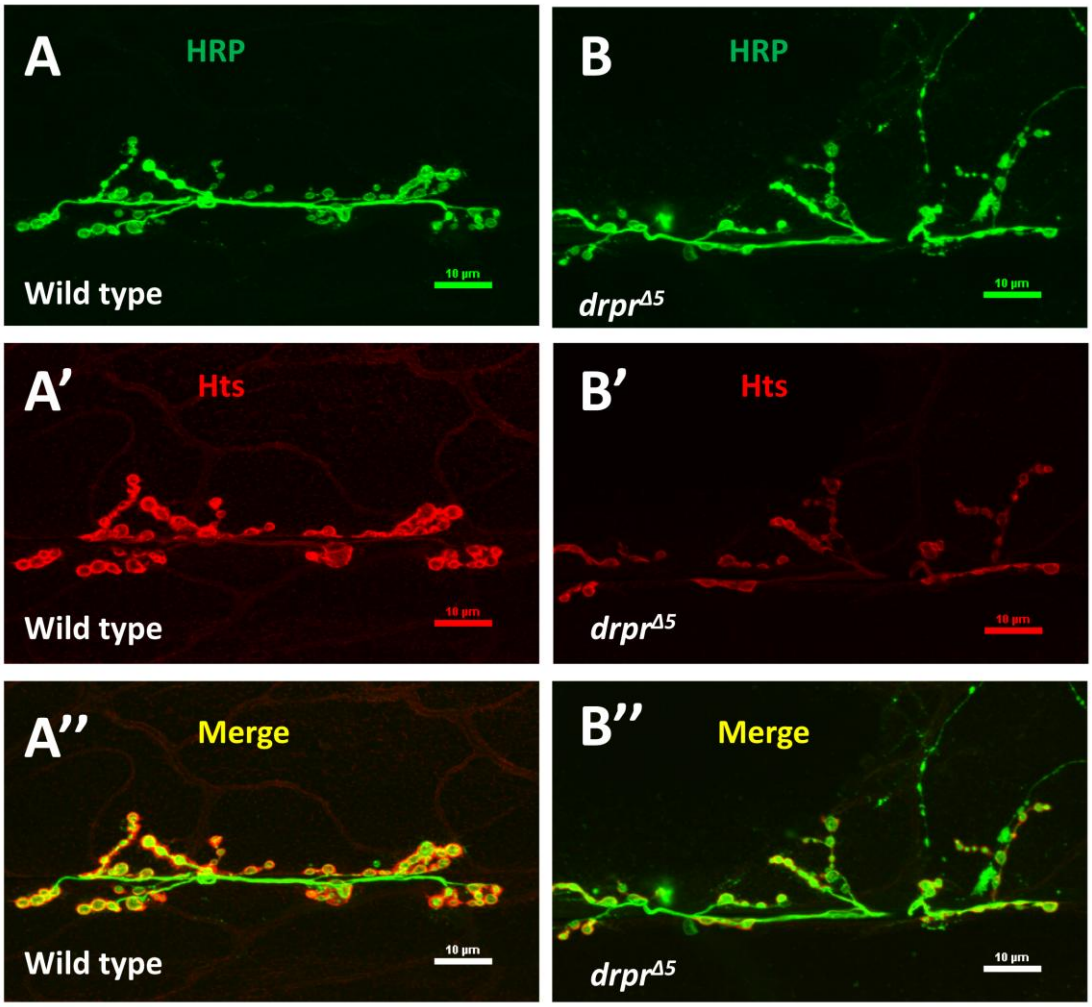
A
HRP
Wild type
10 µm
B
HRP
drpr^Δ5
10 µm
A'
Hts
Wild type
10 µm
B'
Hts
drpr^Δ5
10 µm
A''
Merge
Wild type
10 µm
B''
Merge
drpr^Δ5
10 µm

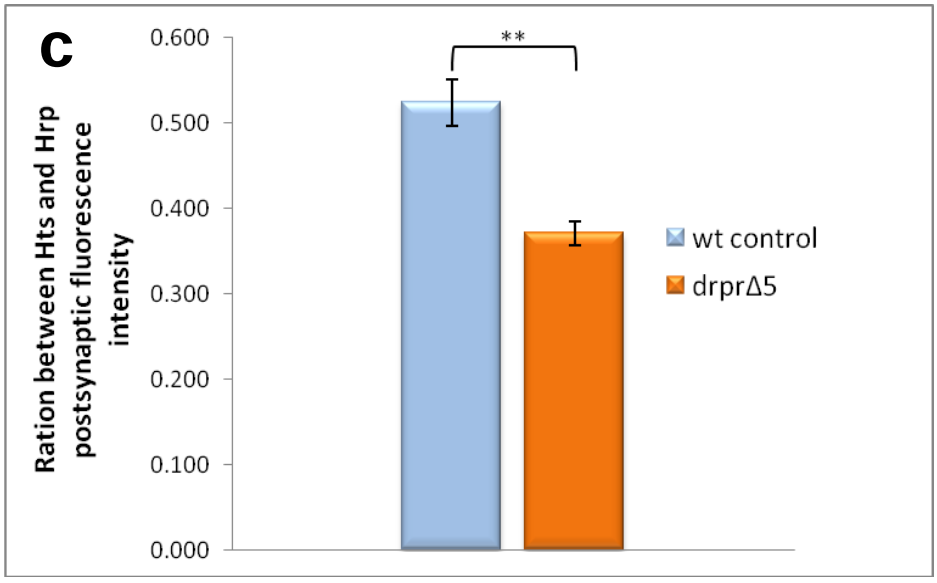
C
Ration between Hts and Hrp postsynaptic fluorescence intensity
0.600
0.500
0.400
0.300
0.200
0.100
0.000
**
wt control
drprΔ5

Figure 3.16. drpr mutant NMJs show decreased Hts immunoreactivity.

Representative immunostainings of NMJs (muscle 6/7, A3 segment) in wild type (A to A'') and *drpr* null mutant larvae (B to B''). Anti-Hrp staining is shown in the green channel (A, B), and anti-Hts staining is shown in the red channel (A', B'). Merged images of the two channels are (A'', B'').Scale bar: 10 µm. (C) Quantification of the ratio between Hts and Hrp synaptic fluorescence intensity. Sample size: wild type=14 NMJs, $drpr^{\Delta 5}$ =18 NMJs. Double asterisks (**) indicate significant difference at $p<0.01$

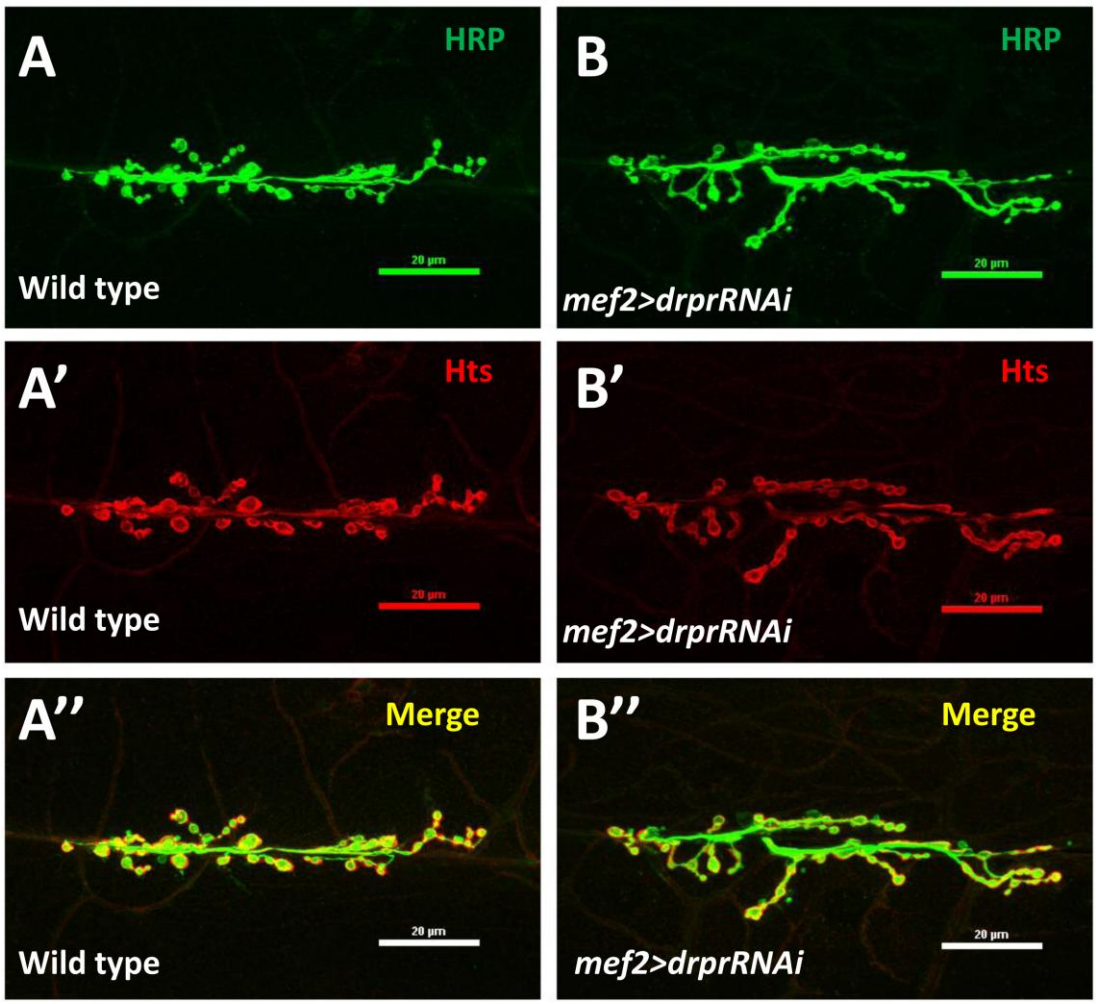
A
HRP
Wild type
20 µm
B
HRP
mef2>drprRNAi
20 µm
A'
Hts
Wild type
20 µm
B'
Hts
mef2>drprRNAi
20 µm
A''
Merge
Wild type
20 µm
B''
Merge
mef2>drprRNAi
20 µm

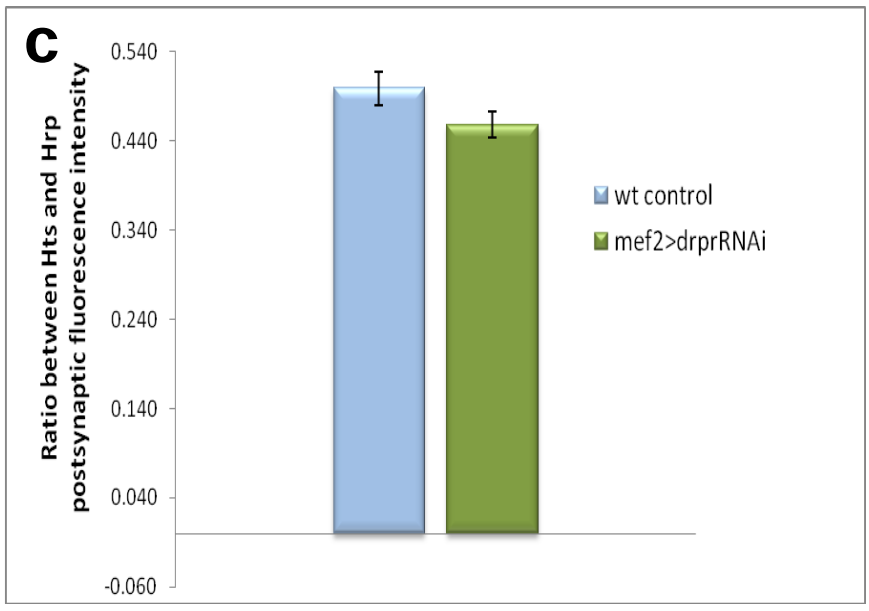
C
Ratio between Hts and Hrp postsynaptic fluorescence intensity
0.540
0.440
0.340
0.240
0.140
0.040
-0.060
wt control
mef2>drprRNAi

Figure 3.17 Hts immunoreactivity is slightly decreased at the NMJ in larvae with muscle specific knock-down of Draper.

Representative immunostainings of NMJs (muscle 6/7, A3 segment) in wild type (A to A'') and larvae with muscle specific Draper knock-down (B to B''). Anti-Hrp staining is shown in the green channel (A, B), and anti-Hts staining is shown in the red channel (A', B'). Merged images of the two channels are (A'', B''). (C) Quantification of the ratio between Hts and Hrp synaptic fluorescence intensity. Sample size: wild type=17 NMJs, *mef2>drprRNAi* =18 NMJs.

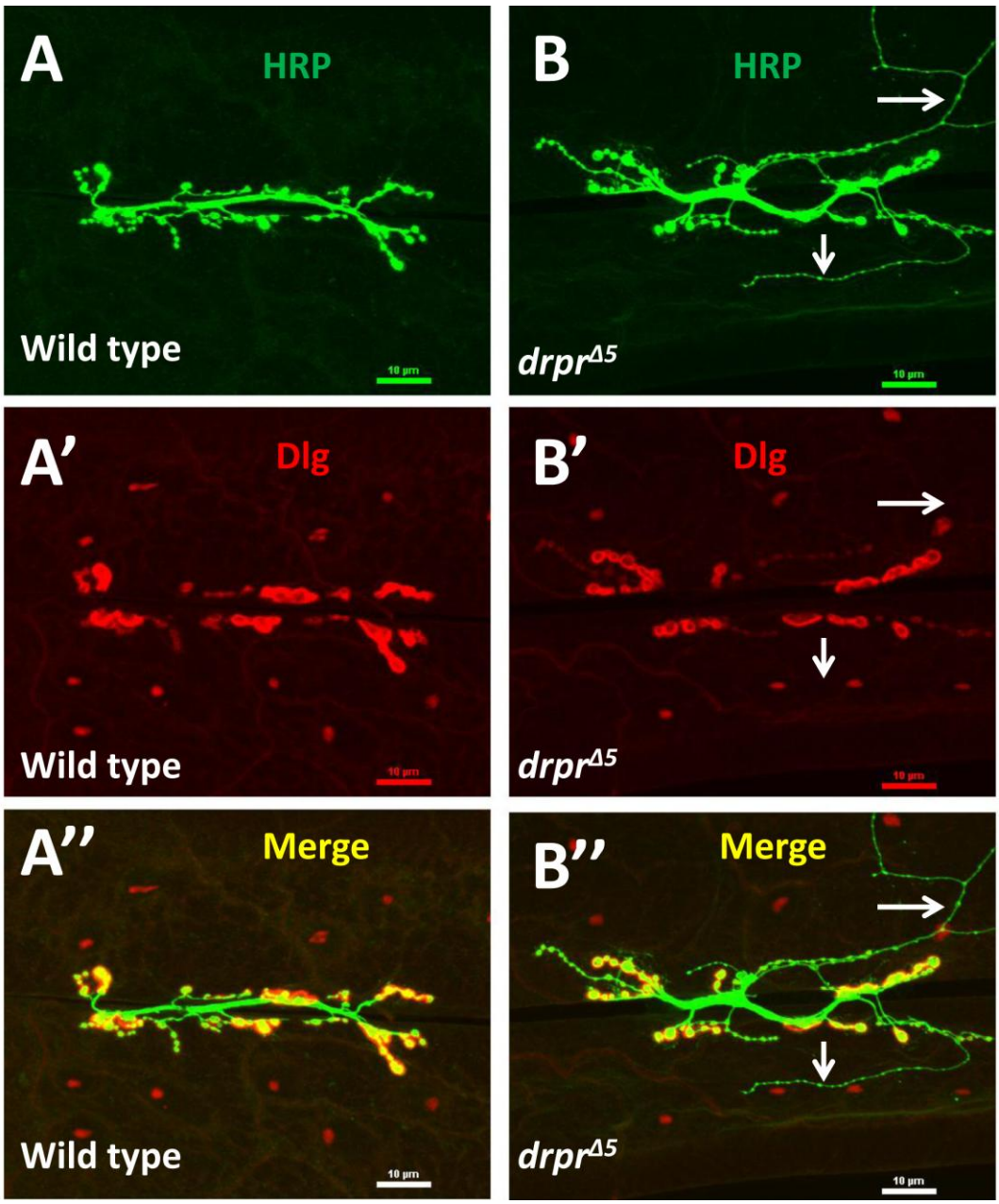

Figure 3.18 drpr null mutant NMJ exhibits long, small-caliber neuronal protrusions.

Representative immunostainings of NMJs (muscle 6/7, A3 segment) in wild type (A to A'') and *drpr* null mutant larvae (B to B''). Anti-Hrp staining is shown in the green channel (A, B), and anti-Dlg staining is shown in the red channel (A', B'). Merged images of the two channels are (A'', B''). 44% of the examined NMJs in *drpr* null mutant larvae showed long, small-caliber neuronal protrusions (indicated by arrows in B-B''. Protrusions were not observed in wild type control. Sample size: wild type=18 NMJs, $drpr^{\Delta 5}$ =18 NMJs.

3.9. Draper regulates Dlg immunoreactivity at the larval NMJ

To study whether the interaction between Dlg and Draper is co-dependent, Dlg immunoreactivity at the NMJ was examined in larvae expressing different levels of Draper, including wild type control, *drpr*$^{\Delta 5}$ null mutant alleles, and larvae with muscle-specific overexpression of Draper-I. The results showed that *drpr*$^{\Delta 5}$ null mutant NMJs had a slight (but not significant) decrease of Dlg immunoreactivity compared to wild type control (**Figure 3.19 A', B' and C**). However, when Draper-I is overexpressed in the muscle, there was a ~40% increase of Draper immunoreactivity at the NMJ compared to wild type control ($p<0.01$, **Figure 3.20 A', B' and C**). These results suggest that Draper is not required for proper Dlg targeting to the NMJ, however upregulating Draper in the muscle promotes Dlg expression or targeting to the NMJ.

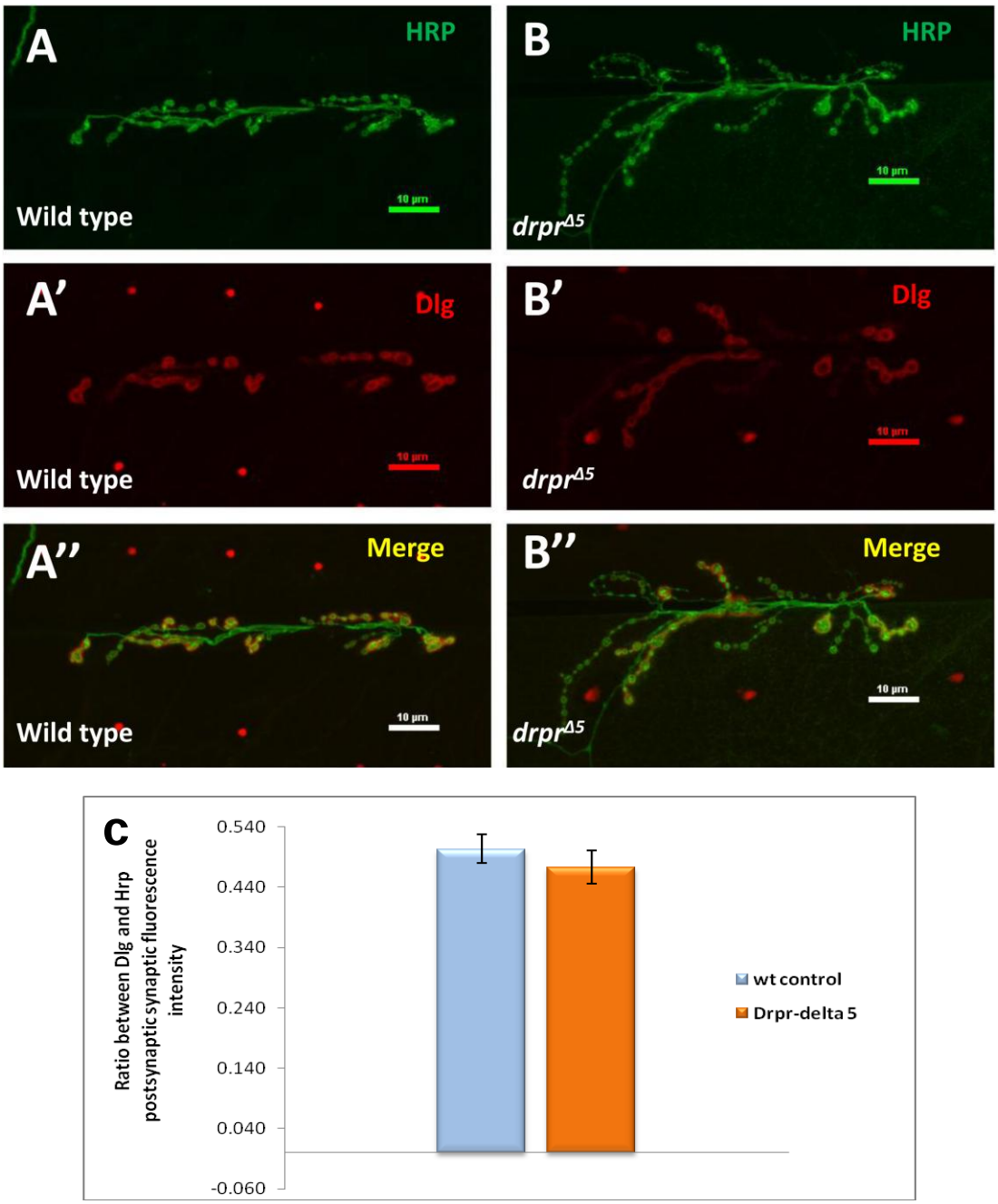

Figure 3.19 drpr mutant NMJs show slightly decreased Dlg immunoreactivity.

Representative immunostainings of NMJs (muscle 6/7, A3 segment) in wild type (A to A'') and *drpr* null mutant larvae (B to B''). Anti-Hrp staining is shown in the green channel (A, B), and anti-Dlg staining is shown in the red channel (A', B'). Merged images of the two channels are (A'', B''). (C) Quantification of the ratio between Dlg and Hrp synaptic fluorescence intensity. Sample size: wild type=21 NMJs, $drpr^{\Delta 5}$ =20 NMJs. No statistically significant difference.

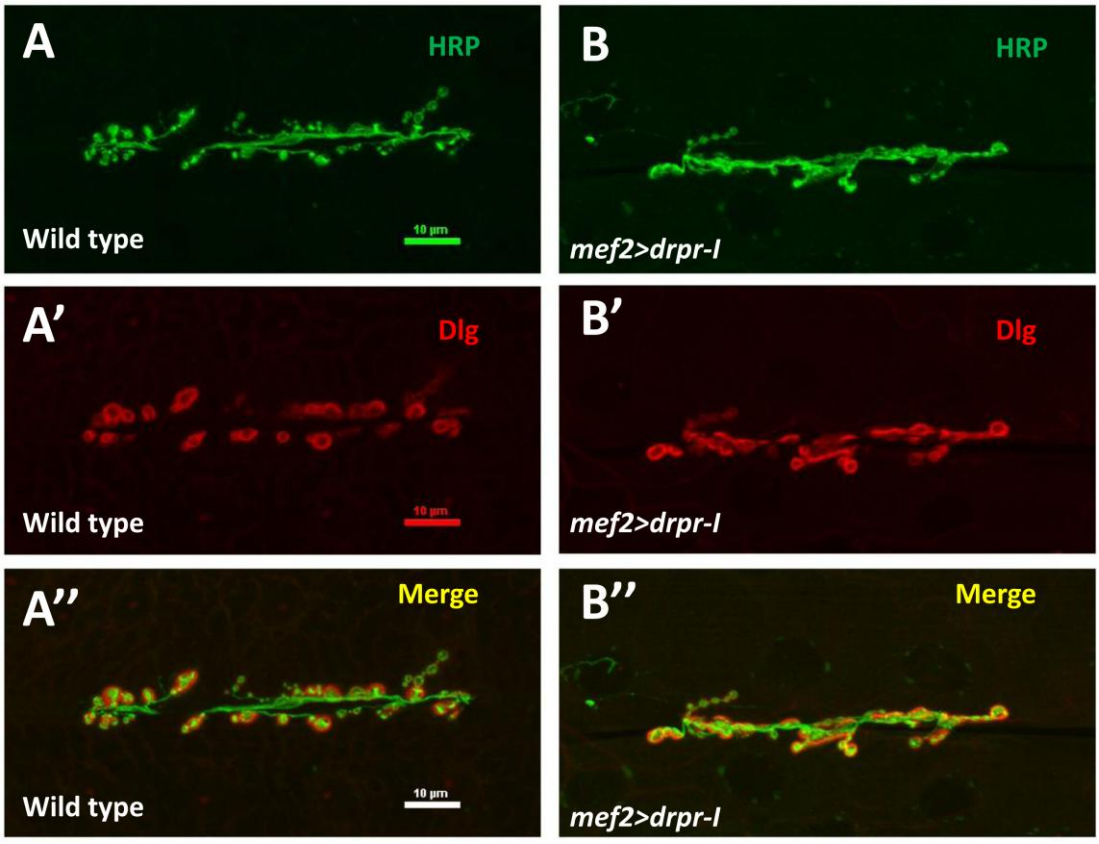
A
HRP
Wild type
10 µm
B
HRP
mef2>drpr-I
A'
Dlg
Wild type
10 µm
B'
Dlg
mef2>drpr-I
A''
Merge
Wild type
10 µm
B''
Merge
mef2>drpr-I

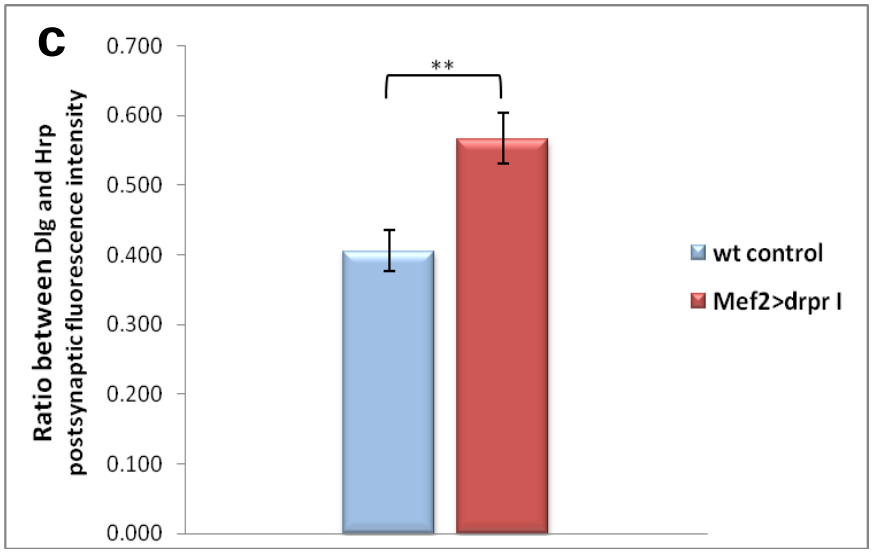
C
Ratio between Dlg and Hrp postsynaptic fluorescence intensity
0.700
0.600
0.500
0.400
0.300
0.200
0.100
0.000
**
wt control
Mef2>drpr I

Figure 3.20. Muscle-specific overexpression of Draper-I causes a 40% increase of Dlg immunoreactivity at the NMJ.

Representative immunostainings of NMJs (muscle 6/7, A3 segment) in wild type (A to A'') and larvae with muscle-specific overexpressing of Draper-I (*mef2>drpr-I*) (B to B''). Anti-Hrp staining is shown in the green channel (A, B), and anti-Dlg staining is shown in the red channel (A', B'). Merged images of the two channels are (A'', B''). (C) Quantification of the ratio between Dlg and Hrp synaptic fluorescence intensity. Sample size: wild type=17 NMJs, *mef2>drpr-I* =22 NMJs. Double asterisks (**) indicate significant difference at $p<0.01$.

4. Discussion

My data demonstrates that muscle-associated Hu-li tai shao (Hts) regulates synaptic development at the Drosophila larval NMJ. This is evidenced by the data showing that overexpression Hts in the muscle promotes NMJ growth, whereas muscle-specific Hts knock-down results in underdevelopment of NMJ. Consistent with the above results I found that adult flies with muscle-specific Hts knock-down exhibit severe neuromuscular defect which is characterized by weakness and shivering leg movement and hence restrained range of motion. This evidence suggests that muscle-assoicated Hts is also required for *Drosophila* adult NMJ stabilization and normal development. These data add to the growing body of evidence indicating that adducin/Hts is a key regulator of synaptic stability and plasticity.

Hts has been previously shown to regulate Drosophila larval NMJ through interacting with other important synaptic proteins localized at the same protein complex, such as Discs-large (Wang *et al*., 2011). Here I focused on studying the potential interaction between Hts and Draper, a trans-membrane engulfment receptor which has been shown to regulate NMJ development (Fuentes-Medel *et al*., 2009). *In vivo* co-localization between Hts and Draper is identified at the postsynaptic region. Draper has also been previously identified as a putative binding partner of Hts in a yeast two-hybrid based screen (Giot *et al*., 2003). These data together indicate that there may be a interaction between Hts and Draper. Furthermore, overexpressing Hts in the muscle is observed to delocalize Draper from the NMJ, yet muscle-specific Hts knock-down gives Draper a 'tighter' localization to the NMJ. Hence I propose that Draper localization to the NMJ is regulated by Hts. The effects of muscle-associated Hts on the targeting of Draper to the synapse highlights a new avenue by which Hts may be exerting its influence on *Drosophila* larval NMJ development.

4.1. Muscle-associated Hts is required for normal Drosophila NMJ development

In the present study I first characterized the function of muscle-associated Hts during *Drosophila* life circle development. Animals with muscle-specific Hts knock-down can successfully pass the embryonic and larval stages and develop into pupae. However, at the end of pupal stage when the majority of wild type control managed to develope into adult flies and emerged from the pupal case, flies with muscle-specific Hts knock-down failed to eclose. This could be caused by: 1) knocking down of muscle-associated Hts causes general developmental defect during pupal stage, so that pupae cannot develop into adult flies; or 2) pupae with muscle-specific Hts have normal pupal development to complete metamorphosis and develop into adult flies, but suffer neuromuscular defect which renders them too weak to break the surrounding pupal case and get trapped inside.

The first point is unlikely to be true. Pupal cases of five late-stage *mef2>htsRNAi* pupae were manually ripped open and the animals trapped inside were gently pulled out. Two were found alive and fully-developed into adult flies. The other three were found dead previously, but they all appeared to be fully-developed into adult flies. These observations indicate that flies with muscle-associated Hts knock-down can complete metamorphosis and develop into adulthood. My second point is supported by the observation that the two rescued *mef2>htsRNAi* flies exhibit severe neuromuscular defects, which is characterized by their inability to crawl and lack of escape behavior. A closer observation under the dissecting microscope showed that they can only partially move their legs with shivering movement. These observed defects probably are the reason that makes the flies unable to break the surrounding pupal case trapping them inside which in turn cause death of the flies by starvation.

I propose that this observed neuromuscular defect in muscle-associated Hts knock-down flies is a direct outcome of underdeveloped neuromuscular junctions, given that Hts is an important structural component of the spectrin-actin cytoskeleton (Zaccai and Lipshitz, 1996a) which has been well recognized to provide synaptic stabilization (Pielage *et al.*, 2005; Koch *et al*., 2008). To test this hypothesis, a rather simple way would be to expose the neuromuscular junctions of these *mef2>htsRNAi* adult flies for

immunohistochemical and electrophysiological analysis. However, due to the diversity and complexity of *Drosophila* adult neuromuscular system (Hebbar *et al*., 2006), the electrophysiological analysis was not conducted in the present study. Instead, the effect of muscle-specific Hts knock-down on 3rd instar larval NMJ development is examined. Results show *mef2>htsRNAi 3rd* instar larvae exhibit significantly underdeveloped NMJ. Therefore I speculate a similar result for the *mef2>htsRNAi* adult fly that of the knock-down of Hts in *Drosophila* adult will cause underdevelopment of its NMJ.

4.2. Relative contributions of pre- and postsynaptic Hts to NMJ development

The mechanisms by which presynaptic Hts regulates *Drosophila* larval NMJ development has been well studied previously by Pielage *et al. (*2011). They present a model in which presynaptic Hts function as a molecular keystone that stabilizes the submembranous spectrin-actin cytoskeleton to achieve synaptic stability and simultaneously influences the shape and growth potential of NMJ via its actin-capping activity (Pielage *et al.*, 2011). I focused on the postsynaptic Hts and demonstrated that muscle-associated postsynaptic Hts can also regulate NMJ development. However, the mechanism in which NMJ growth is regulated by the postsynaptic Hts differs from the presynaptic Hts.

4.2.1. Loss of presynaptic Hts, but not postsynaptic Hts, causes synaptic retraction

At synapses, the submembranous spectrin-actin cytoskeleton support the overall synaptic framework. At the Drosophila NMJ, several mutations have been identified to destabilize presynaptic spectrin-actin cytoskeleton and as a result cause synaptic retraction (Pielage *et al*., 2005; Eaton *et al*., 2002; Koch *et al*., 2008). Hence the structural integrity of spectrin-actin cytoskeleton is essential for synapse stabilization. In consistent with the well established function of Hts/adducin as the cross-linker of spectrin and actin that participates in the stabilization of submembranous spectrin-actin cytoskeleton (Matsuoka *et al*., 2000; Bennett and Baines, 2001; Zaccai and Lipshitz,

1996a), it has been shown that loss of presynaptic Hts results in a dramatic increase in the number of synaptic retractions at the larval NMJ (Pielage *et al*., 2011).

Here I present evidence that knocking down of postsynaptic Hts results in underdeveloped NMJs with decreased bouton numbers. Similarly, NMJs lacking muscle-associated spectrin also exhibit reduced number of boutons (Pielage *et al.*, 2006), suggesting that disruption of spectrin cytoskeleton integrity interfere with normal NMJ development. However, no evidence of increased level of synaptic retraction was found in synapses with postsynaptic knock-down of Hts in one of my preliminary study (data not shown). This is Consistent with the discovery by Pielage *et al*. (2005) in which they claim that postsynaptic knock-down of spectrin does not cause synapse retractions. These indicate that the structural integrity of spectrin cytoskeleton is uniquely required in the presynaptic nerve terminal to achieve synapse stabilization and prevent synaptic retraction.

In its place though, evidence show that loss of postsynaptic spectrin causes obvious defects in the integrity of subsynaptic reticulum (SSR, Pielage *et al*., 2006). Correspondingly, *hts* null mutant NMJs causes less compact, underdeveloped SSRs (Pielage *et al*., 2011). Although, the functions of SSR and how it affects NMJ development remain unclear, it can be proposed that the structural defect of SSR may cause NMJ underdevelopment in Hts or spectrin postsynaptic knock-down larvae.

4.2.2. Presynaptic Hts restrains NMJ growth, while postsynaptic Hts promotes NMJ growth

When Hts is knocked down presynaptically, the NMJs at muscle 4 undergoes overgrowth (Pielage *et al*., 2011). This NMJ overgrowth is characterized by increased bouton numbers and the presence of small-caliber, actin-rich synaptic protrusions (Pielage *et al.*, 2011). It was speculated that this presynaptic knock down of Hts-induced NMJ overgrowth is caused by loss of the actin capping activity of Hts (Pielage *et al*., 2011). Based on work in other systems, loss of actin-capping activity at the plasma membrane could reasonably favor the formation of actin-based filopodia which might promote the elaboration of small-caliber synaptic protrusions and NMJ growth (Bear *et al*., 2002; Mejillano *et al*., 2004; Menna *et al.*, 2009). Consistent with such a model, presynaptic overexpression of Hts, thereby increasing the actin capping activity, was

found sufficient to inhibit the growth of small-caliber type II and type III nerve terminals in muscle 12/13 (Pielage *et al.*, 2011). These data indicate that presynaptic Hts with its actin-capping activity restrains the growth potential of NMJ.

Conversely, here I present evidence that overexpression of postsynaptic Hts promotes NMJ growth in muscle 6/7. Moreover, no small-caliber, actin-rich processes were observed at muscle 6/7 NMJ in larvae with postsynaptic knock-down of Hts. These data indicate that postsynaptic Hts regulate NMJ growth in a different way that is independent to the actin-capping activity.

In *hts* null mutant larvae, where both pre- and postsynaptic Hts are knocked off, NMJs at muscle 6/7 are severely underdeveloped (Wang *et al*., 2011), representing a similar phenotype exhibited by larvae with postsynaptic Hts knockdown. This suggests that in muscle 6/7 the function of postsynaptic Hts prevails in regulating the NMJ development. It is important to note that, unlike most other larval muscles, muscle 6 and 7 are only innervated by type Ib and type Is boutons (Guan *et al*., 1996). Thus the growth-restraining function of presynaptic Hts observed on small-caliber type II and type III boutons may not apply to the type I boutons in muscle 6/7 (Pielage *et al*., 2011). The regulatory role of presynaptic Hts in muscle 6/7 NMJ growth is currently being investigated.

4.3. Postsynaptic Hts regulates NMJ growth via interacting with Draper

Although the function of postsynaptic Hts in larval NMJ development has been characterized in the present study, the underlying mechanisms remain unknown. The spectrin-actin cytoskeleton has been termed a “protein accumulation machine”, serving as a scaffold for synaptic protein recruitment and interactions (Dillon and Goda, 2005). Therefore it is possible that postsynaptic Hts exerts its influence on NMJ development via local interaction with other synaptic proteins at the postsynaptic spectrin cytoskeleton. Here I focused on studying the potential interaction between Hts and Draper, a trans-membrane engulfment receptor which has been shown to regulate NMJ development (Fuentes-Medel *et al*., 2009).

4.3.1. Draper localization at the Drosophila larval NMJ

Draper is claimed to localize to the peripheral glia and postsynaptic region of Drosophila larval NMJ (Fuentes-Medel *et al*., 2009). And from my experiment Draper is observed to co-localize with Hts at postsynaptic regions. However, the localization patterns of the two are different. Hts immunoreactivity evenly distributed to the peripheral portion of each bouton and forms a donut-like shape pattern, while Draper immunoreactivity forms a discontinuous ring where some portions have stronger staining than the others. This suggests that Draper tends to localize in clusters. Weak Draper staining is also observed in the extrasynaptic muscle area. Some scattered stainings of Draper were found beyond the synaptic bouton, which could be either glia staining or the engulfed membrane vesicles in the muscle. Draper has not yet been reported to localize to presynaptic neurons. However, MEGF10 and MEGF11, the mammalian homologs of Draper has recently been identified as the membrane markers of two subtypes of neurons in the retina (Kay *et al*., 2012), implying that Draper may also have presynaptic neuronal localization. Consistently, Draper immunoreactivity is also found to partially overlap the Hrp immunoreactivity in this study (**Figure 3.5B’’’, 3.7A’’’ and 3.7B’’’**). In summary, Draper is universally expressed in all the three components of Drosophila larval NMJ system, including the presynaptic neuron, the postsynaptic muscle and the glia. Draper may have important functions in initiating intercellular signaling and communications among these three NMJ components during synapse development.

4.3.2. Muscle-associated Hts regulates Draper localization at postsynaptic region

To show that muscle-associated Hts regulates Draper localization at the postsynaptic regions, muscle-specific knock-down of Hts causing a ‘tighter’ localization of Draper at postsynaptic region was shown, with a 20% increase of Draper relative fluorescent intensity at postsynapse region compared to wild type. A similar 25% increase of Draper relative fluorescent intensity at the postsynaptic region is also detected in *hts* null mutant larvae where both pre- and postsynaptic Hts are knocked off.

These data indicate that this 'tighter' Draper targeting to the postsynaptic NMJ is predominantly caused by postsynaptic muscle-associated Hts.

Next I examined Draper localization in larvae with muscle-specific overexpression of Hts proteins. When endogenous Hts proteins are overexpressed in the muscle, Draper immunoreactivity is shown to be delocalized from the postsynaptic NMJ area. In a later experiment, muscle-specific overexpression of Add1, an adducin-like isoform of Hts proteins in animals showed that Draper immunoreactivity delocalized from the postsynapse in a diffusing pattern. Likewise, the relative fluorescence intensity of Draper at postsynaptic NMJ is decreased in these animals. This indicates that overexpression of Add1 in the muscle is sufficient to cause Draper delocalization. Whether other isoforms of Hts do contribute to the delocalization of Draper needs further study to be conducted in the future.

4.3.3. Muscle associated Hts does not affect Draper expression

There are three isoforms of Draper (Draper-I, -II, and -III), and only Draper-I and Draper-III are expressed in neuromuscular system (Fuentes-Medel *et al*., 2009). Western blotting of Draper did not reveal any significant changes in either Draper-I or Draper-III protein level among wild type control, *mef2>htsRNAi* and *mef2>hts*^{S705S} larval body wall lysates, indicating that muscle-associated Hts does not affect Draper expression level in larval body wall muscles. A limitation is that the body wall preparations used in this experiment are not purely composed by muscles, some innervating nerves and peripheral glial tissues are remnantly imbedded in the muscles. However, given that the amount of imbedded nerve and glial tissues is very small, I assume that they will only have negligible impact on the result.

4.3.4. How does muscle-associated Hts regulate Draper localization?

4.3.4.1. Draper delocalization is not caused by general muscle defect

The delocalization of Draper observed in muscle-associated Hts gain of function animals could be caused by a general developmental defect of muscle resulting from ectopic Hts overexpression, which would affect the proper targeting of all the postsynaptic proteins to the NMJ. To evaluate this possibility, I examined the

immunoreactivities of two postsynaptic proteins, Pak and Glutamate receptor IIb (GluR-IIb), in animals (*mef2>hts*^{S705S}) with muscle-specific Hts overpression. Immunoreactivities of these two proteins are tightly targeted to the postsynaptic area, with no diffusing staining observed. The relative fluorescence intensity of Pak at postsynaptic NMJ in *mef2>hts*^{S705S} animals is even slightly higher than wild type control. These data suggest that other postsynaptic proteins could be properly localized to the NMJ area in *mef2>hts*^{S705S} animals. Hence the delocalization of Draper seen in *mef2>hts*^{S705S} animals should not be caused by general developmental defect of muscle.

The relative fluorescence intensity of GluRIIb at NMJ is decreased in *mef2>hts*^{S705S} animals compared to wild type control. But since the immunostaining of GluRIIb is still tight and sharp at the NMJ, it is unlikely that this decreased GluR-IIb level is caused by general morphological defect of the muscle. Postsynaptic Hts has been shown to affect synaptic targeting of Discs-large (Dlg) (Wang *et al*., 2011), which has been shown to regulate GluRIIb composition at Drosophila NMJ (Chen and Featherstone, 2005). Thus, it is possible that the decreased GluRIIb staining in *mef2>hts*^{S705S} animals is caused by the delocalization of DLG induced by muscle-specific Hts overexpression.

4.3.4.2. Dlg as the speculated mediator of Hts/Draper interaction

It is well known that Draper is a trans-membrane receptor containing multiple extracellular EGF repeats, a single transmembrane domain and an intracellular domain (Ziegenfuss *et al*., 2008). However, little information was gathered from the literature on how Draper localizes to the membrane. A potential mechanism would be that Draper is anchored to the membrane through binding to certain scaffolding proteins in the submembranous cytoskeleton. Interestingly, Draper has been shown to co-localize with Dlg at postsynaptic NMJ (Fuentes-Medel *et al*., 2009). Moreover, both Draper and Dlg have been shown to be delocalized from the NMJ in a similar diffusing pattern when Hts is overexpressed in the muscle (in the present study and Wang *et al*., 2011). These data suggest that Dlg could be the potential scaffolding protein for proper Draper localization to the membrane. Thus when Dlg is delocalized from the NMJ by Hts overexpression, Draper can no longer localize to the postsynaptic membrane. To test this hypothesis, I examined the immunoreactivity of Draper at the NMJ in larvae expressing different levels

of Dlg in the muscle. Supporting to my hypothesis, I showed that when Dlg is knocked-down in the muscle, it gives a 'fuzzy' Draper immunostaining at the NMJ indicating that Draper cannot be properly localized to the NMJ. Moreover, Larvae with muscle-specific overexpression of Dlg-A showed a 20% increase of Draper immunoreactivity at the NMJ compared to wild type control (**Figure 3.15A', B' and D**). The above data collectively suggest that Dlg is required for the proper localization of Draper to the NMJ by recruiting and anchoring Draper to the postsynaptic NMJ. There is no significant change of Draper immunoreactivity detected in larvae overexpressing Dlg-S97 compared to wild type (**Figure 3.15 A',C' and D**), suggesting that only the isoform Dlg-A interacts with Draper at postsynaptic NMJ. Co-immunoprecipitation is needed to confirm the colocalization between Dlg and Drpr.

4.3.5. The potential Hts-Draper interaction could be co-dependent

Here I showed evidence that Hts affects Drpr localization at the NMJ via a potential Hts-Drpr protein interaction. Interestingly, I also showed evidence that this Hts-Draper interaction could be co-dependent by showing that *drpr* null mutant larvae have significantly decreased levels of Hts immunoreactivity at the NMJ (**Figure 3.14**). Consistently, about 44% of *drpr* null mutant larvae show long, small-caliber neuronal protrusions at the NMJ, which were previously observed in *hts* loss of function flies but never is seen in wild type flies. This suggests that *drpr* loss of function also affects Hts function at the NMJ. There is only a slight decrease of Hts immunoreactivity in larvae with muscle-specific *drpr* knock down (*mef2>drprRNAi*) compared to wild type (**Figure 3.15**). A possible explanation is that the effectiveness of the RNAi knock-down is low so that the residual level of Draper in the muscle is sufficient for normal Hts expression.

4.4. The function of muscle-associated Draper in NMJ development

The function of muscle-associated Draper during Drosophila larval NMJ development was firstly studied by Fuentes-Medel *et al*. (2009), where loss of Draper in the muscle is shown to hamper NMJ growth. In the same study, Increased number of 'ghost boutons' (immature boutons without postsynaptic membranes surrounding them)

was also observed in larvae with muscle-specific knock-down of Draper. Hence Fuentes-Medel *et al*. (2009) speculated that muscle-associated Draper functions to initiate the engulfment of presynaptic derived 'ghost boutons', and that failure of muscle to clear 'ghost boutons' negatively regulates synaptic growth (Fuentes-Medel *et al*., 2009). However, there is no direct evidence provided that the accumulation of 'ghost boutons' is the main cause of NMJ underdevelopment. It is possible that muscle-associated Draper actually regulates NMJ development though other uncovered mechanisms, and that the accumulation of 'ghost boutons' just has a trivial effect on NMJ growth. Two potential functions of muscle-associated Draper are discussed below.

4.4.1. Muscle-associated Draper may initiate homotypic interaction during cell-cell recognition events

In the mammalian retina, neurons of numerous individual subtypes display orderly spatial arrangements called mosaics (Cook and Chalupa, 2000). The phenomenon of retinal mosaicism implies a molecular system for cell-cell recognition, where neurons of the same subtype recognize, repel and separate from each other to ensure that each cell type evenly distributed across the retina (Kay *et al.*, 2012). MEGF10, the mammalian homolog of Draper, has been identified as the homotypic repellent ligand expressed in starburst amacrine cells (SACs) during retinal mosaicism. SACs use MEGF10 as part of a receptor complex that detects MEGF10 on their homotypic neighbours to initiate repulsive signaling and separate from each other (Kay *et al*., 2012). During *Drosophila* larval NMJ synaptogenesis, Cell-cell recognition events also take place when neuronal growth cones firstly make contact with myopodia processed from muscles. Neuronal axons select their target muscle counterparts to form synapses by recognizing the attractive or repulsive cues from the muscle (Nose 2012). It is possible that Draper, like its mammalian homolog MEGF10, also serves as a signaling ligand during synaptogenesis. A good way to evaluate this possibility is to use the embryonic driver *H94-GAL4* to achieve unbalanced level of Draper between muscle 6 and muscle 7 (by specifically expressing Draper transgene in muscle 6, but not in muscle 7), and then examine if there is a shift of bouton distribution in muscle 6/7 compared to wild type. This experimental method is described in Mosca *et al*., 2012.

4.4.2. Draper may be involved in the Wg signaling pathway

Wingless (Wg) is a member of the Wnt family of secreted glycoproteins which function in synapse formation and maturation (Pachard *et al*., 2003). At Drosophila NMJ, Wg is secreted from presynaptic terminals and presumably binds to postsynaptic transmembrane DFrizzled2 receptor (DFz2). DFz2 in turn becomes internalized and transported to perinuclear areas, where its cytoplasmic C-terminus tail is cleaved and enters the nucleus to activate transcription of target genes that is required for synaptic growth and differentiation (Mathew *et al*., 2005).

When the Wg signaling is disturbed, the growth of NMJs is hampered and 'ghost boutons' are formed (Packard *et al*., 2002). These characteristics are strikingly similar to those previously observed in larvae with muscle-specific knock-down of Draper (Fuentez-Medel., 2009), suggesting a potential relationship between muscle-associated Draper and the Wg pathway. Given that Draper is an engulfment receptor which has well established function to initiate membrane internalization (Fullard *et al*., 2009), it is possible that Draper is involved in the internalization process of DFz2. Therefore, loss of Draper in the muscle may impede the endocytosis of DFz2 and consequently block the Wg signaling. A proper way to evaluate this hypothesis is to compare the level of DFz2 internalization (as described in Mathew *et al*., 2005) between larvae with muscle-specific Draper knock-down and wild type control.

4.5. Concluding remarks

I have provided the evidence that postsynaptic Hts is an important regulator of *Drosophila* NMJ development. Loss of postsynaptic Hts hampers larval NMJ development, whereas upregulating postsynaptic Hts results in overdeveloped larval NMJs. In addition, loss of postsynaptic Hts leads to severe motor defects in the late stage pupae, suggesting that postsynaptic Hts also affects NMJ development during metamorphosis. These findings complement our understanding of the function of Hts in addition to the previously well studied function of presynaptic Hts in synaptic development (Pielage *et al*., 2011). Given that high degree of sequence conservation between Hts and mammalian adducin, it is likely that at least part of our understanding

into Hts regulation and function at the NMJ may be extrapolated to help shed light on the role of adducin in mammalian neuronal development and neurological disorders. For example, neuromuscular junction dismantlement has been identified as an early hallmark of ALS with unknown mechanisms (Fischer *et al*., 2004; Parkhouse *et al*., *2008). Given the close relationship between postsynaptic Hts and Drosophila* neuromuscular junction development, and that adducin is misregulated in the spinal cords of ALS patients (Hu *et al*., 2003a), it is possible that aberrant regulation of adducin also presents at the NMJ and contributes to NMJ dismantlement in ALS.

The protein-protein interaction between Hts and Draper is also suggested in this study, which highlight a new avenue by which Hts may be exerting its influence on NMJ development, and open up worthwhile possibilities for future studies. Draper is a transmembranous molecule with multiple EGF-repeats in its extracellular domain (Fuentes-Medel *et al*., 2009). The extracellular EGF-repeats of Teneurin are speculated to initiate trans-synaptic signaling during Drosophila larval NMJ development (Mosca *et al*., 2012). It is possible that by interacting with Hts, Draper could transduce the signaling initiated from submembranous Hts to other synaptic counterparts.

Although the cross-talk between Hts and Draper is important during NMJ development, Draper is probably not the main downstream regulator of Hts during NMJ development. Here Draper is shown to be delocalized by Hts overexpression in the muscle. Muscle-specific Draper knockdown has been previously shown to hamper NMJ growth by a ~50% decrease in type Ib bouton number (Fuentes-Medel *et al*., 2009). If Draper was the main downstream regulator of Hts during NMJ development, we should expect to see underdeveloped NMJs in larvae overexpressing Hts in the muscle. In fact, overexpressing Hts in the muscle results in overdeveloped NMJs. It is possible that Hts interacts with multiple synaptic proteins and the effects of these interactions contribute together to the final phenotype of NMJ in animals with different Hts manipulation. Future study is needed to indentify other interacting candidate with Hts during Drosophila larval NMJ development.

References

Adams M D, Celniker S E*, et al.* (2000). "The genome sequence of Drosophila melanogaster." *Science* 287(5461): 2185-2195.

Ashley J, Packard M, Ataman B, and Budnik V. (2005). Fasciclin II signals new synapse formation through amyloid precursor protein and the scaffolding protein dX11/Mint. The Journal of Neuroscience 25(25): 5943-5955

Ataman B, Budnik V, and Thomas U. (2006). Scaffolding proteins at the Drosophila neuromuscular junction. INTERNATIONAL REVIEW OF NEUROBIOLOGY, VOL.75, DOI: 10.1016/S0074-7742(06)75009-7.

Atwood HL, Karunanithi S, Georgiou J, and Charlton MP. (1997). Strength of synaptic transmission at neuromuscular junctions of crustaceans and insects in relation to cacium entry. Invert Neuosci 3: 81-87.

Awasake T., Tatsumi R., Takahashi K et al. (2006). Essential role of the apoptotic cell engulfment genes Draper and ced-6 in programmed axon pruning during Drosophila metamorphosis. Neuron 50: 855-867.

Karunanithi S, Marin L, Wong K, Atwood HL. (2002). Quantal size and variation determined by vesicle size in normal and mutant Drosophila glutamatergic synapses. J Neurosci 22: 10267-10276.

Barber SC and Shaw PJ. (2010). Oxidative stress in ALS: Key role in motor neuron injury and therapeutic target. Free Radical Biology and Medicine 48: 629-641.

Bate M (1990). "The embryonic development of larval muscles in Drosophila." *Development* 110(3): 791-804.

Bear JE, Svitkina TM, Krause M, Schafer DA, Loureiro JJ, Strasser GA, Maly IV, Chaga OY, Cooper JA, Borisy GG and Gertler FB. (2002). Antagonism between Ena/VASP proteins and actin filament capping regulates fibroblast motility. Cell Biol. 161, 557-570.

Bednarek E and Caroni P. (2011). β-Adducin is required for stable assembly of new synapses and improved memory upon environmental enrichment. Neuron 69: 1132-1146.

Bennett V. (1990). Spectrin-based membrane skeleton: a multipotential adapter between plasma membrane and cytoplasm. Phys. Rev. 70: 1029-1065.

Bennett V and Baines AJ. (2001). Spectrin and ankyrin-based pathways: Metazoan inventions for integrating cells into tissues. Physiol. Rev. 81: 1353-1392.

Beumer K., Matthies H., Bradshaw A. and Broadie K. (2002). Integrins regulate DLG/FAS2 via a CaMkinase II-dependent pathway to mediate synapse elaboration and stabilization during postembryonic development. Development. 129, 3381-3391

Brent JR, Werner KM, McCabe BD. (2009). Drosophila larval NMJ dissection. J. Vis. Exp. (24), e1107 10.3791/1107, DOI : 10.3791/1107

Broadie K S and Bate M (1993). "Development of the embryonic neuromuscular synapse of Drosophila melanogaster." *J Neurosci* 13(1): 144-166.

Budnik V (1996). Synapse maturation and structural plasticity at Drosophila neuromuscular junctions. Curr Opin Neurobiol 6: 858-867.

Budnik V, Koh YH, Guan B, Hartmann B, Hough C, Woods D, Gorczyca M. (1996). Regulation of synapse structure and function by the *Drosophila* tumor suppressor gene *dlg*. Neuron 17: 627-640.

Chen K and Featherstone DE. (2005). Discs-large (DLG) is clustered by presynaptic innervations and regulates postsynaptic glutamate receptor subunit composition in Drosophila. BMC Biol 3:1.

Chevalier-Larsen E and Holzbaur EL. (2006). Axonal transport and neurodegenerative disease. Biochim Biophys Acta 1762: 1094-1108.

Chui V. (2011). The regulation and function of Hu-li tai shao (Hts) at the Drosophila neuromuscular junction. Master of science Thesis@SFU.

Citterio L, Tizzoni L, Gatalano M, Zerbini G, Bianchi G, Barlassina C. (2003). Expression analysis of the human adducing gene family and evidence of ADD2 beta4 multiple splicing variants. *Biochem Biophys Res Common 309*: 359-367.

Cook JE and Chalupa LM. (2000). Retinal mosaics: new insights in to an old concept. Trends Neurosci. 23: 26-34.

Crossley AC. (1978). The morphology and development of the Drosophila muscular system. In: The genetics and Biology of Drosophila (Ashburner M WT, ed), pp499-560. London, New York: Academic Press.

DiAntonio A, Petersen SA, Heckmann M, Goodman CS. (1999). Glutamate receptor expression regulates quantal size and quantal content at the Drosophila neuromuscular junction. J Neurosci 19: 3023-3032.

Dillon C and Goda Y. (2005). The actin cytoskeleton: integrating form and function at the synapse. Annu Rev Neurosci 28: 25-55.

Duffy JB. (2002). GAL4 system in Drosophila: a fly geneticist's Swiss army knife. Genesis 34: 1-15.

Eaton BA, Fetter RD and Davis GW. (2002). Dynactin is necessary for synapse stabilization. Neuron 34: 729-741.

Eisen A and Krieger C. (1998). Amyotrophic lateral sclerosis: A synthesis of research and clinical practice. Cambridge, UK. 303 pp.

Freeman M.R., Delrow J., Kim J., Johnson E. and Doe C.Q. (2003). Unwrapping glial biology: gcm target genes regulating glial development, diversification, and function. Neuron 38: 567-580.

Fischer LR, Culver DG, Tennant P, Davis AA, Wang M, Castellano-Sanchez A, Khan J, Polak MA, and Glass JD. (2004). Exp Neurol. 185(2); 232-240.

Fouquet W, Owald D, Wichmann C, Mertel S, Depner H, Dyba M, Hallermann S, Kittel RJ, Eimer S and Sigrist SJ. (2009). Maturation of active zone assembly by *Drosophila* Bruchpilot. *J. Cell Biol.* 186: 129-145.

Fuentes-Medel Y, Logan M, Ashley J, Atama B, Budnik V and Freeman M. (2009). Glia and muscle sculpt neuromuscular arbors by engulfing destabilized synaptic boutons and shed presynaptic debris. PLoS BIOLOGY. 7, 1-15.

Fullard J, Kale A and Baker NE. (2009). Clearance of apoptotic corpses. Apoptosis 14: 1029-1037.

Gilligan DM, Sarid R and Weese J. (2002). Adducin in platelets: activation-induced phosphorylation by PKC and proteolysis by calpain. Blood. 99: 2418-2426.

Giot L, Bader JS, et al. (2003). "A protein interaction map of Drosophila melanogaster." Science 302(5651): 1727-1736.

Goda Y and Davis GW. (2003). Mechanisms of synapse assembly and disassembly. Neuron 40, 243-264.

Goeliner B. and Aberle H. (2011). The synaptic cytoskeleton in development and disease. Dev Neurobiol. doi: 10.1002/dneu.20892.

Gorczyca M, Augart C and Budnik V (1993). "Insulin-like receptor and insulin-like peptide are localized at neuromuscular junctions in Drosophila." *J Neurosci* **13**(9): 3692-3704.

Gruenbaum LM, Gilligan DM, Picciotto MR, Marinesco S, and Carew TJ. (2003). Identification and characterization of Aplysia adducin, and Aplysia cytoskeletal protein homologous to mammalian adducins: increased phosphorylation at a protein kinase C consensus site during long-term synaptic facilitation. J. Neurosci. 23, 2675-2685.

Gu J, Lee CW, Fan Y, Komlos D, Tang X, Sun C, Yu K, Hartzell HC, Chen G, et al. (2010). ADF/cofilin-mediated actin dynamics regulate AMPA receptor trafficking during synaptic plasticity. Nat. Neurosci. 13, 1208-1215.

Guan B, Hartmann B, Kho Y H, Gorczyca M and Budnik V (1996). "The Drosophila tumor suppressor gene, dlg, is involved in structural plasticity at a glutamatergic synapse." Curr Biol 6(6): 695-706.

Hebbar S, Hall RE, Demski SA, Subramanian A and Fernandes JJ. (2006). The adult abdominal neuromuscular junction of Drosophila: a model for synaptic plasticity. Journal of Neurobiology. DOI 10.1002/neu.

Hu JH, Chernoff K, Pelech S and Krieger C. (2003a). Protein kinase and protein phosphatase expression in the CNS of G93a mSOD over-expressing mice. J. Neurochem. 85: 422-431.

Hu JH, Zhang H, Wagey R, Krieger C. and Pelech SL. (2003b). Protein kinase and protein phosphatase expression in amyotrophic lateral sclerosis spinal cord. J. Neurochem. 85: 432-442.

Hoang B and Chiba A (2001). "Single-cell analysis of Drosophila larval neuromuscular synapses." Dev Biol 229(1): 55-70.

Honkura N, Matsuzaki M, Noquchi J, Ellis-Davies GC and Kasai H. (2008). The subspine organization of actin fibers regulates the structure and plasticity of dendritic spines. Neuron 57(5): 719-729.

Hoy R R. (2006, 2007). "Project Fruitfly: Genetic Dissection of Neural Systems and Behaviour." from http://hoylab.cornell.edu/fruitfly/shaker/physiology/.

Inaki M, Shinza-Kameda M, Ismat A, Frasch M and Nose A. (2010). Drosophila Tey represses transcription of the repulsive cue Toll and generates neuromuscular target specificity. Development 137(13): 2139-2146.

Jan LY and Jan YN. (1976a). Properties of the larval neuromuscular junction in Drosophila melanogaster. J Physiol 262: 189-214.

Jan LY and Jan YN (1976b). "L-glutamate as an excitatory transmitter at the Drosophila larval neuromuscular junction." J Physiol 262(1): 215-236.

Jan LY, Jan YN. (1982). Antibodies to horseradish peroxidase as specific neuronal markers in Drosophila and in grasshopper embryos. Proc Nacl Acad Sci USA 79: 2700-2704.

Jia X X, Gorczyca M and Budnik V (1993). "Ultrastructure of neuromuscular junctions in Drosophila: comparison of wild type and mutants with increased excitability." J Neurobiol 24(8): 1025-1044.

Johansen J, Halpern M E, Johansen K M and Keshishian H (1989a). "Stereotypic morphology of glutamatergic synapses on identified muscle cells of Drosophila larvae." J Neurosci 9(2): 710-725.

Johansen J, Halpern M E and Keshishian H (1989b). "Axonal guidance and the development of muscle fiber-specific innervation in Drosophila embryos." J Neurosci 9(12): 4318-4332.

Karunanithi S, Marin L, Wong K and Atwood HL. (2002). Quantal size and variation determined by vesicle size in normal and mutant Drosophila glutamatergic synapses. J Neurosci 22(23): 10267-10276.

Keshishian H and Chiba A (1993). "Neuromuscular development in Drosophila: insights from single neurons and single genes." Trends Neurosci 16(7): 278-283.

Kay JN, Chu MW and Sanes JR. (2012). MEGF10 and MEGF11 mediate homotypic interactions required for mosaic spacing of retinal neurons. Nature 483(7390): 465-471.

Koch I, Schwarz H, Beuchle D, Goellner B, Langegger M and Aberle H. (2008). Drosophila Ankyrin 2 is required for synaptic stability. Neuron 58: 210-222.

Koh Y H, Popova E, Thomas U, Griffith L C and Budnik V (1999). "Regulation of DLG localization at synapses by CaMKII-dependent phosphorylation." *Cell* **98**(3): 353-363.

Koh YH, Gramates LS and Budnik V. (2000). Drosophila larval neuromuscular junction: molecular components and mechanisms underlying synapic plasticity. Microsc Res Tech 49: 14-25

Krieger C, Hu JH and Pelech S. (2003). Aberrant protein kinases and phosphoproteins in amyotrophic lateral sclerosis. Trends in Pharmacological Sciences 24 (10): 535-541.

Kuhlman PA, Hughes CA, Bennett V and Fowler VM. (1996). A new function for adducin, calcium calmodulin regulated capping of the barbed ends of actin filaments. J. Biol. Chem. 271: 7986-7991.

Lahey T, Gorczyca M, Jia X X and Budnik V (1994). "The Drosophila tumor suppressor gene dlg is required for normal synaptic bouton structure." Neuron 13(4): 823-835.

Li X, Matsuoka Y, and Bennett V. (1998). Adducin preferentially recruits spectrin to the fast growing ends of actin filaments in a complex requiring the MARCKS-related domain and a newly defined oligomerization domain. J. Biol. Chem. 273, 19329-19338.

Lin, H., Yue, L. and Spradling, A. C. (1994). The Drosophila fusome, a germline-specific organelle, contains membrane skeletal proteins and functions in cyst formation.Development 120,947 -956.

Lin Y, and Koleske AJ. (2010). Mechanisms of synapse and dentrite maintenance and their disruption in phychiatric and neurodegerenative disorders. Annu. Rev. Neurosci. 33: 349-378.

Luo L. (2002). Actin cytoskeleton regulation in neuronal morphogenesis and structural plasticity. Annu. Rev. Cell Dev. Biol. 18, 601-635.

Luo L. and O'Leary D.D. (2005). Axon retraction and degeneration in development and disease. Annu Rev Neurosci 28: 127-156.

MacDonald J.M., Beach M.G., Porpiglia E., Sheehan A.E., Watts R.J. and Freeman M.R. (2006). The Drosophila cell corpse engulfment receptor Draper mediates glial clearance of severed axons. Neuron 50: 869-881.

Martin LJ and Chang Q. (2012) Inhibitory synaptic regulation of motoneurons: A new target of disease mechanisms in Amyotrophic lateral sclerosis. Mol Neurobiol 45: 30-42.

Mathew D, Ataman B, Chen J, Zhang Y, Cumberledge S and Budnik V. (2005). Wingless signaling at synapses in through cleavage and nuclear import of receptor DFrizzled2. Science 310: 1344-1347.

Matsuoka Y, Hughes CA and Bennett V. (1996). Adducin regulation. Definition of the calmodulin-binding domian and sites of phosphorylation by protein kinases A and C. J Biol. Chem. 271: 25157-25166.

Matsuoka Y, Li X, and Bennett V. (1998). Adducin is an in vivo substrate for protein kinases C: phosphorylation in the MARCKS-related domain inhibits activity in promoting spectrin-actin complexes and occurs in many cells, including dentritic spines of neurons. J. Cell Biol. 142: 485-497.

Matsuoka Y, Li X and Bennett V. (2000). Adducin: structure, function and regulation. Cell. Mol. Life Sci. 57(6), 884-895

McPhee CK, Logan MA, Freeman MR and Baehrecke EH. (2010). Activation of autophagy during cell death requires the engulfment receptor Draper. Nature 465(7301): 1093-1096.

Mejillano MR, Kojimo S, Applewhite DA, Gertler FB, Svitkina TM and Borisy GG. (2004). Lamellipodial versus filopodial mode of the actin nanomachinery: Pivotal role of the filament barbed end. Cell 118: 363-373.

Menna E, Disanza A, Cagnoli C, Schenk U, Gelsomino G, Frittoli E, Hertzog M, Offenhauser N, Sawallisch C, Kreienkamp HJ et al. (2009). Eps 8 regulates axonal filopodia in hippocampal neurons in response to brain-derived neurotrophic factor (BDNF). PLos Biol. 7, e1000138.

Miller, C.; Drosophila melanogaster (On-line), Animal Diversity Web; 2000. Accessed October 27, 2008 @http://animaldiversity.ummz.umich.edu/site/accounts/information/Drosophila_melanogaster.html.

Monastirioti M, Gorczyca M, Rapus J, Eckert M, White K and Budnik V (1995). "Octopamine immunoreactivity in the fruit fly Drosophila melanogaster." J Comp Neurol 356(2): 275-287.

Mosca TJ, Hong W, Dani VS, Favaloro V, Luo L. (2012). Trans-synaptic Teneurin signling in neuromuscular synapse organization and target choice. Nature 484(7393): 237-41.

Nose A. (2012). Generation of neuromuscular specificity in Drosophila: novel mechanisms revealed by new technologies. Frontiers in Molecular Neuroscience 5: 1-11.

Packard M, Koo ES, Gorczyca M, Sharpe J, Cumberledge S and Budnik V. (2002). The Drosophila Wnt, Wingless, provides an essential signal for pre- and postsynaptic differentiation. Cell 111: 319-330

Packard M, Mathew D and Budnik V. (2003). Wnts and TGF beta in synaptogenesis: old friends signaling at new places. Nat Rev Neurosci 4: 113-120

Parkhouse WS, Cummingham L, McFee I, Miller JM, Whitney D, Pelech SL and Krieger C. (2008). Neuromuscular dysfunction in the mutant superoxide dismutase mouse model of amyotrophic lateral sclerosis. Amyotroph Lateral Scler 9 (1): 24-34.

Petrella H, Smith-Leiker T, and Cooley L. (2007). The Ovhts polyprotein is cleaved to produce fusome and ring canal proteins required for Drosophila oogenesis. Development 134, 703-712.

Pielage J, Fetter RD and Davis GW. (2005). Presynaptic spectrin is essential for synapse stabilization. Current Biology 15: 918-928.

Pielage J, Fetter RD and Davis GW. (2006). A postsynaptic spectrin scaffold defines active zone size, spacing, and efficacy at the Drosophila neuromuscular junction. J Cell Biol 175(3): 491-503.

Pielage J, Bulat V, Zuchero B, Fetter RD and Davis GW. (2011) Hts/adducin controls synaptic elaboration and elimination. Neuron 69: 1114-1131.

Porro F, Rosato-Siri M, Leone E, Costessi L, Iaconcig A, Tongiorgi E, Muro AF. (2010). Beta-adducin (ADD2) KO mice show synaptic plasticity, motor coordination and bahavioural deficits accompanied by changes in the expression and phosphorylation levels of the alpha- and gamma-adducin subunits. Genes Brain Behav 9: 84-96.

Ritzenthaler S, Suzuki E and Chiba A (2000). "Postsynaptic filopodia in muscle cells interact with innervating motoneuron axons." Nat Neurosci 3(10): 1012-1017.

Rorbertson RM. (1993). Effects of temperature on synaptic potentials in the locust flight system. J Neurophysiol 70: 2197-2204.

Roos J and Kelly RB. (1999). The endocytic machinery in nerve terminals surrounds sites of exocytosis. Current Biology 23: 1411-1414.

Rose D and Chiba A. (2000). Synaptic target recognition at Drosophila neuromuscular junctions. Microsc Res Tech 49(1): 3-13.

Rowland LP and Shneider NA. (2001). Amyotrophic lateral sclerosis. N Engl J Med 344: 1688-1700.

Ruiz-Canada C and Budnik V. (2006). Introduction on the use of the Drosophila embryonic/larval neuromuscular junction as a model system to study synapse development and function, and a brief summary of pathfinding and target recognition. Int Rev Neurobiol 75: 1-31.

Seidel B, Zuschratter W, Wex H, Garner CC and Gundelfinger ED. (1995). Spacial and sub-cellular localization of the membrane cytoskeleton-associated protein alpha-adducin in the rat brain. Brain Res. 700: 13-24.

Schuster CM, Davis GW, Fetter RD, and Goodman CS. (1996a). Genetic dissection of structural and functional compoments of synaptic plasticity. I. Fasciclin II controls synaptic stabilization and growth. Neuron 17: 641-654.

Schuster CM, Davis GW, Fetter RD, and Goodman CS. (1996b). Genetic dissection of structural and functional compoments of synaptic plasticity. II. Fasciclin II controls presynaptic structural plasticity. Neuron 17: 655-667.

Schymick JC, Talbot K, Traynor GJ. (2007) Genetics of amyotrophic lateral sclerosis. Hum Mol Genet 16:R233–R242

Shan X, Hu JH, Cayabyab FS and Krieger C. (2005). Increased phosphor-adducin immunoreactivity in a murine model of amyotrophic lateral sclerosis. Neuroscience 134(3): 833-846.

Sone M, Suzuki E, Hoshino M, Hou D, Kuromi H, Fukata M, Kuroda S, Kaibuchi K, Nabeshima Y, Nabeshima Y, Hama C. (2000). Synaptic development is controlled in the periactive zones of Drosophila synapses. Development 127(19): 4157-68.

Strong MJ, Kesavapany S, Pant HC. (2005). The pathobiology of amyotrophic lateral sclerosis: a proteinopathy? J Neuropathol Exp Neurol 64: 649-664.

Sun M and Xie W, (2012). Cell adhesion molecules in Drosophila synapse development and function. Sci China Life Sci 55: 20-26, doi: 10.1007/s11427-012-4273-3.

Thomas U, Kim E, Kuhlendahl S, Koh YH, Gundelfinger ED, Sheng M, Garner CC and Budnik V. (1997). Synaptic clustering of cell adhesion molecule Fasciclin II by Discs-large and its role in the regulation of presynaptic structure. Neuron 19: 787-799.

Toba G, Ohsako T, Miyata N, Ohtsuka T, Seong KH, Aigaki T. (1999). The gene search system. A method for efficient detection and rapid molecular identification of genes in *Drosophila* melanogaster. Genetics 151 (2): 725-37.

Vincent C. (2011). The regulation and function of Hu-li Tai shao (Hts) at the Drosophila neuromuclar junction. SFU MSc Thesis (MBB).

Vukojevic V, Gschwind L, Vogler C, Demougin P, J-F de Quervain D, Papassotiropoulos A and Stetak A. (2012). A role for α-adducin (ADD-1) in nematode and human memory. The EMBO Journal 31: 1453-1466.

Wang S, Yang J, Tsai A, Kuca T, Sanny J, Lee J, Dong K, Harden N and Krieger C. (2011). Drosophila adducing regulates Dlg phosphorylation and targeting of Dlg to the synapse and epithelial membrane. Developmental Biology 357: 392-403.

Whittaker KL, Ding D, Fisher WW, Lipshitz HD. (1999) Different 3' untranslated regions target alternatively processed hu-li tai shao (hts) transcripts to distinct cytoplasmic locations during Drosophila oogenesis. J Cell Sci 112 (pt 19): 3385-3398.

Wilson P. (2005). Centrosome inheritance in the male germ line of *Drosophila* requires *hu-li tai-shao* function. *Cell Biol. Int*. 29, 360-369.

Woods D F and Bryant P J (1991). "The discs-large tumor suppressor gene of Drosophila encodes a guanylate kinase homolog localized at septate junctions." Cell 66(3): 451-464

Xia R., Liu Y., Yang L., Gal J, Zhu H and Jia J. (2012). Motor neuron apoptosis and neuromuscular junction perturbation are prominent features in a Drosophila model of Fus-mediated ALS. Molecular Neurodegeneration 7: 10.

Yue, L. and Spradling, A. C. (1992). hu-li tai shao, a gene required for ring canal formation during Drosophila oogenesis, encodes a homolog of adducin. Genes Dev. 6, 2443-2454.

Zaccai M, Lipshitz HD. (1996a). Role of Adducin-like (hu-li tai shao) mRNA and protein localization in regulating cytoskeletal structure and function during Drosophila Oogenesis and early embryogenesis. Dev Genet 19: 249-257

Zaccai M, Lipshitz HD. (1996b). Differential distributions of two adducing-like protein isoforms in the Drosophila ovary and early embryo. Zygote 4: 159-166.

Zhang J. (2012). Genetic redundancies and their evolutionary maintenance. Adv Exp Med Biol 751: 279-300.

Zhang Y, Guo H, Kwan H, Wang J W, Kosek J and Lu B (2007). "PAR-1 kinase phosphorylates Dlg and regulates its postsynaptic targeting at the Drosophila neuromuscular junction." *Neuron* **53**(2): 201-215.

Zhou Q, Xiao M, and Nicoll RA. (2011). Contribution of cytoskeleton to the internalization of AMPA receptors. Proc. Natl. Acad. Sci. USA 98, 1261-1266.

Zhou Z., Hartwieg E. and Horvitz H.R. (2001). CED-1 is a transmembrane receptor that mediates cell corpse engulfment in C. elegans. Cell 104: 43-56

Ziegenfuss JS, Biswas R, Avery MA, Hong K, Sheehan A, Yeung Y, Stanley ER and Freeman MR. (2008). Draper-dependent glial phagocytic activity is mediated by Src and Syk family kinase signalling. Nature 453: 935-940.

Zito K, Fetter R D, Goodman C S and Isacoff E Y (1997). "Synaptic clustering of Fascilin II and Shaker: essential targeting sequences and role of Dlg." *Neuron* **19**(5): 1007-1016

Zito K, Parnas D, Fetter RD, Isacoff EY and Goodman CS. (1999). Watching a synapse grow: noninvasive confocal imaging of synaptic growth in Drosophila. Neuron 22: 719-729.

Appendix.

DVD: Third instar larvae with muscle-specific Hts knock down show severe neuromuscular defect

Creator:

Mannan Wang

Description:

This DVD contains two supplementary videos from which **Figure 3.2** origins. Flies in late pupal stage were released from their pupal shells. Their neuromuscular functions were evaluated. The movement of a representative wild type adult fly and a fly with muscle-specific knock down (*mef2>htsRNAi*) were recorded. Compared to wild type, the *mef2>htsRNAi* fly exhibits sereve neuromuscular defects, indicating muscle-associated Hts is required for *Drosophila* neuromuscular development.

Filename:

Supplementary video- A wild type type fly.avi

Supplementary video- A *mef2>htsRNAi* fly.avi